The role of sphingosine-1-phosphate lyase (SPL) in the brain

Studies in brain-targeted SPL-deficient mice

Dissertation

zur

Erlangung des Doktorgrades (Dr. rer. nat.)

der

Mathematisch-Naturwissenschaftlichen Fakultät

der

Rheinischen Friedrich-Wilhelms-Universität Bonn

vorgelegt von

Daniel Nicolae Mitroi

aus Bukarest, Rumänien

Bonn, Oktober 2016

Angefertigt mit Genehmigung der Mathematisch-Naturwissenschaftlichen Fakultät der Rheinischen Friedrich-Wilhelms-Universität Bonn

1. Gutachter: PD Dr. Gerhild van Echten-Deckert

2. Gutachter: Prof. Dr. Walter Witke

Tag der Promotion: 20. Februar 2017

Erscheinungsjahr: 2017

TABLE OF CONTENTS

ABBREVIATIONS

AD	alzheimer's disease
Akt	serine/threonine kinase
AL	autophagolisosomes
ALS	amyotrophic lateral sclerosis
APP	amyloid precursor protein
APP-CTFs	amyloid precursor protein C-terminal fragments
APP-FL	amyloid precursor protein full length
ASM	acid sphingomyelinase
ATF	activating transcription factor
ATG	autophagy realated protein
BAPTA-AM	1,2-Bis(2-aminophenoxy)ethane-N,N,N′,N′-tetraacetic acid tetrakis(acetoxymethyl ester)
Bcl-2	B-cell lymphoma 2
BSA	bovine serum albumin
cDNA	complementary deoxyribonucleic acid
CerS	ceramide synthase
CERT	ceramide transfer protein
CMA	chaperone-mediated autophagy
CNS	central nervous system
DMSO	dimethyl sulfoxide
DUBs	deubiquitinating enzymes
DRAM	DNA damage-regulated autophagy modulator protein
EGFP	enhanced green fluorescent protein
eIF2α	eukaryotic initiation factor 2 alpha
EM	electron microscopy
ER	endoplasmatic reticulum
GAP-43	growth associated protein 43
GFAP	glial fibrillary acidic protein
GFP	green fluorescent protein
GPBP	goodpasture antigen binding protein
HD	Huntington's disease
HDAC	histone deacetylase
HRP	horseradish peroxidase
ICF	immunocitofluorescence
IHC	immunohistochemestry
IHF	immunohistofluorescence
IP	immunoprecipitation
IRE1	inositol requiring 1
Jnk	c-Jun N-terminal kinase
L	lysosome
LAMP-2	lysosomal associated membrane protein 2
LC3	microtubule-associated protein 1A/1B-light chain 3
LIR	LC3-interacting region

MG-132	*N*-benzyloxycarbonyl-L-leucyl-L-leucyl-L-leucinal
mRNA	messenger ribonucleic acid
mRFP	monomeric red fluorescent protein
mTOR	mammalian target of rapamycin
MUNC18	mammalian uncoordinated 18
NCS1	neuronal calcium sensor 1
NeuN	neuronal nuclei
NPC	Niemann-Pick disease, type C
OQ	other quadrant
P	phagophore
PBS	phosphate buffer saline
PCR	polymerase chain reaction
PD	Parkinson's disease
PDGF	platelet-derived growth factor
PE	phosphatidylethanolamine
PERK	protein kinase RNA-like endoplasmatic reticulum kinase
PFA	paraformaldehyde
PI3K	phosphatidylinositol-4,5-biphosphate 3-kinase
PKB	protein kinase B
PLP	pyridoxalphosphate
PSD95	postsynaptic density protein 95
S1P	sphingosine 1-phosphate
S1PR	sphingosine 1-phosphate receptor
SK	sphingosine kinase
SL	sphingolipid
SM	sphingomyelin
SNAP25	synaptosome associated protein 25kDa
SNARE	SNAP (soluble NSF attachment protein) receptor
SNCA	synuclein alpha
Sph	sphingosine
SPL	sphingosine 1-phosphate lyase
SPP	sphingosine 1-phosphate phosphohydrolase
SPT	serine palmitoyltransferase
SQSTM1	sequestosome 1
SVs	synaptic vesicles
THI	2-acetyl-4-tetrahydroxybutyl imidazole
TQ	targeted quadrant
UBA	ubiquitin-associated
UPR	unfolded protein response
UPS	ubiquitin-proteasome system
USP14	ubiquitin-specific protease 14
UVRAG	UV radiation resistance associated gene
VAMP2	vesicle-associated membrane protein 2
WB	western blotting

ABSTRACT

The bioactive lipid sphingosine 1-phosphate (S1P) is a degradation product of sphingolipids that are particularly abundant in neurons. It was shown previously that neuronal S1P accumulation is toxic leading to ER-stress and an increase in intracellular calcium. To clarify the neuronal function of S1P, a brain-specific knockout mouse model was generated, in which S1P-lyase (SPL), the enzyme responsible for irreversible S1P cleavage was inactivated ($SPL^{fl/fl/Nes}$ mice).

SPL cleaves S1P into ethanolamine phosphate, which is directed towards the synthesis of phosphatidylethanolamine (PE) that is an anchor to autophagosomes for LC3-I. In the brains of $SPL^{fl/fl/Nes}$ mic significantly reduced PE levels were detected. Accordingly, autophagy alterations involving decreased conversion of LC3-I to LC3-II and increased beclin-1 and p62 levels were apparent. Alterations were also noticed in downstream events of the autophagic-lysosomal pathway like increased levels of lysosomal markers and aggregate prone proteins such as amyloid precursor protein, α-synuclein and tau protein. Genetic and pharmacological inhibition of SPL in cultured neurons promoted these alterations while addition of PE was sufficient to restore LC3-I to LC3-II conversion, and control levels of p62, APP and α-synuclein. Rapamycin, which is an agonist of autophagy by inhibition of mTOR kinase, had no effect on autophagy in neuronal cultures from $SPL^{fl/fl/Nes}$ mice suggesting that the impaired autophagy seen in $SPL^{fl/fl/Nes}$ mice is mTOR independent. Electron and immunofluorescence microscopy showed accumulation of unclosed phagophore-like structures, reduction of autophagolysosomes and altered distribution of LC3 in $SPL^{fl/fl/Nes}$ brains. Experiments using mRFP-EGFP-LC3 provided further support for blockage of the autophagic flux at initiation stages upon SPL deficiency due to PE paucity.

Developmental ablation of SPL in the brain ($SPL^{fl/fl/Nes}$) caused marked accumulation of S1P and sphingosine. These changes in lipid composition lead to morphological, molecular and behavioral abnormalities. We observed altered presynaptic architecture including a significant decrease in number and density of synaptic vesicles (Mitroi et al. in press), and decreased expression of several presynaptic proteins in hippocampal neurons from $SPL^{fl/fl/Nes}$ mice. At the molecular level, accumulation of S1P induced a calcium mediated activation of the ubiquitin-proteasome system (UPS) which resulted in a decreased expression of the deubiquitinating enzyme USP14 and several presynaptic proteins. Upon inhibition of proteasomal activity, expression of USP14 and of preysnaptic proteins were restored. In addition, these mice displayed cognitive deficits.

These findings identify S1P metabolism as a novel player in modulating synaptic architecture, and emphasize a formerly overlooked direct role of SPL in neuronal autophagy.

ZUSAMMENFASSUNG

Das bioaktive Lipid Sphingosin-1-phosphat (S1P) ist ein Abbauprodukt von Sphingolipiden, die besonders reichlich in Neuronen vorkommen. Es wurde bereits infrüheren Studien gezeigt, dass die Akkumulation von S1P neurotoxisch ist. Sie bewirkt eine Zunahme des intrazellulären Calciums und löst ER-Stress aus. Um die neuronale Funktion von S1P weiter aufzuklären, wurde eine gehirnspezifische Knockout-Maus erzeugt, bei der S1P-Lyase (SP)L, das Enzym welches die irreversible S1P Spaltung katalysiert, inaktiviert wurde ($SPL^{fl/fl/Nes}$ Mäuse).

SPL spaltet S1P in Ethanolaminphosphat, das zur Synthese von Phosphatidylethanolamin (PE) genutzt wird. PE verankert LC3-I in Autophagosomen als LC3-II. In den Gehirnen von $SPL^{fl/fl/Nes}$ Mäusen wurden deutlich reduzierte PE Spiegel beobachtet. Als Folge davon war die verminderte Umwandlung von LC3-I zu LC3-II signifikant reduziert. Des Weiteren wurde eine erhöhte Expression von Beclin-1 und p62beobachtet. Veränderungen wurden auch in nachgelagerten Ereignisse im autophagasomal-lysosomalen Weg beobachtet. Neben einer Erhöhung an lysosomalen Markern, kam es auch zu einem Anstieg von Aggregat anfälligen Proteinen wie Amyloid-Vorläufer-Protein, α-Synuclein und Tau-Protein in Gehirnen der $SPL^{fl/fl/Nes}$ Mäuse.. Sowohl die genetische als auch die pharmakologische Hemmung der SPL in kultivierten Neuronen führten zu den gleichen Veränderungen , während die Zugabe von PE ausreichend war um sowohl die LC3-I zu LC3-II-Konvertierung als auch den Gehalt an p62, APP und α-Synuclein auf Kontrollniveau wieder herzustellen. Rapamycin, welches durch die Hemmung der mTOR-Kinase als Autophagieantagonist fungiert, hatte keinen Effekt auf die Autophagie in SPL-defizienten Neuronen. Dieses Ergebnis zeigt dass die durch das Ausschalten von SPL fehlerhafte Autophagie mTOR unabhängig ist. Mit Hilfe der Elektronen- und Immunfluoreszenzmikroskopie konnte zudem eine Akkumulation von noch nicht vollständig geschlossenen Phagophorartigen Strukturen, eine Reduzierung der Autophagolysosomen sowie eine veränderte Verteilung von LC3 in $SPL^{fl/fl/Nes}$ Gehirnen gezeigt werden. Unter Verwendung von mRFP-EGFP-LC3 konnte ein zusätzlicher Beweis für die Blockierung des Autophagie-Flusses bei SPL-Defizienz in Neuronen aufgrund eines PE-Mangelserbracht werden.

Die entwicklungsabhängige Ablation von SPL im Gehirn verursacht auch eine deutliche Zunahme von S1P und Sphingosin. Diese Veränderungen in der Lipidzusammensetzung führen zu morphologischen, molekularen und Verhaltensauffälligkeiten. Wir beobachteten Veränderungen der präsynaptischen Architektur einschließlich einer signifikanten Abnahme der Anzahl und Dichte von synaptischen Vesikeln (Mitroi et al. in press) sowie eine verminderte Expression mehrerer präsynaptischen Proteine in hippocampalen Neuronen aus $SPL^{fl/fl/Nes}$ Mäusen. Auf molekularer Ebene, induzierte die Akkumulation von S1P eine Calcium-vermittelte Aktivierung des Ubiquitin-Proteasomalen-Systems (UPS), die zu einer verminderten Expression des deubiquitinierenden Enzyms USP14 und einiger präsynaptischen Proteine führte. Durch Hemmung der proteasomalen Aktivität, konnte sowohl die Expression von USP14 als auch jene

derpräysnaptischen Proteine wiederhergestellt werden. Darüber hinaus zeigten diese Mäuse kognitive Defizite.

Diese Ergebnisse identifizieren eine neue Rolle des S1P Stoffwechsels bei der Modulation der synaptischen Architektur und zeigen erstmalig eine vormals übersehene Bedeutung der SPL für die neuronale Autophagie.

1. INTRODUCTION

Sphingosine 1-phosphate (S1P), sphingosine and ceramide are important metabolites of the sphingolipid network that have emerged as bioactive signaling molecules mediating critical cellular functions (Hannun et al. 2008). S1P is an evolutionarily conserved catabolic intermediate of sphingolipid metabolism that has been suggested as regulate crucial functions in the brain including neural development, differentiation and survival (Mizugishi et al. 2005, van Echten-Deckert et al. 2014). Its deficiency has resulted in embryonic lethality associated with disturbed neurogenesis including neural tube closure (Mizugishi et al. 2005). On the other hand its accumulation has turned out to be neurotoxic leading to neuronal death (Hagen et al. 2009, Hagen et al. 2011). Alternatively, S1P is proposed as a neuroprotective factor early lost in the pathogenesis of Alzheimer's (Couttas et al. 2014).

The dynamic balance of S1P, which is maintained by sphingosine kinases (SK1 and SK2) catalyzing its formation, and S1P phosphatases (SPP1 and SPP2) and S1P-lyase (SPL), catalyzing its degradation, is a critical determinant of S1P associated cellular functions (Spiegel et al. 2003). In particular, the diverse roles of S1P in autophagy are increasingly being recognized (Taniguchi et al. 2012, Harvald et al. 2015). Ethanolamine phosphate, derived from the breakdown of S1P by SPL, can be used in the synthesis of PE, an abundant membrane lipid. However, in most cell types, redirection of S1P degradation by SPL toward phosphoethanolamine formation does not constitute the major pathway for de novo PE synthesis. Autophagy competes for a common PE pool with major cellular PE-consuming pathways (Wilson-Zbinden et al. 2015). Autophagy is crucial for the survival of post-mitotic cells with high energy demands like neurons (Nixon 2013). It is employed by neurons not only for homeostatic and waste-recycling functions but also as an effective strategy for eliminating aggregate prone proteins, normally diluted by cell division in mitotic cells (Komatsu et al. 2006). Accordingly, defective autophagy is often associated with neuronal dysfunction and enhanced autophagy in neurons is currently being focused on, as an approach in combating neurodegenerative diseases (Hara et al. 2006, Komatsu et al. 2006, Menzies et al. 2015). Recent reports have deciphered how S1P related autophagic pathways might affect neurodegeneration (Moruno Manchon et al. 2015). These controversial findings point to a tight regulation of S1P levels in the brain.

S1P accumulation in SPL-deficient neurons has been associated with increased cytosolic calcium levels (Hagen et al. 2011) and ER-stress (Hagen-Euteneuer et al. 2012), which has mediated apoptotic neuronal death (Hagen et al. 2011). Based on these findings and due to early postnatal death of systemic SPL knockouts (Hagen-Euteneuer et al. 2012), it was assumed that brain-specific ablation of SPL might serve as a tool for clarifying the role of neuronal S1P. Therefore a mouse model was generated, with the developmental neural-specific ablation of SPL and its consequences explored.

1.1 Sphingolipids

1.1.1 Sphingolipid metabolism

Sphingolipids (SLs) represent a major class of natural lipids consisted of a sphingoid base backbone, and are ubiquitous constituents of membranes in eukaryotes. An essential molecule in sphingolipid biology is ceramide (Chen et al. 2010) formed of sphingosine N-acylated with fatty acids. A range of charged, neutral, phosphorylated, or glycosylated moieties are attached to ceramide further creating complex sphingolipids (Merrill et al. 2007). One example is phosphoryl choline which attached to ceramide makes sphingomyelin, the most abundant mammalian sphingolipid.

During the last couple of decades the biochemical pathways of SL metabolism (Huwiler et al. 2000, Futerman et al. 2005) and the intracellular compartments of synthesis and degradation (endoplasmic reticulum (ER)/Golgi apparatus and lysosomes, respectively) have been broadly characterized (Futerman et al. 2005, Futerman 2006).

SL synthesis starts with the condensation of serine and palmitoyl CoA by serine palmitoyl transferase (Hanada 2003) to form 3-keto-dihydrosphingosine, which is subsequently reduced by 3-ketosphinganine reductase to produce dihydrosphingosine, followed by acylation by a (dihydro)-ceramide synthase (Lass or CerS) (Pewzner-Jung et al. 2006). Ceramide is formed by the desaturation of dihydroceramide (Causeret et al. 2000) (Fig.1). Ceramide may be degraded by one of many ceramidases (Galadari et al. 2006, Xu et al. 2006) forming sphingosine, which may be recycled into sphingolipid pathways, or it can be phosphorylated by sphingosine kinases (Hait

et al. 2006), SK1 or SK2. The product S1P can be dephosphorylated back to sphingosine by specific intracellular S1P phosphatases (Johnson et al. 2003) and, also by non-specific extracellular and intracellular lipid phosphate phosphatases (Brindley 2004, Sigal et al. 2005). S1P can also be cleaved irreversibly by S1P lyase with generation of ethanolamine phosphate and hexadecenal (which can be oxidized to palmitate (reduced to palmitol and reused) (Bandhuvula et al. 2007).

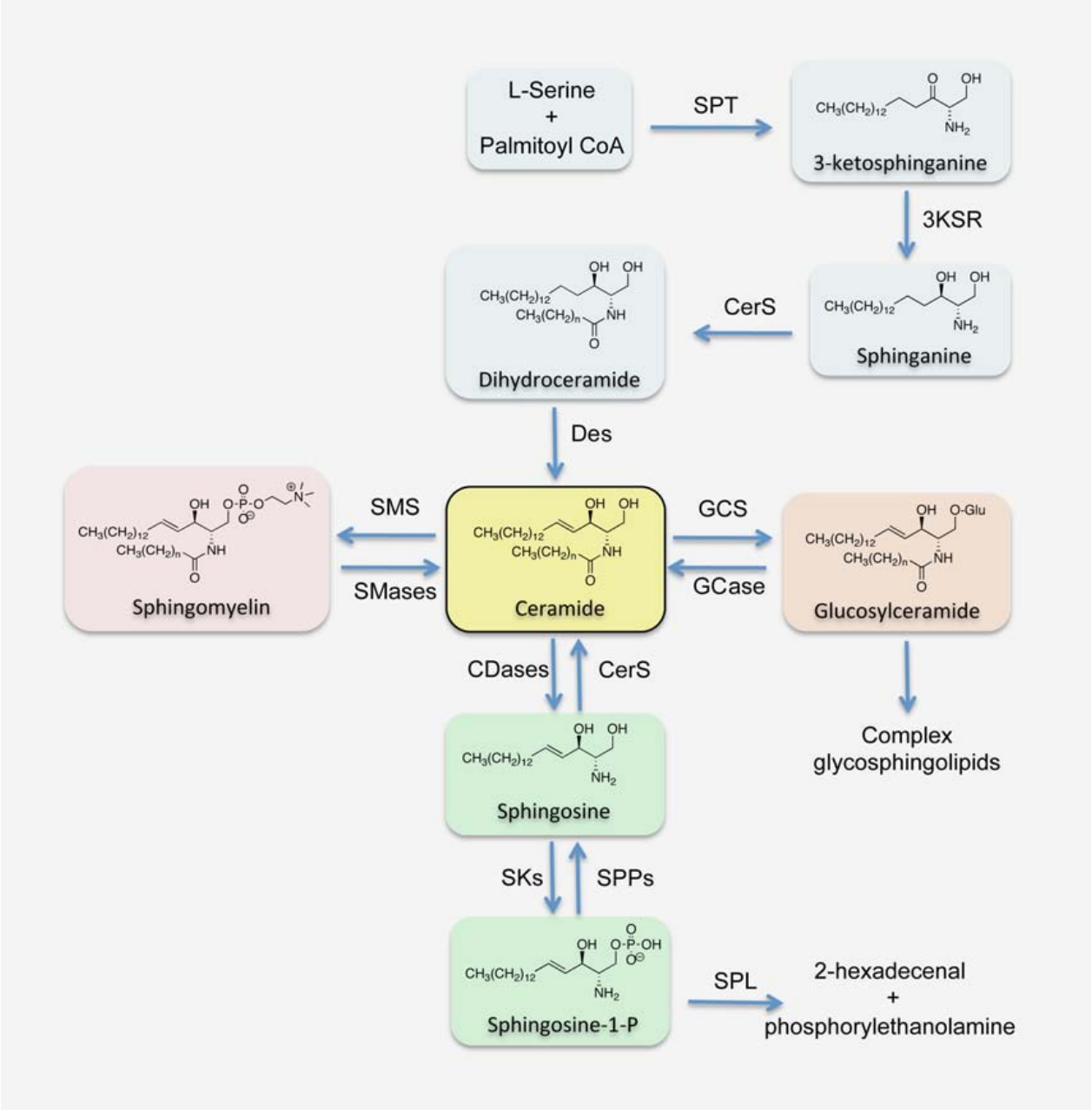

Figure 1. Schematic view of sphingolipid metabolism. SPT, serine palmitoyl transferase; 3KSR, 3-ketosphinganine reductase; CerS, ceramide synthases; Des, dihydroceramide desaturase; SMS, sphingomyelin synthases; SMases; sphingomyelinases; GCS, glucosylceramide synthase; GCase, glucocerebrosidase; CDases, ceramidases; SKs, sphingosine kinases; SPPs, sphingosine-1-phosphate phosphatases; SPL, sphingosine-1-phosphate lyase (Bedia et al. 2011).

1.1.2 Sphingosine 1-phosphate lyase

The first report of cloning of an SPL gene was published in 1997 (J.D. Saba 1997). In this article, the *Saccharomyces cerevisiae DPL1 (DHS1P lyase)* gene was identified by its ability to suppress sphingosine-induced growth inhibition. Subsequently, SPL homologs from *Mus musculus, Homo sapiens, Drosophila melanogaster*, *Caenorhabditis elegans, Dictyostelium discoideum* and *Leishmania major* were identified and confirmed by means of biochemical assay as encoding functional SPL enzymes and functional complementation of yeast *dpl1* mutants (J. Zhou 1998, P.P. Van Veldhoven 2000, G. Li 2001, D.R. Herr 2003, J. Mendel 2003, K. Zhang 2007). To date, genomic sequencing has revealed the existence of putative SPL genes in a wide variety of organisms including fungi, plants and mammals. The human SPL gene, *Sgpl1*, encodes a predicted protein of 568 amino acids with a molecular mass of 63.5 kDa (P.P. Van Veldhoven 2000). The amino acid sequence of the murine SPL homolog displays 84% identity and 92% similarity to human SPL. Similarity in primary sequence is also found in SPL homologs from *D. melanogaster, L. major, C. elegans, D. discoideum* and *S. cerevisiae.*

Immunofluorescence and subcellular fractionation studies have confirmed the primary location of SPL within the endoplasmic reticulum (ER), although the possibility that some SPL may localize to other organelles has not been definitively ruled out (P.P. Van Veldhoven 2000, M. Ikeda 2004, U. Reiss 2004). It has not yet been established just how SPL is specifically localized in the ER, although removal of the first 58 amino acids leads to its expression in the soluble fraction of Escherichia coli (P.P. Van Veldhoven 2000). SPL has not been found in serum, in plasma or in the extracellular space, and there are no reports of ecto-enzymes or secreted isoforms. Thus, SPL seems to be restricted to the intracellular environment. This allows SPL to act like an S1P “sink”, creating a gradient between circulating and tissue S1P levels that has physiological importance (Fyrst et al. 2008).

SPL function appears to be critical for mammalian development. *Sgpl1* expression has been observed throughout the development of mouse embryos (M. Ikeda 2004, Schmahl J 2007). Homozygous *Sgpl1* knockout mice do not survive beyond 3–4 weeks after birth, and they exhibit significant growth failure and anemia (Serra et al. 2010). Several congenital defects have been reported, including vascular abnormalities, skeletal defects, thoracic malformation of the sternum, ribs and vertebrae, and renal abnormalities (Fyrst et al. 2008). Embryonic fibroblasts from *Sgpl1* knockout mice have been shown to have migration defects *in vitro* (Schmahl et al. 2007). These vascular and cell migration defects are reminiscent of pathological changes observed in PDGF receptor and S1P1 receptor knockout mice (Y. Liu et al. 2000). Together with the identification of *Sgpl1* as a downstream target of PDGF signaling, this information suggests that SPL may play a role in the regulation of mammalian angiogenesis and other developmental processes (Fyrst et al. 2008).

1.1.3 Involvement of sphingolipids in neurodegenerative diseases

Multiple sclerosis (MS) is a chronic autoimmune disease characterized by blood-brain barrier break down, immune cell infiltration of the CNS, demyelination, astrogliosis, and neurodegeneration (Pelletier et al. 2012). S1P signaling activity is relevant to disease pathogenesis, as demonstrated by the efficacy of FTY720, a structural analog of S1P, in the treatment of relapsing-remitting MS (Brinkmann et al. 2010). S1P action likely occurs at multiple cellular sites within the immune, vascular, and nervous systems (Brinkmann et al. 2010).

Intracellular aggregation and protein misfolding are characteristics of many late-onset neurodegenerative diseases, also known as proteinopathies. These proteinopathies include Alzheimer's disease (AD), Parkinson's disease (PD), tauopathies and Huntington's disease (HD), and the proteins that accumulate are thought to be toxic. This belief is supported by overexpression in mouse models of HD, the presence of autosomal dominant tauopathies caused by mutations in the gene encoding tau, and PD due to triplication of the α-synuclein (SNCA) locus (Rubinsztein 2006). Even though inducing clearance of intracellular aggregate-prone proteins could constitute a therapeutic strategy, compromised clearance may increase or contribute to disease by increasing levels of key substrates such as aggregate-prone proteins

(Hara et al. 2006, Komatsu et al. 2006) and dysfunctional mitochondria (Kim et al. 2011), enhancing susceptibility to cell death (Boya et al. 2005, Ravikumar et al. 2006); and disturbing flux through the ubiquitin-proteasome system (Korolchuk et al. 2009). The role of lipid homeostasis in the brain, particularly that of membrane lipids, in AD pathogenesis has been recognized and considered in multiple studies (Lane et al. 2005, Walter et al. 2013). Neuronal membranes contain a highly specific and characteristic pattern of complex sphingolipids and therefore is it not surprising that neuronal function and survival is dependent on the metabolism of these lipids (van Echten-Deckert et al. 2014). Neuronal levels of S1P are tightly regulated at very low concentrations in the picomolar range (Hagen et al. 2009, Hagen-Euteneuer et al. 2012). A direct role of S1P in neuronal Aβ generation has been reported recently (Takasugi et al. 2011). Moreover, SPL knock-out cells showed strong accumulation of APP and potentially amyloidogenic APP C-terminal fragments, which have been associated with impaired lysosomal degradation (Karaca et al. 2014).

The integral component of the brain is formed by sphingolipids and therefore a proper sphingolipid homeostasis is crucial for the normal functioning of neurons. Several neurological diseases like Niemann-Pick disease (type I), Gaucher's disease, and Tay-Sacks disease result from the dysfunction of enzyme activities that handle complex sphingolipids (Rao et al. 2008). Niemann-Pick disease is a lysosomal storage disease, caused by mutations in the *Sphingomyelin phosphodiesterase* genes and is accompanied by a group of fatal inherited metabolic disorders. The complete or partial deficiency of acid sphingomyelinase (ASM) resulting from these mutations causes cell death due to the accumulation of sphingomyelin. Ledesma et al. (Ledesma et al. 2011) reviewed the neuronal impact in the acid sphingomyelinase knockout mouse model. Besides changes in the lipid content of neurons, this also includes a possible impairment in the neuronal signaling that may lead to Purkinje cells death, altered axonal polarity, altered calcium homeostasis, abnormal endocytosis function, and even an increased susceptibility to infection because of dysfunctional microglia (Ledesma et al. 2011). Although the primary defect in NPC (Niemann-Pick disease, type C) is related to cholesterol transport in endosomal-lysosomal compartments, SLs also accumulate in these compartments. Thus NPC might also be classified as a SL storage disorder (van Echten-Deckert et al. 2012). In addition, brains of NPC patients also showed accumulation of amyloidogenic APP CTFs and Aβ42 as compared to control brains (Jin et al. 2004). To sum up, evidence suggests that even minor changes in sphingolipid balance may

play an essential role in the development of neurodegenerative diseases, including Alzheimer's disease (Mielke et al. 2010), amyotrophic lateral sclerosis (Cutler et al. 2002), Parkinson's disease (France-Lanord et al. 1997), and dementia (Haughey et al. 2004).

1.2 Autophagy and ubiquitin-proteasome system

Two major pathways accomplish regulated protein catabolism: the ubiquitin-proteasome system (UPS) and the autophagy-lysosomal system (Fig. 2). The UPS accomplishes selective degradation of short-lived proteins. Degradation by the proteasome is spatially and temporally controlled largely by highly specific targeting of proteins by conjugation with polyubiquitin chains (Ciechanover 2005). Autophagy is a cellular catabolic process used to maintain cellular homeostasis. It is responsible for the degradation and recycling of long-lived proteins, protein aggregates and damaged organelles, via autophagolysosomes (Ravikumar et al. 2010, Chen et al. 2011). Recent studies have shown that autophagy also has additional functions, including organelle clearance, antigen presentation, elimination of microbes, in addition to regulation of development and cell death (Mizushima 2005). Autophagy occurs under basal conditions and it is stimulated by different types of cellular stress, such as nutrient starvation, oxidative stress, hypoxia, endoplasmic reticulum (ER) stress, mitochondrial damage, and is also stimulated by the application of treatment with some pharmacological agents (Kroemer et al. 2010). Three types of autophagy have been described: macroautophagy, microautophagy, and chaperone-mediated autophagy (CMA) (Klionsky 2005). Macroautophagy, more simply known as autophagy, occurs when cytoplasmic components are surrounded by double membrane structures called autophagosomes that mature by first fusing with late endosomes or by fusing directly with lysosomes in the formation of autolysosomes. In the final stage the autolysosome content, together with its inner membrane, is degraded by lysosomal hydrolases (Ravikumar et al. 2010, Chen et al. 2011). Microautophagy involves the direct engulfment of the cytoplasm on the lysosomal surface, while CMA translocates unfolded, soluble proteins directly across the limiting lysosomal membrane (Massey et al. 2006) (Fig. 2). The role of autophagy in recycling is complementary to that of the UPS, which degrades proteins to generate oligopeptides that are

subsequently degraded into amino acids, while replenishing the cell's supply of free ubiquitin (Nedelsky et al. 2008).

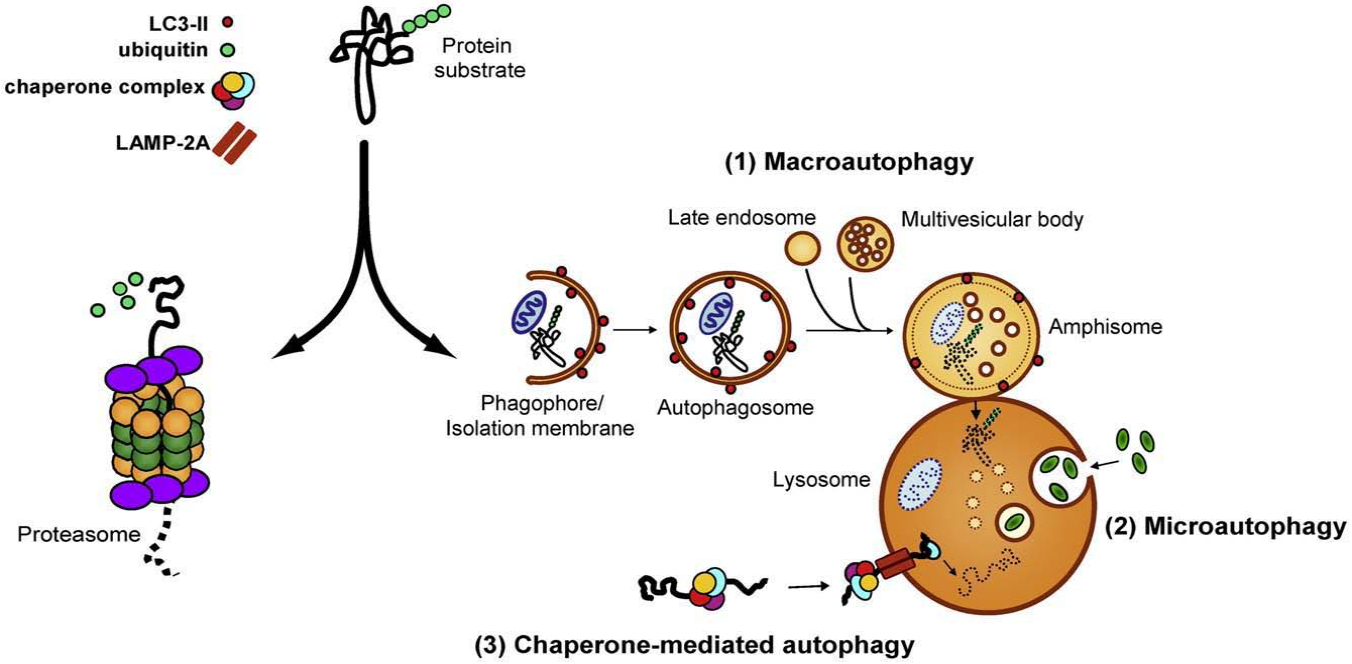

Figure 2. The ubiquitin-proteasome system (UPS) and autophagy are two major intracellular protein degradation systems. Proteasome-mediated degradation involves covalent addition of ubiquitin chains to target proteins followed by proteolytic cleavage through proteasome. Recent studies suggest that some ubiquitinated substrates could also be prone for the autophagy-lysosomal system. Multiple types of autophagy involve distinct routes in which cytoplasmic components are delivered for lysosome-mediated degradation. (1) Macroautophagy is a multistep process by which cytosolic components are engulfed by an isolation membrane to form autophagosomes that are delivered to lysosomes. (2) Microautophagy, cytosolic contents are directly engulfed by lysosomes. (3) Chaperone-mediated autophagy involves recognition of a peptide signal that induces receptor-mediated translocation into the lysosome (Nedelsky et al. 2008).

1.2.1 Autophagy

Autophagy is begun by the formation and elongation of a double-layered isolation membrane (the origin of which is not precisely known) called phagophore, which enwraps and sequesters parts of the cytoplasm containing autophagic substrates, to form autophagosomes. A set of Atg genes regulates the formation of autophagosomes, where Atg stands for autophagy-related. Atg genes

were originally discovered in yeast where the nomenclature was taken from Klionsky et al. (Klionsky et al. 2003). According to their function these can be grouped into the Atg1 complex regulating vesicle nucleation (Atg1, Atg13 and Atg17 controlling autophagosomal induction), the PI3K complex III (including phosphatidyl inositol 3-phosphate kinase vps34, Beclin 1 (Atg6 orthologue) UVRAG (UV radiation resistance associated gene)), and two interconnected ubiquitin-like conjugation systems that mediate vesicle elongation and sealing. Formation of the Atg5-Atg12 conjugate is one of the first of these conjugation systems mediated by the E1-like enzyme, Atg7, and the E2-like enzyme, Atg10. The second of these systems involves conjugation of Atg8 (in mammalian cells also known as microtubule-associated protein 1 light chain 3, LC3) with the lipid, phosphatidylethanolamine, regulated by Atg7, along with Atg3, as the E2-like enzyme (Suzuki et al. 2007). After the formation of the autophagosome, Atg5-Atg12 conjugate is removed, while LC3 remains attached to the vesicle. Thus, LC3 serves as a reliable autophagosomal marker that can be used to evaluate the rates of autophagosome formation and degradation (Klionsky et al. 2008). Autophagosomes are transported along microtubules in a dynein-dependent manner and fuse with endosomes or fuse directly with lysosomes where autophagosomal contents are degraded by lysosomal hydrolases (Ravikumar et al. 2005).

1.2.2 The ubiquitin-proteasome system (UPS)

Proteins are targeted for degradation by the UPS via a series of enzymatic reactions that tag them with ubiquitin, a small 76-amino acid residue (Ciechanover et al. 1980, Hershko et al. 1980). UPS clients are marked by polyubiquitylation for transportation by a shuttling machinery, which is not very well understood, to proteasome, a specialized organelle, where proteins are degraded to oligopeptides, which are released into the cytoplasm or nucleoplasm. Oligopeptides can be further digested into amino acids by soluble peptidases. The specificity and selectivity of the ubiquitylation process is delineated by a combination of three types of enzymes (Hershko et al. 1983). The initiation of the reaction is made by activating ubiquitin E1 enzymes, two of these known in mammals, and by transferring it onto E2 ubiquitin-conjugating molecules (it is thought that around 40 are encoded in the mammalian genome). One of several hundred E3 ligases, which

are capable of binding the ubiquitin-carrying E2 enzyme, selects a substrate, resulting in the transfer of the ubiquitin onto lysine residues (Pickart et al. 2004, Randow et al. 2009). As a result of this type of reaction, the substrate becomes monoubiquitylated in one or more places. For proteasomal targeting the initial modifications are insufficient, since ubiquitin itself contains lysine residues in positions 6, 11, 27, 31, 33, 48 and 63, that would be able to accept another ubiquitin moiety in a second round of ubiquitylation. This will lead to the generation of different types of polyubiquitin chains. For delivery to the proteasome, it is believed that at least four ubiquitin chains are ideal (Thrower et al. 2000), interconnected via K48 residues and characterized by a closed conformation (Fushman et al. 2010). The proteasome is a barrel–shaped proteolytic organelle found throughout the cell. It consists of a 20S central complex and two 19S lid complexes. The 19S complexes bind cargo-loaded shuttling proteins, deubiquitylate the substrates and control access to the six proteolytic sites of the inner core of the 20S subunit (Kopp et al. 1986, Lowe et al. 1995). The catalytic activities of the proteasome have different specificities, and are considered trypsin-, chymotrypsin- and peptidyl-glutamyl peptide-hydrolyzing-like (Heinemeyer et al. 1997). Protein substrates have to be partially-unfolded prior to entry into the 20S subunit since the proteasomal catalytic pore is relatively narrow in size. Thus, protein complexes and aggregates can only be degraded if they are disassembled. This makes them unlikely substrates of proteasome (Nandi et al. 2006).

Deubiquitinating enzymes (DUBs) remove covalently attached ubiquitin from proteins, thereby controlling substrate activity and/or abundance (Sowa et al. 2009). Mammalian proteasomes are associated with three DUBs: RPN11, UCH37, and USP14 (Lee et al. 2010, Nag et al. 2012). Both USP14 and UCH37 associate reversibly with the 19S regulatory particle, whereas RPN11 is an intrinsic subunit of the proteasome lid subcomplex of the 19S regulatory particle; therefore, the modulation of their functions may affect the proteasomal uptake of the protein substrate for degradation (Tian et al. 2014). USP14, in particular, can inhibit proteasomes *in vitro*, and also inhibits protein turnover in cells (Lee et al. 2010).

1.2.3 Presynaptic protein degradation by the ubiquitin proteasome system

Some studies provide information about the function of UPS in the presynaptic terminals. One of these studies has shown that some components of the UPS, like E1 and the proteasome, are found in the presynaptic boutons at the neuro-muscular junction in *Drosophila* (Speese et al. 2003). Using a conditional fluorescent reporter of proteasome activity, these studies have demonstrated that the proteasome is active in these boutons. Proteasome inhibition provoked a 50% increase in excitatory junctional current amplitude when compared to controls. The rapid increase suggests a local degradation of proteins by the UPS. DUNC-13, a protein regulating synaptic vesicle priming seems to be involved in this process. Speese et al. (Speese et al. 2003) showed that DUNC-13 accumulates at the presynaptic site upon proteasome inhibition. Syntaxin-1 and synaptophysin, two other synaptic vesicle proteins involved in neurotransmitter release, are also regulated by UPS (Chin et al. 2002, Wheeler et al. 2002). At the presynaptic terminal deubiquitinating enzymes are also found. They can decrease the total content of ubiquitinated substrates within a matter of seconds (Chen et al. 2003). USP14, a deubiquitinating enzyme of the presynapse was reported to have been involved in the regulation of synaptic transmission (Bhattacharyya et al. 2012). Thus, an ataxic mouse model with a loss of functional mutation of USP14 exhibits decreased frequency and increased amplitude of miniature end plate potentials at the neuromuscular synapses (D'Amato et al. 1965). Hippocampal short-term plasticity, but not its long-term plasticity, is also impaired, which suggests that UPS activity and ubiquitin recycling are important modulators of neurotransmitter release and plasticity (Wilson et al. 2002).

1.2.4 Relationship between the proteasomal system and autophagy

1.2.4.1 Ubiquitin as a unifying factor linking the UPS and selective autophagy

Autophagy was believed to be a non-specific process that degrades cytoplasmic proteins and organelles in conglomerate, a situation that may occur during periods of starvation when cell survival depends on autophagy (Ciechanover 2005). Organelles like the ER or mitochondria were the first evidence of selective autophagy, as early as in the 1970s, although further understanding of such selectivity was impossible until more recent insights into the molecular mechanisms of selective autophagy (Klionsky 2007). While there is still scant evidence for this process, it is assumed that, during selective autophagy, certain autophagic substrates may be specifically targeted for degradation, in the process of being randomly taken up along with an amount of cytoplasm. The importance of this issue becomes evident when we are aware that ubiquitylation plays a significant role as a signal of selective autophagy, just as in the ubiquitin proteasome pathway. Therefore, it might be tempting to consider that the degradation of cellular targets is regulated by ubiquitin in both the UPS and autophagic processes. Certainly, many proteins have been shown to be target substrates for both degradative systems. In some circumstances the ubiquitylated substrates, normally digested by the UPS, can also be degraded by autophagy, and vice versa (Fuertes et al. 2003, Fuertes et al. 2003, Wooten et al. 2008). Moreover, impairment of proteasomal activity was found to activate autophagy, thought to be a compensatory mechanism allowing the cell to reduce the levels of UPS substrates (Iwata et al. 2005, Ding et al. 2007, Pandey et al. 2007, Milani et al. 2009). Nonetheless, the total contribution of autophagy to the degradation of the overall pool of ubiquitylated proteins in the cell is still unclear. It is also unknown whether ubiquitylation is an essential mechanism for targeting many proteins to autophagy. The exact type of ubiquitin modification recognized by each pathway seems to vary, although ubiquitylation may appear to function as a universal tag for substrate degradation via both catabolic systems. It is known that K48-linked polyubiquitin chains are targeted to the UPS and the substrates recognised by autophagosome-lysosome pathway are believed to be modified either by K63-linked chains (adopting a more open conformation than

K48 chains), or may simply be monoubiquitylated (Welchman et al. 2005). Thus, despite the use of ubiquitin in both catabolic pathways, the structural complexity of different polyubiquitin chains may be sufficient to maintain the selectivity and specificity of the UPS and autophagy in their substrates. However, some potential overlap may result from the incomplete specificity of the different adaptor molecules that have been thought to retrieve the ubiquitylated substrates of each degradative pathway. In this group, there are several proteins that seem to serve as linkers between ubiquitylated cargo and the phagophore, including p62 (also called SQSTM1/A170), NBR1 (neighbour of BRCA1 gene 1), HDAC6 (histone deacetylase 6) and Alfy (Kirkin et al. 2009). These proteins have the capacity to interact directly or indirectly with both ubiquitin and components of autophagic machinery, thus providing the type of link that would be provided by an adaptor molecule. The most established of these adaptors, p62, is itself an autophagy substrate that forms homo-oligomers to which ubiquitylated proteins are recruited via its UBA (ubiquitin associated) domain (Bjorkoy et al. 2005, Komatsu et al. 2007, Pankiv et al. 2007, Kirkin et al. 2009). These complexes have been described as serving to sequester ubiquitylated substrates that are recognised by the autophagic machinery (p62 interacts directly with LC3 via a dedicated LIR motif (Pankiv et al. 2007)), and then engulfed and degraded (Bjorkoy et al. 2005, Kirkin et al. 2009). The UBA domain of p62 seems to have a higher preference for monoubiquitin or polyubiquitin chains with open conformations (K63-linked), compared to those with a closed conformations (K48-linked) (Long et al. 2008). This may suggest a preference of autophagy for substrates tagged with single ubiquitin, short chains, or with longer K63 chains, and might also still allow K48 chain-tagged substrates to be recruited in autophagosomes, especially in circumstances where the UPS is compromised, and when the concentration of K48-polyubiquitylated proteins is sufficient to allow such chains to interact effectively with p62 (Fuertes et al. 2003, Long et al. 2008). A small accumulation of primarily K63-linked polyubiquitin-tagged proteins was observed in p62-deficient mouse tissues. The interpretation of this effect is complex, since p62 also appears to have a function as an adaptor in the proteasomal degradation of some ubiquitylated proteins. p62 appears to have a ubiquitin-independent role in the degradation of some autophagic substrates (Geetha et al. 2008, Wooten et al. 2008). Nevertheless, these studies are consistent with the notion that p62 can serve as an adaptor that is required for the autophagic degradation of ubiquitylated proteins (Kirkin et al. 2009, Kirkin et al. 2009).

1.2.4.2 Impairment of the UPS is compensated by upregulation of autophagy

One of the proposed links between the UPS and autophagy is based on the observation that impairment of the UPS leads to increased autophagic function (Iwata et al. 2005, Ding et al. 2007, Pandey et al. 2007). This is a compensatory mechanism, allowing cells to reduce the accumulation of UPS substrates. Treatment of both cells and mice with rapamycin to upregulate autophagy has been demonstrated to protect against cell death caused by proteasome inhibition (Pan et al. 2008). Moreover increase of autophagy has been shown to protect against loss of proteasome activity in Drosophila (Pandey et al. 2007). Unfortunately, there is little consensus on the exact mechanism(s) of this cross-talk, as several potential explanations have been suggested. One possible mechanism involves the induction of the unfolded protein response (UPR) by the activation of endoplasmic reticulum (ER) stress, due to the accumulation of misfolded proteins. The UPR is an ER-to-nucleus signaling pathway that results in the transcriptional activation of a variety of genes, including those involved in protein folding and degradation in the ER. This pathway activation has been shown by a number of studies to also activate autophagy (reviewed in (Hoyer-Hansen et al. 2007)). There are diversities in the exact mechanics of this phenomenon, and it is most likely to depend on the cell type and stimulus for the UPR. Investigations into the direct link between proteasome inhibition, UPR and autophagy have been carried out in two studies using the proteasome inhibitor bortezomid. These studies demonstrate the importance of the transcription factor ATF4 in the upregulation of autophagy genes following proteasome inhibition (Milani et al. 2009, Zhu et al. 2010). However, the study of Zhu et al. (Zhu et al. 2010) suggests that the mechanism for increased ATF4 level is the activation of the PERK arm of the UPR requiring the phosphorylation of eIF2a, whereas Milani et al. (Milani et al. 2009) suggest that direct stabilization of the ATF4 protein due to the loss of proteasome activity, independent of the upstream activity of PERK, results in its increased activity (Milani et al. 2009). In addition these studies differ in the downstream targets of ATF4 action, showing on one hand an increase in ATG5 and ATG7 transcription (Zhu et al. 2010), and on the other hand in LC3 expression (Milani et al. 2009). Another study has suggested that compensatory autophagy upregulation following treatment with MG-132, or bortezomib, is mediated by the IRE1 arm of the UPR and its downstream target c-Jun NH2-terminal kinase (Jnk1) (Ding et al. 2007, Wei et al. 2008). Jnk1,

in turn, may induce autophagy by phosphorylation of Bcl-2, thereby disrupting its autophagy–inhibitory interaction with Beclin 1 (Ding et al. 2007, Wei et al. 2008). Independently of the UPR, proteasome inhibition in dopaminergic neurons has been shown to induce autophagy via a mechanism requiring p53 (Du et al. 2009). The protective effect of the compensatory upregulation of autophagy in proteasome-inhibited cells has also been suggested to be dependent on HDAC6 (Iwata et al. 2005, Pandey et al. 2007). However, the role for HDAC6 in this process is not thought to be through signaling to increase autophagic flux, but rather through ensuring efficient delivery of substrates to the autophagic machinery for degradation. There is a general consensus about a compensatory role of autophagy following proteasomal inhibition, but the exact mechanisms of this link require further clarification (Fig. 3). These different mechanisms may not be mutually-exclusive and may also be of different importance in different cell types or at different time-points after the proteasome is inhibited.

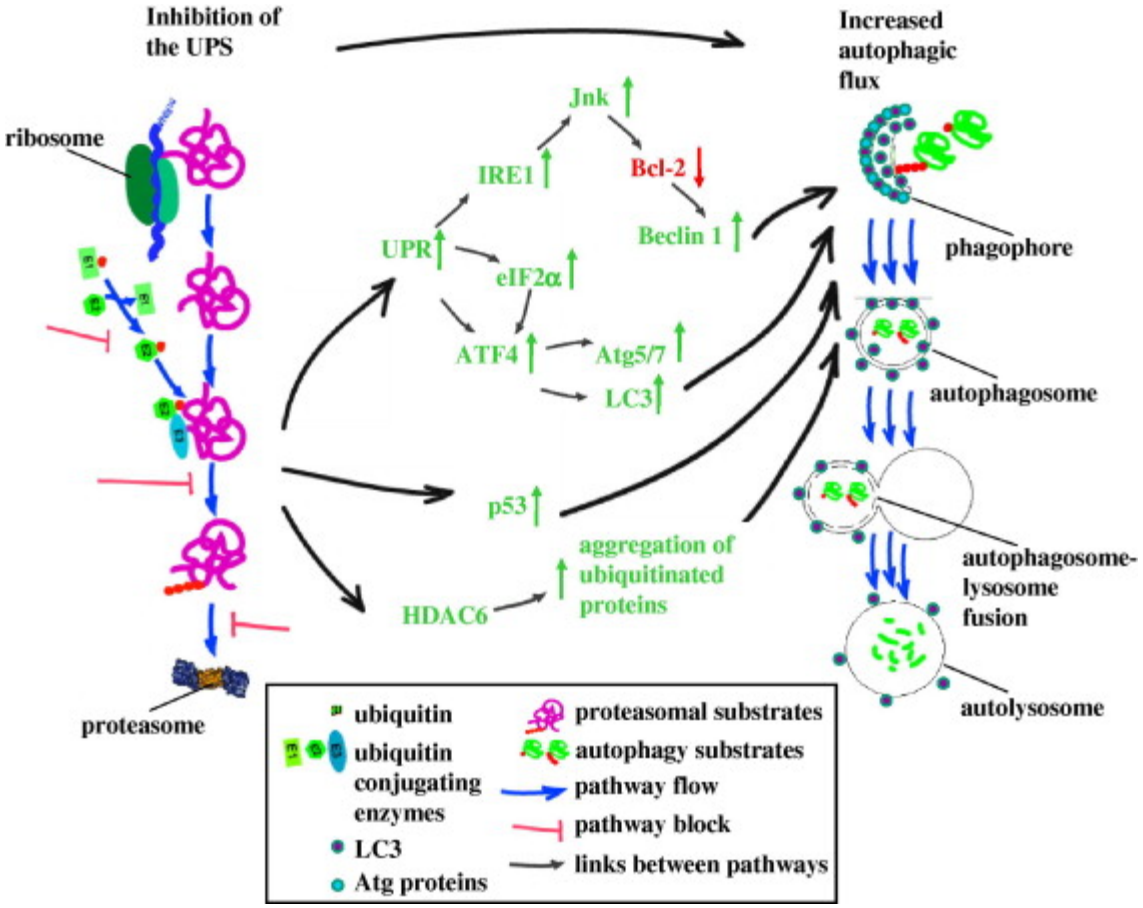

Figure 3. Possible mechanisms of compensatory autophagic upregulation following UPS inhibition. Unfolded protein response, elevated levels of p53 and the increased aggregation of ubiquitylated proteins mediated by HDAC6, have all been implicated in the cross-talk between the UPS and autophagy (Korolchuk et al. 2010).

1.2.4.3 Effect of autophagy on the UPS

Genetic studies in mice demonstrated that inactivation of autophagy by the knockout of essential autophagic genes (Atg5 or Atg7) results in the accumulation and aggregation of ubiquitylated proteins (Hara et al. 2006, Komatsu et al. 2006). One interpretation is that ubiquitylated proteins could be degraded by autophagy, although it is currently unknown whether the type of polyubiquitin chains accumulating in autophagy-deficient tissues is consistent with the proposed specificity of autophagy for K63-linked polyubiquitin chains. The extent to which autophagy contributes to the degradation of the total pool of cellular ubiquitylated proteins, or whether the accumulation of ubiquitylated autophagic substrates can alone explain the profound accumulation of ubiquitin seen in autophagy-deficient mice. Another possibility is that autophagosomal clients that initially are not ubiquitylated, remain long enough in autophagy-deficient cells to eventually become modified by ubiquitin. Finally, autophagy impairment could impact on the flux through the UPS. Indeed, some findings support the latter hypothesis. Impaired autophagy was found to cause impaired degradation of specific UPS clients (Korolchuk et al. 2009, Korolchuk et al. 2009, Qiao et al. 2009). These data suggest that the decreased UPS flux in autophagy-compromised cells was not due to impaired catalytic activity of proteasomes isolated from them. Instead, it was found that the block in the UPS function is mediated by accumulation of p62, as its knockdown rescued the levels of UPS substrates in autophagy-deficient cells. In addition, overexpression of p62 alone was sufficient to inhibit the UPS, an effect partially dependent on its UBA domain. Since p62 competes with other ubiquitin-binding proteins involved in proteasomal degradation, like p97/VCP (valosin-containing protein), for binding to ubiquitylated proteins, it was proposed that elevated levels of p62 may deny such shuttling proteins access to ubiquitylated UPS substrates (Fig. 4) (Korolchuk et al. 2009, Korolchuk et al. 2009). These findings help to explain how knockout of p62 rescues the increased levels of soluble and aggregated ubiquitylated proteins observed in autophagy-deficient tissues (Komatsu et al. 2007). Thus, p62 has been

implicated in two different, but not mutually- exclusive, mechanisms of cross-talk between the UPS and autophagy. In the physiological state, where autophagy operates at normal rates, p62 could serve to deliver ubiquitylated proteins for autophagosomal destruction (Bjorkoy et al. 2005, Pankiv et al. 2007, Kirkin et al. 2009). In contrast, in situations where autophagy becomes impaired (which occurs in a variety of pathological conditions, including certain neurodegenerative conditions, such as lysosomal storage disorders), p62 becomes a Trojan horse due to its binding (probably non-selectively because of elevated levels) to ubiquitylated proteins and preventing their delivery to the proteasome for degradation (Korolchuk et al. 2010). The lack of compensation for autophagy dysfunction by the UPS is in agreement with the fact that p62, when accumulating, oligomerizes and therefore would be too bulky to be a good substrate for the proteasome with its narrow catalytic pore. A special case of coordination between the two degradative systems comes from Goldberg and colleagues, who demonstrated that both the UPS and autophagy contribute to muscle atrophy in physiological conditions, like fasting, as well as in diseases characterized by muscle wasting (Zhao et al. 2007). In this case, coordinate upregulation of both catabolic pathways was induced by the FoxO3 transcription factor downstream of the IGF-1/PI3K/Akt signaling axis.

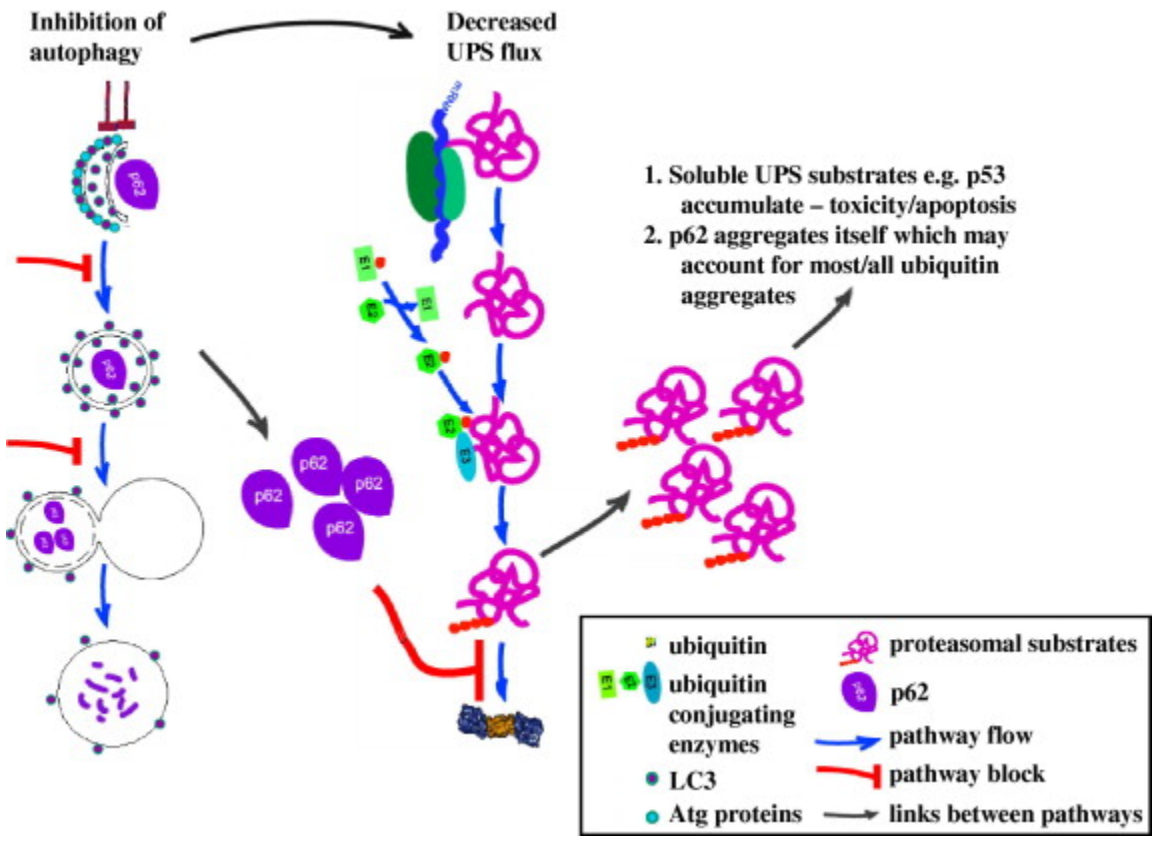

Figure 4. Inhibition of autophagy impairs the UPS function. p62, which accumulates due to autophagy blockade, binds ubiquitylated proteins and prevents their delivery to and degradation by the proteasome. Toxicity due to elevated levels of certain UPS substrates, like p53, and accumulation of ubiquitinated p62-positive aggregates are the components of the autophagic deficiency phenotype (Korolchuk et al. 2010).

1.2.5 Role of autophagy and the ubiquitin-proteasome system in neuroprotection

First studies which provided evidence for the protective role of autophagy in the context of disease was initially provided by a series of in vitro studies demonstrating that disease-causing proteins are frequently degraded by autophagy. The neuroprotective role of autophagy was provided by a series of animal studies in which impairment of the autophagy-lysosomal system was consistently found to induce neurodegeneration. Knockout of cathepsin D, a lysosomal protease highly expressed in the nervous system, caused accumulation of autophagosomes and lysosomes with accompanying neural dysfunction and degeneration (Koike et al. 2000, Koike et al. 2005, Shacka et al. 2007). The importance of autophagy in neurodegeneration was further

underscored by two studies examining conditional knockout of autophagy in murine central nervous system. Deficiency of Atg5 or Atg7, both critical proteins for autophagosome formation, caused neurodegeneration characterized by ubiquitin-positive neuropathology (Hara et al. 2006, Komatsu et al. 2006).

1.2.6 Regulation of autophagy by sphingolipids

The regulation of the delicate balance between proliferation and cell death is another important aspect where sphingolipids act as second messengers. Specifically, S1P and ceramide have proved important in the regulation of cell fate (Scarlatti et al. 2004, Taniguchi et al. 2012), however, their effects on cell fate are very different (Le Stunff et al. 2002, Lavieu et al. 2006). Both acting through autophagy, S1P is believed to promote cell survival and proliferation, whereas ceramide has been found to induce growth arrest and cell death (Ogretmen et al. 2004). S1P has been found to upregulate autophagic activity under serum-starved conditions in PC-3 prostate cancer cells. By applying small interfering RNA and dihydro-S1P, it was demonstrated that this process is regulated through S1P5-dependent pathways. In addition, mTOR signaling was inhibited upon exogenous S1P treatment (Chang et al. 2009). The role of S1P in autophagy regulation has been further investigated by manipulating its synthesis by sphingosine kinases (SK) or its degradation by S1P phosphatases (SPP) or S1P lyase (SPL). It has been shown that overexpression of SK1 in MCF-7 cells stimulates survival autophagy by increasing the formation of LC3-positive autophagosomes. In contrast to ceramide-induced autophagy in the same cell line, the SK1-induced autophagy proceeded independently of ceramide synthase activity, and was characterized by the inhibition of mTOR (independently of Akt/PKB signaling) and by the lack of Beclin 1 accumulation. Both SK1 activity and autophagy were enhanced upon nutrient starvation, resulting in cell protection from cell death and apoptotic features (Lavieu et al. 2006). In contrast, pharmacological inhibition of SK by dimethylsphingosine, the SK1 and SK2 dual inhibitor SK1-2 or the SK2- specific inhibitor ABC294640, resulted in increased autophagic features and death in A-489 kidney carcinoma cells (Beljanski et al. 2010). The autophagy induced by ABC294640 was associated with decreased levels of phospho-Akt and up-regulation

of Beclin 1, similar to the ceramide-induced autophagy described in Scarlatti *et al.*'s work (Scarlatti et al. 2004). However, the increased cytotoxicity observed in A-489 cells when combining SK inhibition and cytotoxics like sorafenib or gemcitabine was not due to enhanced autophagy, as there was no significant difference in the levels of LC3-II or Beclin 1 compared with cells treated with the individual compounds (Beljanski et al. 2011).

Concerning S1P degradation, depletion of SPP1 has been reported to promote autophagy but without leading to autophagic cell death. This was mediated by ER stress, since downregulation of the expression of two major ER stress transducers, activating transcription factor 6 (ATF6) and inositol-requiring transmembrane kinase/endonuclease (IRE1a), completely abrogated SPP1-regulated autophagy (Lepine et al. 2011). In this process, depletion of SPP1 induced Akt phosphorylation that protects cells from apoptosis; the class III PI3K/Beclin 1 complex and mTOR were not involved. Furthermore, it has been demonstrated that the autophagy induced by downregulation of SPP1 was mediated by intracellular S1P and not by secreted S1P, as treatment with exogenous S1P at concentrations that activate cell surface S1P receptors did not cause autophagy (Lepine et al. 2011).

1.2.7 Behavioral phenotyping of mouse models of neurodegeneration

Neurodegenerative disorders, such as amyotrophic lateral sclerosis (ALS), Huntington's (HD), Parkinson's (PD) and Alzheimer's diseases (AD), are characterized by the loss of structure and function of specific neuronal circuitry in the brain. As a result of this loss, behavioral symptoms occur progressively. For understanding the causes of neurodegeneration several animal models of neurodegenerative disorders have been generated and characterized. Behavioral science plays a crucial role by identifying specific symptoms in these animal models of human disorders.

Open-field test. The simplest tests of locomotor activity involve observing and recording an animal's movements around an open arena. When placed in the center of a field, a mouse will typically run to the walled edge and then explore its way around the whole arena while remaining close to the wall. Over time, as the animal habituates to the new environment and its anxiety

reduces, the mouse will increasingly venture out towards central parts of the arena before returning to the edges. Exploitation of this behavioural profile forms the basis of the study of open-field locomotor activity test in mice (Brooks et al. 2009).

In the *object placement recognition* test the mouse is placed in an enclosure where it is exposed to two objects for a defined time. The mouse is removed and later re-tested in the same environment, in which one of the two previously used objects has been moved in another part of the habitat. The time spent on exploring the object in the new location in the arena is recorded and reflects ability to remember what is new and what is old (Fig. 5 A) (Tuscher et al. 2015).

The *Morris water maze* measures spatial reference memory. Mice are trained in a circular pool filled with an opaque liquid. Distant visual cues are provided for navigation around the pool. A platform is hidden just below the water surface. Mice swim until they find the platform. There are different ways to perform the test and also many parameters to assess memory, including path length and time to find the platform (escape latency). The test can be divided into two phases, an acquisition phase followed by a reversal phase during which the platform is moved to the opposite corner (Fig. 5 B) (Gotz et al. 2008).

Contextual fear conditioning is the most basic of the conditioning procedures. It involves taking an animal and placing it in a novel environment, providing an aversive stimulus, and then removing it. When the animal is returned to the same environment, it generally will demonstrate a freezing response if it remembers and associates that environment with the aversive stimulus. Freezing is a species-specific response to fear, which has been defined as “absence of movement except for respiration.” This may last for seconds to minutes depending on the strength of the aversive stimulus, the number of presentations, and the degree of learning achieved by the subject (Fig. 5 C) (Curzon et al. 2009).

Rotarod. The rotarod was specifically designed for making automated measurements of neurological deficits in rodents (Dunham et al. 1957), and is one of the most commonly used tests of motor function in mice (Fig. 5 D). Early designs use a rotating rod of ~3 cm diameter, on which the mouse is placed and has to maintain its balance; a trip switch on the floor below is set to record the latency until the mouse falls from the rotating rod. Mice are tested on separate trials at a series of fixed speeds, or speed increases can be incorporated into a single trial by using an

accelerating version of the test (Jones et al. 1968). In accelerating versions, the range of rod rotation speeds can differ markedly between studies, but typically revolutions of the rod accelerate smoothly from 0 to 40 rpm over a 5 minute period. The accelerating test is quicker and more efficient, but it confounds motor coordination at different speeds with fatigue, whereas the fixed-speeds test provides separate data on each range of rotation speeds and is probably more sensitive (Monville et al. 2006). The fixed-speeds test has been used to demonstrate that the age of onset of transgenic phenotypes is dependent on task difficulty and the sensitivity of the test to motor symptoms (Carter et al. 1999). There are several common confounds of the rotarod test. The first is that some animals may cling to the beam, and rotate with it, rather than fall when they lose balance. This is due to some commercial models having a rod that is grooved to aid grip, but to which the mice can cling by their claws; a simple solution is to cover the rod with a layer of coarse rubber. The second confound relates to individual animals that refuse the test and simply fall as soon as they are placed on the rod. This is especially relevant in longitudinal assessments, during which the animals can learn over repeated tests that the consequences of falling are innocuous. Fortunately these animals are relatively rare and their performance is conspicuous relative to that of the other mice in the cohort, thus they can be (and need to be) excluded as ‘outliers’ in any statistical analysis. A third confound relates to mouse weight: heavy mice perform worse than light mice. Thus, genetic or lesion-induced weight loss can offset motor disability and potentially skew results. Finally, and particularly with the accelerating version of the rotarod, speed is confounded by fatigue at progressively longer latencies. However, demonstration of differential deficits at higher rotation rates in a series of fixed-speed tests (Carter et al. 1999) can be used to ensure that a more rapid fall is indeed attributable to problems with motor coordination rather than to greater susceptibility to fatigue. Despite these confounds, the rotarod remains one of the main tests of motor function in the mouse owing to its ease of use and sensitivity (Brooks et al. 2009).

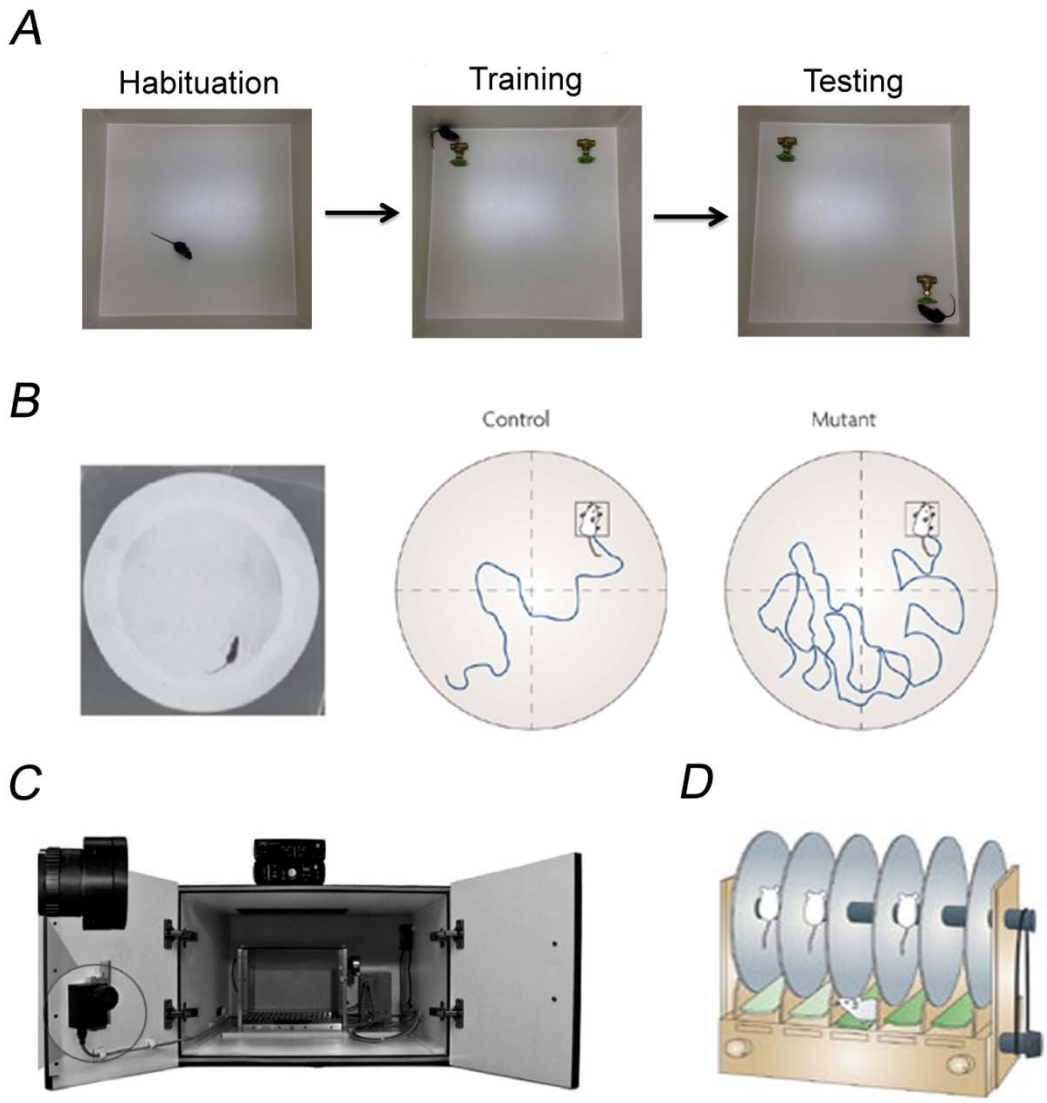

Figure 5. Tests used to asses neurodegeneration in mice. A. Object palcement recognition (modified from (Tuscher et al. 2015)), B. Morris water maze (Gotz et al. 2008), C. Contextual fear conditioning (Curzon et al. 2009), D. Rotarod (Brooks et al. 2009).

1.3 Objectives of the study

The bioactive lipid sphingosine 1-phosphate (S1P) is a component of the degradation pathway of sphingolipids that are particularly abundant in neurons. Its accumulation turned out to be neurotoxic leading to neuronal death (Hagen et al. 2009, Hagen et al. 2011). Alternatively, S1P is proposed as a neuroprotective factor that is lost early in Alzheimer pathogenesis (Couttas et al. 2014). Mice with systemic deletion of SPL exhibit a quite severe phenotype and their life expectancy is limited to only 6-8 weeks (Hagen-Euteneuer et al. 2012). Therefore, a brain-specific knockout mouse model of the enzyme responsible for irreversible S1P cleavage, S1P-lyase (SPL), was generated. The aim of this study was to clarify the role of SPL, and respectively the accumulation of S1P in the brain.

One of the objectives of the present study was to explore the impact of SPL knockout on the levels of brain lipids and hence on brain architecture and function. Note that earlier findings in primary cultured cerebellar neurons generated from mice with systemic SPL deletion resulted in a considerable accumulation of S1P and its metabolic precursor sphingosine with no changes in ceramide and sphingomyelin in brains of these mice (Hagen-Euteneuer et al. 2012).

In a recent study conducted in SPL-deficient MEFs an accumulation of APP most probably due to an impaired autophagy has been reported (Karaca et al., 29014). Thus another objective of the thesis was to investigate the involvement of SPL ablation in the autophagasom-lysosomal system and to uncover the molecular mechanism that could link SPL deficiency to neuronal autophagy. SPL links sphingolipid and phospholipid metabolism via its reaction product phosphoethanolamine (Fyrst et al. 2008). Of interest, phosphatidylethanolamine (PE) levels were shown to be decreased in neurodegeneration especially in brain regions highly affected by AD (Prasad et al. 1998). PE plays an important role in autophagosome formation and closure as it lipidates LC3-I. Thereby SPL activity might affect autophagy and hence essential physiological processes in the brain.

2. MATERIALS AND METHODS

2.1 Materials

Antibodies. Monoclonal antibodies against synapsin-1, synaptophysin, PSD95, Bassoon, SNAP25, VAMP2, GFAP, beclin-1, LC3, p62, α-synuclein, IDE, Piccolo, NCS-1, GAP-43, Munc18, and ß-Actin (8H10D10), anti synaptotagmin1 polyclonal antibody, as secondary antibodies including HRP-linked anti-rabbit and anti-mouse IgG, and fluorescent secondary antibodies (anti-rabbit IgG (H+L), $F(ab')_2$ Fragment-Alexa Fluor 488 conjugated and anti-mouse IgG (H+L), $F(ab')_2$ Fragment-Alexa Fluor 555 conjugated) were from Cell Signaling Technology (Cambridge, UK). Anti-piccolo polyclonal serum was from Synaptic Systems (Göttingen, Germany), anti-syntaxin1a polyclonal antibody from Abcam (Cambridge, UK), anti-ubiquitinylated proteins, clone FK2 (mouse monoclonal IgG1) from Millipore (Darmstadt, Germany), rabbit polyclonal anti USP14 was from Thermo Fisher (Rockford, IL, USA), Atg5 (MBL Life Science (Nagoya, Japan), LAMP-2 (University of Iowa (Iowa City, IA, USA) Cathepsin D (kind gift of Prof. Dr. Stefan Hoening, Cologne. Polyclonal anti-APP C-terminal (Eurogentec (Liege, Belgium).

Chemicals. PE, THI, Epoxomicin, Rapamycin and BAPTA-AM were purchased from Sigma-Aldrich (Darmstadt, Germany) and MG-132 from Enzo Life Sciences (Loerrach, Germany).

2.2 Mice

All animal experiments were conducted in accordance with the guidelines of the Animal Care Committee of the University of Bonn and of the CBMSO/CAM.

The *Sgpl1*$^{flox/flox}$ lines were generated as recently described. (Degagne et al. 2014) *Sgpl1*$^{flox/flox}$ mice, harbouring "floxed" exons 10-12 on both *Sgpl1* alleles were crossbred with mice expressing *nestin-Cre* transgene. Thus SPL$^{fl/fl/Nes}$ mice in which "floxed" exons are excised by *Cre* recombinase were obtained.

2.3 Neuronal cultures

Granular cells were cultured from the cerebella of 6-day-old mice as previously described. (van Echten-Deckert et al. 1997) Briefly, neurons were isolated by mild trypsinization (0.05%, w/v) and dissociated by passing them repeatedly through a constricted Pasteur pipette in a DNase solution (0.1%, w/v). The cells were then suspended in Dulbecco's Modified Eagle's Medium containing 10% heat-inactivated horse serum supplemented with 100 units/ml penicillin and 100 mg/ml streptomycin and plated onto 15 mm sterile glass coverslips placed in 6-well plates, 35mm in diameter, and precoated overnight at 37° C with 0.01 mg/ml of Poly-L-Lysin dissolved in 1 x PBS (5×10^5 cells/well). 24 h after plating, cytosine-ß-D-arabinofuranosid hydrochloride (Sigma-Aldrich, St. Louis, MO, USA) was added to the medium (4×10^{-5} M) to arrest the division of non-neuronal cells. After 10 days in culture cells were used for experiments as indicated.

Primary cultures of hippocampal neurons were prepared from embryonic day 18 (E18) Wistar rats as described in Kaech and Banker. (Kaech et al. 2006) Hippocampi were dissected and placed into ice-cold Hank's solution with 7mM HEPES and 0.45% glucose. The tissue was then treated with 0.005% trypsin (trypsin 0.05% EDTA; (Invitrogen; Life Technologies Co.) and incubated at 37 °C for 16 min and then treated with DNase (72 µg ml^{-1}; Sigma-Aldrich) for 1 min at 37°C. Hippocampi were washed three times with Hank's solution. Cells were dissociated in 5 ml of plating medium (Minimum Essential Medium supplemented with 10% horse serum and 20% glucose) and cells were counted in a Neubauer Chamber. Cells were plated into dishes pre-coated with poly-D-lysine (Sigma-Aldrich) (75.000 in a 3cm dish for ICF and 150.000 in a 3 cm dish for WB) and placed into a humidified incubator containing 95% air and 5% CO_2. The plating medium was replaced with equilibrated Neurobasal media supplemented with B27 and GlutaMAX (Gibco; Life Technologies Co.). On day in vitro (DIV) 7 the culture medium was replaced with medium without GlutaMAX. Cultures were used at 14 DIV.

2.4 Organotypic adult brain slice cultures

For hippocampal slice cultures 9 month old adult mice were used. Coronal slices of 200 µm thickness were stored in artificial cerebrospinal fluid (ACSF) gassed with carbogen until cultivated. The slices were carefully placed onto sterile inserts with 8 µm pore size membrane

(Sarstedt 83.3930.800) in 6 well plates. Slices were kept 37 ^{o}C and 5% CO_2 with 4 ml/well of the following culture medium: 50% MEM/HEPES (Gibco), 25% heat inactivated horse serum (Gibco/Lifetech, Austria), 25% Hanks' solution (Gibco), 2 mM $NaHCO_3$ (Merck, Austria), 6.5 mg/ml glucose (Merck, Germany), 2 mM glutamine (Merck, Germany), pH 7.2 (Ullrich et al. 2011). Slices were incubated for 24 h with and without PE and processed further for Western Blotting.

2.5 Lipid extraction and quantification

Lipid measurements were performed according to an established protocol using liquid chromatography coupled to triple-quadrupole mass spectrometry (LC/MS/MS) (Bode et al. 2012). Tissue samples were homogenized using the Stomacher Model 80 MicroBiomaster Blender (Seward) in 5 ml PBS after addition of C17-base sphingosine (Sph) and C15-base ceramide (Cer) as internal standards (300 pmol/sample, Avanti Polar Lipids). One ml supernatants were transferred into glass centrifuge tubes and mixed with 200 µl of 6 N hydrochloric acid and 1 ml methanol, and vigorously vortexted for 5 min in the presence of 2 ml chloroform. Aqueous and chloroform phases were separated by centrifugation for 3 min at 1900 x *g*, and the lower chloroform phase was transferred into a new glass centrifuge tube. After a second round of lipid extraction with additional 2 ml chloroform, the two chloroform phases were combined and vacuum-dried at 50 °C for 50 min using a vacuum concentrator. The extracted lipids were dissolved in 100 µl methanol/chloroform (4:1, v/v) and stored at -20 °C. Detection was performed with the QTrap triple-quadrupole mass spectrometer (ABSciex, Concord, Canada) interfaced with the 1100 series chromatograph (Agilent, Santa Clara, California, USA), the Hitachi Elite LaChrom column oven (VWR, Radnor, Pennsylvania, USA), and the Spectra System AS3500 autosampler (Thermo Separation Products). Positive electrospray ionization (ESI) LC/MS/MS analysis was used for detection of sphingosine 1-phosphate (S1P), Sph, sphingomyeline (SM), and phosphatidylcholine (PC), positive atmospheric pressure chemical ionization (APCI) for detection of Cer, hexosylcerebrosides (GalCerBr), and cholesterol (Chol), and negative ESI for detection of phosphatidylethanolamine (PE). Multiple reaction monitoring (MRM) transitions were as follows: S1P m/z 380/264, C17-S1P m/z 366/250, C17-Sph m/z 286/268, C15-Cer m/z 524/264 (positive mode) 522/266 (negative mode), C16-Cer m/z 538/264,

C18-Cer m/z 566/264, CerBr (24:1) m/z 810/264, SM (16:0) m/z 703/184, SM (18:0) 731/184, PC (34:1) m/z 760/184, PC (34:2) m/z 758/184 PE (36:2) m/z 742/281; PE plasmalogen (36:2) m/z 728/281, Chol m/z 369/161. Liquid chromatographic resolution of all analytes was achieved using a 2 x 60 mm MultoHigh C18 reversed phase column with 3 µm particle size (CS-Chromatographie Service). The column was equilibrated with 10% methanol and 90% of 1% formic acid in H_2O for 5 min, followed by sample injection and 15 min elution with 100% methanol with a flow rate of 300 µl/min. Standard curves were generated by adding increasing concentrations of the analytes to 300 pmol of the internal standard. Linearity of the standard curves and correlation coefficients were obtained by linear regression analyzes. Data analyzes were performed using Analyst 1.6 (ABSciex, Concord, Canada).

2.6 Reverse transcription and real-time PCR

Total RNA was extracted from brains using RNeasy Mini Kit (QIAGEN, Hilden, Germany), and treated with RNase-free DNase (QIAGEN) according to the manufacturer's instructions. Reverse transcription of 1 µg of total RNA was performed using the First Strand cDNA Synthesis Kit (ProtoScript II, New England BioLabs, Frankfurt am Main, Germany). The primers for real-time PCR were designed using the online tool from Life Technologies „Custom Primers - OligoPerfect™ Designer" and obtained from the same company. They are listed as follows: name: forward primer, reverse primer: bassoon: 5'TACACCGCTCTTCCTGCTCT3', 5'TGTACTCGCTGCCAGACTTG3'; synapsin-1: 5'TCCAGAAGATTGGGCAGAAC3', 5'TCAGACATGGCAATCTGCTC3'; synaptophysin: 5'AGTACCCATTCAGGCTGCAC3', 5'CCGAGGAGGAGTAGTCACCA3'; syntaxin 1: 5'GAACAAAGTTCGCTCCAAGC3', 5'ATTCCTCACTGGTCGTGGTC3'; vamp2: 5'TGACGGTTCCCATCACCTCTC3', 5'CTGTGGGGTTTGCTTTTGTT3'; psd-95: 5'TTTCTCCCACACACATTCCA3', 5'ACCTTCCACTCATGCAAACC3'; s1p-lyase: 5'TTTCCTCATGGTGTGATGGA3', 5'CCCCAGACAAGCATCCAC3'; β-actin: 5'CCACAGCTGAGAGGGAAATC3', 5'TCTCCAGGGAGGAAGAGGAT3'; 12.5 µl of Power SyBR Green (Applied Biosystems, Carlsbad, California, USA), 2 µl of each primer, 1.5 µl of cDNA, and 9 µl of H_2O were loaded into a 96 well plate and PCR performed in a 7300 Real Time PCR System (Applied Biosystems, Carlsbad, California, USA). Results were calculated using the relative C_T method. The fold

increase or decrease was determined relative to controls after normalizing to β-actin as housekeeping gene.

2.7 Western blotting and immunoprecipitation

Total brains, hippocampi or cultured neurons were homogenized twice for 2 min using metallic beads at a frequency of 20 Hz in RIPA buffer (20 mM Tris-HCl, pH 7.5, 150 mM NaCl, 1 mM EDTA, 1 mM EGTA, 1% NP-40, 1% NaDC, 2.5 mM $Na_4P_2O_7$, 1 mM b-glycerophosphate, 1 mM Na_3VO_4, 1 µg/ml leupeptin). Samples were kept on ice for 1 h followed by centrifugation at 13,000 rpm at 4°C for 1 h. The protein concentration of the supernatants was determined using the Pierce BCA protein assay kit (Thermo Scientific, Waltham, MA). Samples were stored at -20°C until use.

Proteins were immunoprecipitated from cleared lysates using primary antibodies (5 µg/ml) and protein G-conjugated sepharose (GE Healthcare, Little Chalfont, UK) for 3 hrs at 4°C. Precipitates were rinsed three times with washing buffer (50 mM Tris/HCl, pH 7.4, 500 mM NaCl, 2 mM EDTA, 0.2% Igepal) for 10 min at 4°C. Precipitates were collected by centrifugation (4,000× g, 4°C, 5 min) and eluted by incubation with SDS sample buffer (25 mM Tris/HCl, pH 6,8, 10% Glycerin, 1,5% SDS, 20 mM DTT) for 10 min at 95°C. Lysates from total brain and cell cultures were incubated with SDS sample buffer for 10 min at 95°C.

Proteins were separated by SDS-PAGE in running buffer (25 mM Tris, 192 mM glycine, 0.1% SDS) at 200 V. Transfer onto nitrocellulose membranes (Porablot NCL, Macherey-Nagel, Düren, Germany) was carried out at 4°C and 300 mA for 2 h in blotting buffer (50 mM Tris, 40 mM glycine, 0.03% SDS, 20% methanol). Membranes were blocked with 5% milk powder in TBS-Tween20 for 1 h, washed and incubated at 4°C overnight with the primary antibody. Then membranes were washed three times for 10 min and incubated for 1 h with an HRP-conjugated secondary antibody. Western Lightning Plus ECL (PerkinElmer, Waltham, MA) was used for detection, VersaDoc 5000 imaging system (Bio-Rad, Hercules, CA) for visualizing the membranes, and ImageJ program for quantification.

2.8 Electron microscopy

Mice were intracardially perfused with PBS and fixative (4% PFA and 2% glutaraldehyde in PBS). Brains were fixed in 4% PFA overnight and sectioned in 200-µm-thick slices. Hippocampal sections were postfixed in 1% osmium tetroxide (in 0.1 M cacodylate buffer), dehydrated in ethanol and embedded in Epon. Serial ultrathin sections of the CA1 region were collected on pioloform-coated, single-hole grids, and stained with uranyl acetate and lead citrate. The sections were examined with a transmission electron microscope (JEM1010, jeol, Akishima, Tokyo, Japan). CA1 neurons identified by position were sampled randomly and photographed at a magnification of x 8.000 with a CMOS 4 k TemCam-F416 camera (TVIPS, Gauting, Germany). The number of autophagic structures and lysosomes was quantified using ImageJ software (National Institute of Health, Bethesda, MD, USA) in 10 randomly selected CA1 neurons from three mice per genotype and age. The area of each cell was also calculated and the values of autophagic structures and lysosomes /µm^2 were statistically compared.

2.9 Immunocytochemistry

Coverslips with cerebellar neurons were washed with phosphate-buffered saline (PBS) and then fixed with 4% paraformaldehyde for 10 min. Then cells were permeabilized with 0.25% Triton-X100-PBS for another 10 min and blocked with 5% BSA in 0.125% Triton X-100 in PBS for 1h. After blocking cells were incubated for 1h with the primary antibody diluted in 2.5% BSA in 0.125% Triton X-100 in PBS. Following washing with 0.125% Triton X-100 in PBS, cells were incubated with a mixture of secondary antibodies conjugated to Alexa Fluor 488, and Alexa Fluor 647 Phalloidin (1:20 in PBS) (for F-actin staining), and DAPI (1:1000 in PBS) for another hour. Reagents were obtained from Cell Signaling Technology (Cambridge, UK). After washing, coverslips were mounted on glass slides and stored at 4^{o}C in the dark until analysis. The slides were imaged using an LSM 710 Axio Observer confocal laser scanning microscope (Carl Zeiss, Oberkochen, Germany).

2.10 Immunohistofluorescence

Mice were intracardially perfused with phosphate buffer saline (PBS) and 4% paraformaldehyde (PFA), fixed with 4% PFA in PBS overnight at 4^{o}C and then cryoprotected in 30% sucrose in PBS for 48 h. Next, samples were frozen in Optimal Cutting Temperature (Tissue-Tek). Sagittal sections (30 µm) were obtained with a CM 1950 Ag Protect freezing microtome (Leica, Solms, Germany). Sections were incubated with the primary antibody 72 hours at 4^{o}C in a PB 0.1 N solution containing 1% bovine serum albumin and 1% Triton X-100. After washing with blocking solution, sections were incubated with donkey Alexa-conjugated secondary antibody overnight at 4^{o}C (Molecular Probes, Eugene, OR, USA and Millipore, Billerica, MA, USA). Finally, sections were washed and mounted with Prolong Gold Antifade (Invitrogen). Images were taken with a confocal LSM710 META microscope (Carl Zeiss AG).

2.11 Proteasomal activity

Proteasomal activity was assessed using the Proteasome Activity Fluorometric Assay Kit, (BioVison, CA, USA). Proteasomal inhibitors epoxomycin and MG-132 were from Merck-Millipore (Darmstadt, Germany) and from Enzo Life Sciences (Loerrach, Germany), respectively.

2.12 THI and PE treatment in cultured neurons

SPL activity was modulated in 14DIV cultured hippocampal neurons from wt rats by addition for 3 hours (h) of 100 µM THI (SPL inhibitor) (Sigma-Aldrich), which was added from a stock prepared in DMSO. For rescue experiments with PE wt neurons were incubated for 3 h with 100 µM THI and 10 µM PE (Sigma-Aldrich). PE was added from a stock prepared in ethanol that ensured a final ethanol concentration of less than 1 % in the neuronal medium to avoid toxicity. Same amounts of DMSO or/and ethanol were added to control neuronal cultures.

2.13 mRFP-EGFP tandem fluorescent-tagged LC3 expression

Primary hippocampal neurons and cerebellar neurons were transfected with mRFP-GFP tandem fluorescent-tagged LC3 (Kimura et al. 2007) using Lipofectamine 2000 reagent (Invitrogen) on DIV 11. After 72 h, hippocampal neurons were treated with 100 µM THI or with 100 µM THI and 10 µM PE for 3 h. Finally neurons were fixed with 4 % PFA for 10 min, stained with DAPI (1/5000; Calbiochem) and analyzed in a confocal LSM710 META microscope (Carl Zeiss AG). The number of RFP-positive structures were quantified with respect to the total number of structures EGFP and RFP-positive per cell.

2.14 Behavioral Analysis

To habituate animals to the investigator, they were handled for 3 days (for approximately 2 min/animal/day) before the onset of behavioral testing. Before the onset of behavioral testing animals were kept for at least 30 min the test room to accommodate to the environment. Between trials used issues were cleaned with terralin to remove odor cues.

Open field. The test apparatus (ActiMot; TSE) was a transparent and infrared light–permeable acrylic test box (45.5 cm × 45.5 cm × 39.5 cm internal measurements). Animals were allowed to freely explore the test arena for 20 minutes. An automated tracking system (Ethovision XT; Noldus) was used to record the total distance traveled by animals.

Object placement recognition. After handling and habituation to the empty test arena, mice were subjected to 3 trials of 6-minute training session, during which they were allowed to explore freely 2 identical objects (small glass bottles) that were placed in defined locations of the test arena. Next day, a 6-minute test session was performed, during which the position of one of the objects was changed, while the position of the other remained unaltered. An automated tracking system (Ethovision XT; Noldus) was used to monitor and record the behavior of the animals. The time the animals spent exploring the object in the novel location and the known location during the test was hand-scored by an observer from the videotape by an observer blinded to the experimental conditions.

Rotarod. An accelerating rotarod (Bioseb, Vitrolles, France) was used to measure motor coordination, balance, and motor learning abilities (Jones et al. 1968). Mice were placed on the rotarod, and the rod rotations were subsequently accelerated from 4 to 40 rpm during the 5-minute trial period. Trials were terminated when animals fell off the rod or when 5 minutes had elapsed, whichever came first. Mice were given 3 trials every day with a 30 min intertrial interval, for 4 consecutive days.

Hidden version of the Morris water maze. The water maze was performed essentially as previously described (Heinen M1 2012). Each animal received 6 daily training trials in the hidden version of the Morris water maze (in blocks of 2 consecutive trials) for 7 consecutive days. Training trials were completed when mice climbed on the escape platform or when 1 minute had elapsed, whichever came first. To evaluate the accuracy with which the animals had learned the position of the escape platform, we performed a probe trial after completion of training on day 3, 5, and 7. We determined the time that mice spent searching in the target quadrant (which previously contained the escape platform) or the other quadrants during the probe trial. Additionally, we analyzed the number of crossings of the exact target location (i.e., where the platform was during training) and compared it with crossings of analogous positions in the other quadrants.

Context fear conditioning. A near infrared video fear conditioning system (Med Associates, Vermont, USA) was used to test context fear conditioning. The training session was 306 seconds total duration; 2-second, 0.75-mA shocks were delivered via the metal grid floor of the chambers after 120, 182 and 244 seconds. A single test session was given on the next day, during which animals were placed in the chamber for 300 seconds to record behavior. Time freezing and average motion were calculated with the Video Freeze® software (Med Associates). To evaluate conditioned fear, we calculated the freezing time on the test day and activity suppression ratios for each animal as activity during test/activity during test + activity during baseline.

2.15 Statistical analysis

All values are presented as means ± SEM. Student's t-test and two-way ANOVA were used for statistical analysis of the data. P values lower than 0.05 were considered significant. In the figures

asterisks indicate P values as follows: * < 0.05; ** < 0.01; *** < 0.001. The GraphPad Prism 5 software was used for statistical analysis.

3. RESULTS

3.1 Generation of a brain-specific SPL knockout mouse model

Mice in which exons 8/9 and 12/13 encoding for the binding site of the SPL cofactor pyridoxalphosphate (PLP) were flanked by *loxP* sites (*floxed, Sgpl1* $^{flox/flox}$*)* were crossbred with the nestin-Cre transgenic mouse line Nes-Cre1 in which Cre-recombinase expression is under the control of the nestin promoter (Dubois et al. 2006). Siblings expressing both, *loxP* sites and Cre-recombinase ($SPL^{fl/fl/Nes}$) exhibited a reduction of about 90 % of SPL in the brain on transcriptional and protein level (Fig. 1 A, B). The residual mRNA amounting to 10 ± 4% is most probably derived from non-neural cells devoid of an active nestin promoter (Dubois et al. 2006). Accordingly, a slight protein band was also detectable (Fig. 1 B). In contrast to systemic SPL deletion, mice lacking SPL only in neural tissue ($SPL^{fl/fl/Nes}$) have no eye-catching phenotype and their lifespan is comparable to that of their wild type littermates, thus representing a promising model to analyze the role of SPL in brain physiology.

3.2 SPL ablation causes sphingosine and S1P accumulation and PE reduction in brains of $SPL^{fl/fl/Nes}$ mice

SPL catalyzes the final step in the sphingolipid degradative pathway and is an important regulator of cellular S1P (Fyrst et al. 2008). Thus SPL on the one hand reduces S1P levels and on the other hand generates hexadecenal and ethanolamine phosphate (Serra et al. 2010). Consistent with earlier findings in primary cultured cerebellar neurons generated from mice with systemic SPL deletion (Hagen-Euteneuer et al. 2012), neural-targeted depletion of SPL resulted in a considerable accumulation of S1P (Fig. 1 C) and its metabolic precursor sphingosine (Fig. 1 D) with no changes in ceramide (not shown) and sphingomyelin (Fig. 1 E) in brains of $SPL^{fl/fl/Nes}$ mice.

Ethanolamine phosphate, one of the products of SPL, is used as a biosynthetic precursor for PE formation (Fyrst et al. 2008). It was therefore not surprising that the content of PE was reduced in brains lacking SPL activity (Fig. 1 F). The reduction of PE levels in both hippocampus and

cerebellum of SPL$^{fl/fl/Nes}$ mice was significant at all ages studied (3, 9 and 12 month-old) excluding the weaning period at which no changes between controls and SPL-deficient mice could be detected (Fig. 1 F).

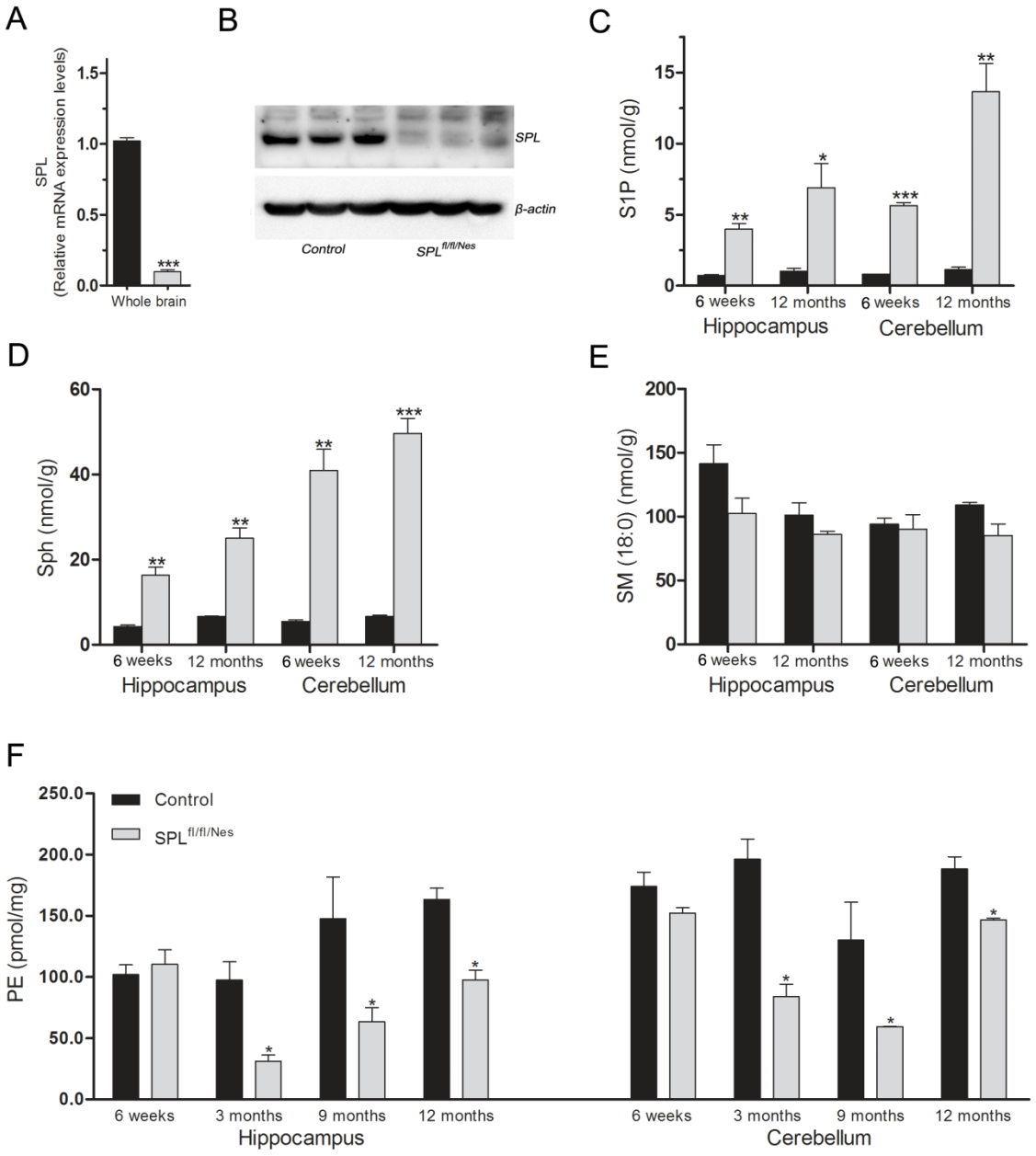

Figure 1. Brain targeted knock-down of SPL and its impact on sphingolipid and phospholipid content. SPL expression was assessed in the indicated brain domains of 6 week old mice of the indicated genotype by **A**, qRT-PCR (unpaired t test, $P < 0.0001$), **B**, Western blotting as described in the Methods section. **C-E**, Sphingolipids from the cerebellum and the hippocampus of mice at the indicated age and genotype

were determined by LC/MS/MS as described in the Methods section. Sphingosine 1-phosphate (S1P) and sphingosine (Sph) increased considerably already after 6 weeks in brains of $SPL^{fl/fl/Nes}$. Bars represent means ± SEM (n≥ 3; two -way ANOVA, $P_{S1P,h6w}$ = 0.041, $P_{S1P,h12m}$ = 0.0458, $P_{S1P,c6w}$ = 0.041, $P_{S1P,c12m}$ = 0.0458,$P_{Sph,h6w}$ =0.0326, $P_{Sph,h12m}$ =0.0284, $P_{Sph,c6w}$ =0.0326, $P_{Sph,c12m}$ =0.0284). **F**, Means ± SEM values of PE levels quantified in pmol/mg tissue by LC/MS/MS in the hippocampus and cerebellum of control and $SPL^{fl/fl/Nes}$ mice at the indicated ages (n ≥ 3; two-way ANOVA, P_{h3m} = 0.041, P_{h9m} = 0.0458, P_{h12m} =0.0326, P_{c3m} =0.0284, P_{h9m} = 0.0474, P_{h12m} =0.0471). The amount of all other lipids determined including ceramides did not change upon SPL

3.2.1 Increase in GPBP, a longer isoform of CERT, in the brain of $SPL^{fl/fl/Nes}$ mice.

Ceramide, sphingosine and S1P are metabolic interconnected (Gault et al. 2010). The accumulation of sphingolipids that are directly involved in the reaction catalyzed by SPL and the normal levels of more complex sphingolipids like ceramide made us wonder whether ceramides might be transported extracellular keeping the regular level of ceramide. The GPBP (Goodpasture antigen-binding protein) and its splice variant the CERT (ceramide transporter) are multifunctional proteins that have been found to play important roles in brain development and biology, and mediates ceramide trafficking (Hanada et al. 2003). Mencarelli et al. suggest that GPBP may be able to transport ceramide to the extracellular space (Mencarelli et al. 2010). Therefore we investigated a possible involvement of GPBP and indeed, we saw an increase in its mRNA level (Fig.2).

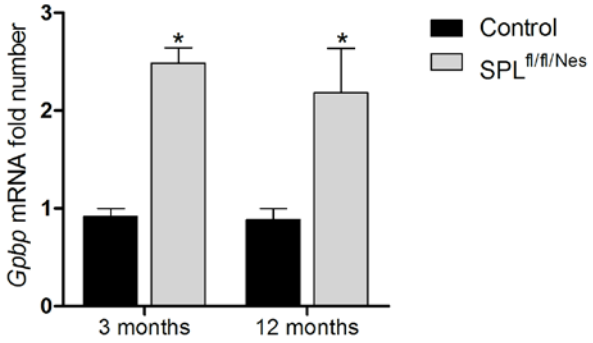

Figure 2. Up-regulation of *Gpbp* (a larger splicing variant of *Cert*) mRNA in $SPL^{fl/fl/Nes}$ mice. Real time analysis of *Gpbp* in the brain (n ≥ 3; two-way ANOVA, P_{3m} = 0.0365, P_{12m} = 0.0483).

3.3 SPL deficiency triggers accumulation of aggregate prone proteins in the brain

SPL ablation was shown to affect APP processing in MEFs (Karaca et al. 2014). Cells lacking functional SPL strongly accumulate full-length APP and it's potentially amyloidogenic C-terminal fragments (CTFs) as compared to cells expressing the functional enzyme (Karaca et al. 2014). Likewise, enhanced levels of both, full-length APP (APP-FL) and of APP-C-terminal fragment (CTFs) were detected in the brains of $SPL^{fl/fl/Nes}$ mice compared to controls (Fig. 3 A). We also found accumulation of α-synuclein in SPL-deficient brains (Fig. 3 B). The accumulation of APP-FL and of α-synuclein was already evident at early stages (3 months of age) and was maintained at all ages analysed. Moreover, we could see an increase in phospho-tau and total tau (Fig. 3 C, D).

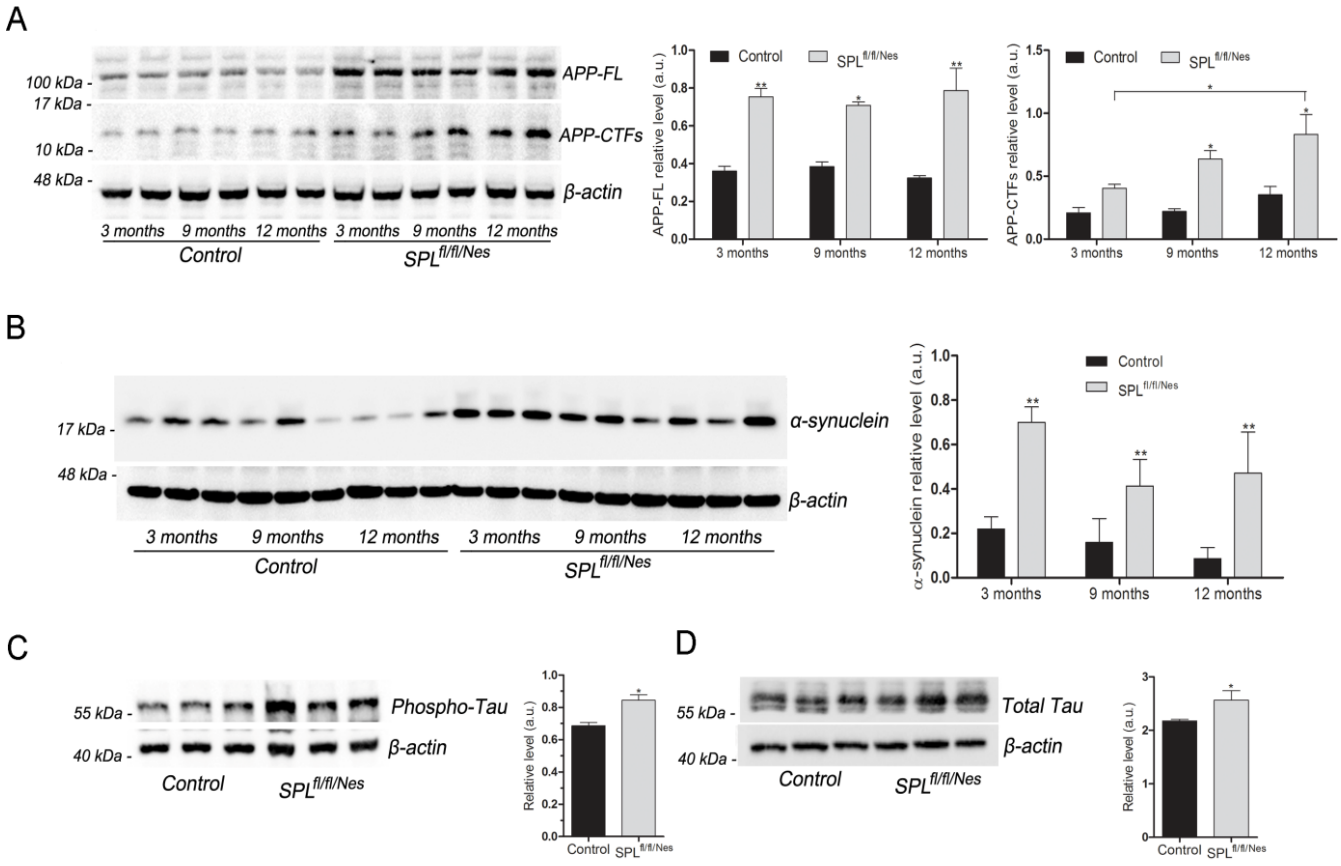

Figure 3. Accumulation of aggregate prone proteins in SPL-deficient brains. Representative Western blot images and graphs showing mean ± SEM in brain extracts of control and $SPL^{fl/fl/Nes}$ mice of the indicated ages for: **A**, APP-FL (full length) and APP-CTFs (C-terminal fragments) ($n \geq 3$; two -way ANOVA, $P_{genotype,\ APP\text{-}FL} = 0.0034$, $P_{time,APP\text{-}CTFs} = 0.0453$, $P_{genotype,APP\text{-}CTFs} = 0.0359$). **B,** α-synuclein ($n \geq 3$;

two-way ANOVA, $P_{genotype}$ = 0.0050). **C,** Western blot analysis of phosphorylated tau (unpaired t test, P = 0.0476) and **D**, total tau in the 12-month-old mice (unpaired t test, P = 0.0483).

3.3.1 Autophagy alterations in the brains of SPL$^{fl/fl/Nes}$ mice

Impairment of autophagy has been implicated in the pathogenesis of neurodegenerative disorders by contributing to the accumulation of aggregate prone proteins (Komatsu et al. 2006). This is the case of APP derived amyloidβ, α-synuclein and of tau protein, which play critical roles in the pathogenesis of AD, Parkinson's disease (PD) and taupathies (Recchia et al. 2004).

There is convincing experimental evidence for the essential role of PE in the regulation of autophagy. (Rockenfeller et al. 2015) Therefore, we investigated whether and how autophagy is affected in brains with neural targeted SPL deletion. First, levels of different autophagic markers were assessed in control and SPL$^{fl/fl/Nes}$ mice brains at different ages. We found increased expression of beclin-1, which is involved in the initiation of autophagosome formation, thus suggesting an elevation of autophagic activity (Fig. 4 A). However, the conversion of LC3-I into LC3-II was considerably hampered in the absence of SPL activity suggesting an impairment of the autophagic flux (Fig. 4 B). Accordingly, the specific autophagic substrate p62 was significantly increased in SPL$^{fl/fl/Nes}$ brains (Fig. 4 C). Electron microscopy analysis in the hippocampus of control and SPL$^{fl/fl/Nes}$ mice of different ages indicated an early (already evident at 3 months of age) and significant decrease of autophagolysosome-like structures in SPL-deficient neurons (Fig. 5 A). These were characterized by electron dense material inside vacuoles of heterogeneous size engulfed by a double membrane. In contrast, the number of phagophore-like structures consisting of curved but unclosed double membranes was increased upon SPL deficiency (Fig. 5 A). These data suggested a block in autophagosome formation. To further analyze this point we performed immunofluorescence analysis of LC3 in hippocampal tissue. LC3 staining in control mice showed a preferential punctate distribution consistent with the incorporation of the protein in autophagosomes as LC3-II (Fig. 5 B). In contrast, LC3 staining in the hippocampus of SPL$^{fl/fl/Nes}$ mice showed a diffuse, less punctated, pattern (Fig. 5 B). This supports the enhanced presence of LC3 in the cytosol as LC3-I and is consistent with the reduced LC3-II/LC3-I ratio evidenced by Western blot (Fig. 4 B).

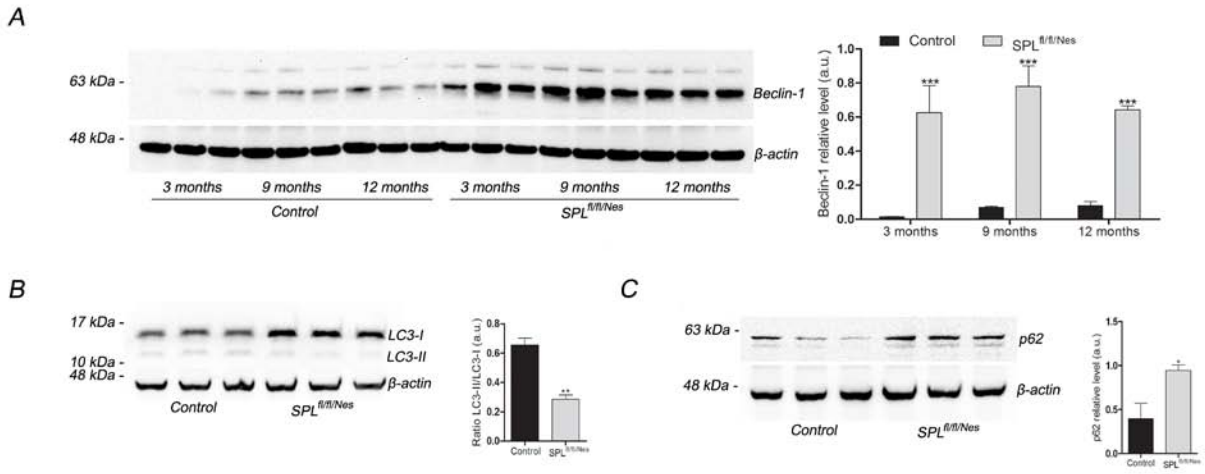

Figure 4. Autophagy is altered in SPL-deficient brains. A, B, C, Western blots and graphs showing mean ± SEM in brain extracts from control and $SPL^{fl/fl/Nes}$ mice for: **A**, Beclin-1 at the indicated ages ($n \geq 3$; two-way ANOVA, $P_{genotype} = 0.0004$), **B**, LC3-I and LC3-II at 12 months of age ($n \geq 3$; unpaired Student's *t* test, $P_{LC3} = 0.0025$) and **C**, p62 at 12 months of age ($n \geq 3$; unpaired Student's *t* test, $P_{p62} = 0.0412$).

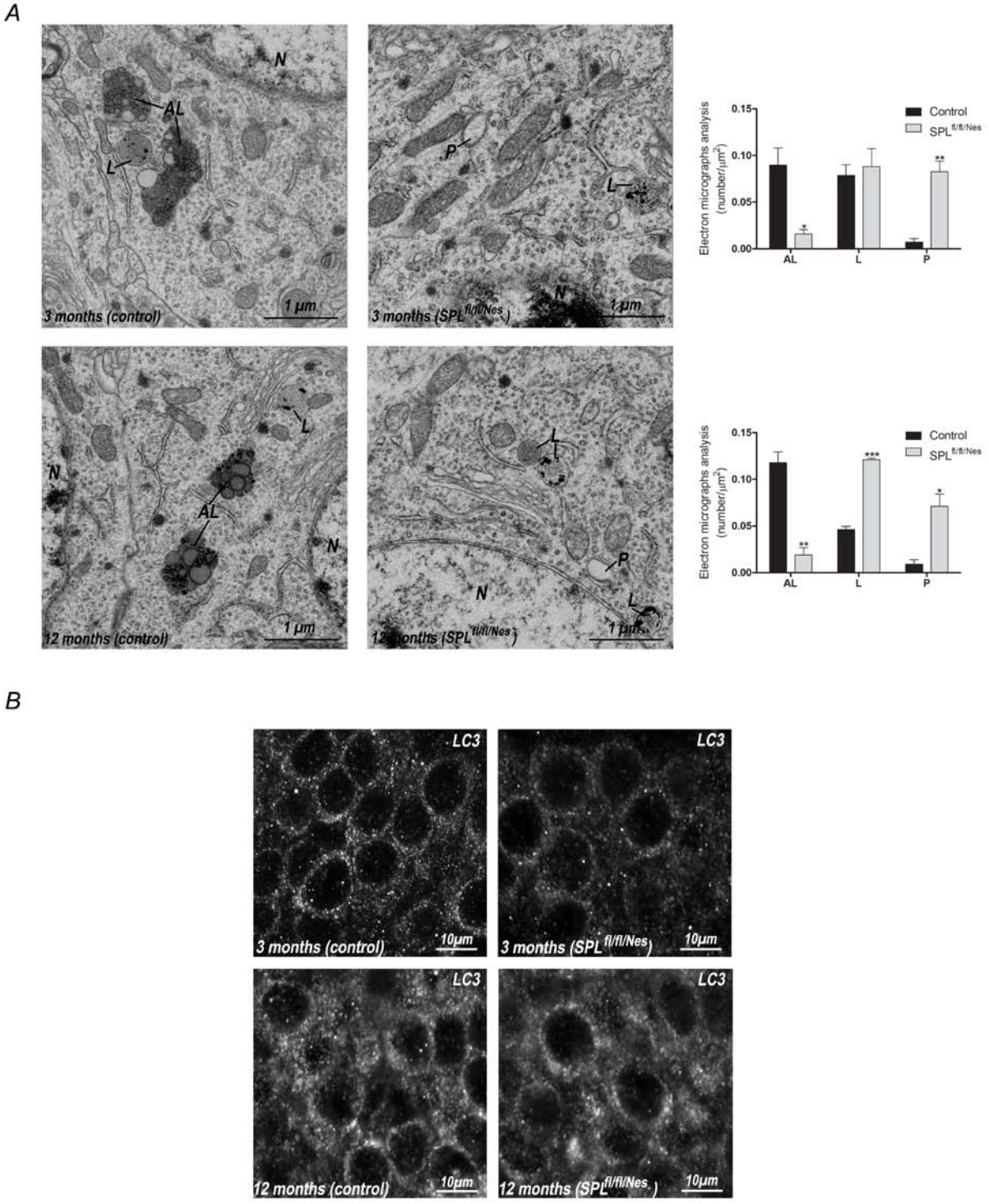

Figure 5. Autophagy morphology is changed in SPL-deficient brains. A, Electron micrographs from CA1 hippocampal neurons of control and $SPL^{fl/fl/Nes}$ mice showing autophagolysosome-like structures (AL), lysosomes (L), and phagophore-like structures (P) (unpaired Student's *t* test, $P_{AL,3m} = 0.0177$ $P_{P,3m} = 0.0031$, $P_{AL,12m} = 0.0021$, $P_{L,12m} < 0.0001$, $P_{P,12m} = 0.0115$). **B**, Representative images of

immunofluorescence analysis of the CA1 hippocampal brain region in control and SPL$^{fl/fl/Nes}$ mice of 3 or 12 months of age using the anti-LC3 antibody.

3.3.2 Lysosomal up-regulation in the brain of SPL$^{fl/fl/Nes}$ mice

Autophagy is intimately connected with lysosomal degradation. Thus, fusion of autophagosomes and lysosomes constitutes the final step of cargo degradation in the autophagic pathway. To assess whether lysosomal alterations exist upon SPL deficiency we first analysed these organelles by electron microscopy. This analysis revealed an increase in lysosome number in the hippocampus of SPL$^{fl/fl/Nes}$ mice compared to control mice that was especially significant at 12 month of age (Fig. 5 D). Biochemical analysis also showed a considerably elevated expression of the lysosome-associated membrane protein-2 (LAMP-2) in brains of SPL$^{fl/fl/Nes}$ mice, which was evident already at 3 months of age and was sustained along aging (Fig. 6 A). We next analysed the expression of the lysosomal protease cathepsin D (Bankowska et al. 1997). Both, the intermediate and active forms of this protease were significantly increased in SPL$^{fl/fl/Nes}$ mice at all ages (Fig. 6 B). However, the ratio active/intermediate form of cathepsin D reveals an absolute increase of active cathepsin in SPL$^{fl/fl/Nes}$ mice brains only in the oldest mice (12 months) analysed.

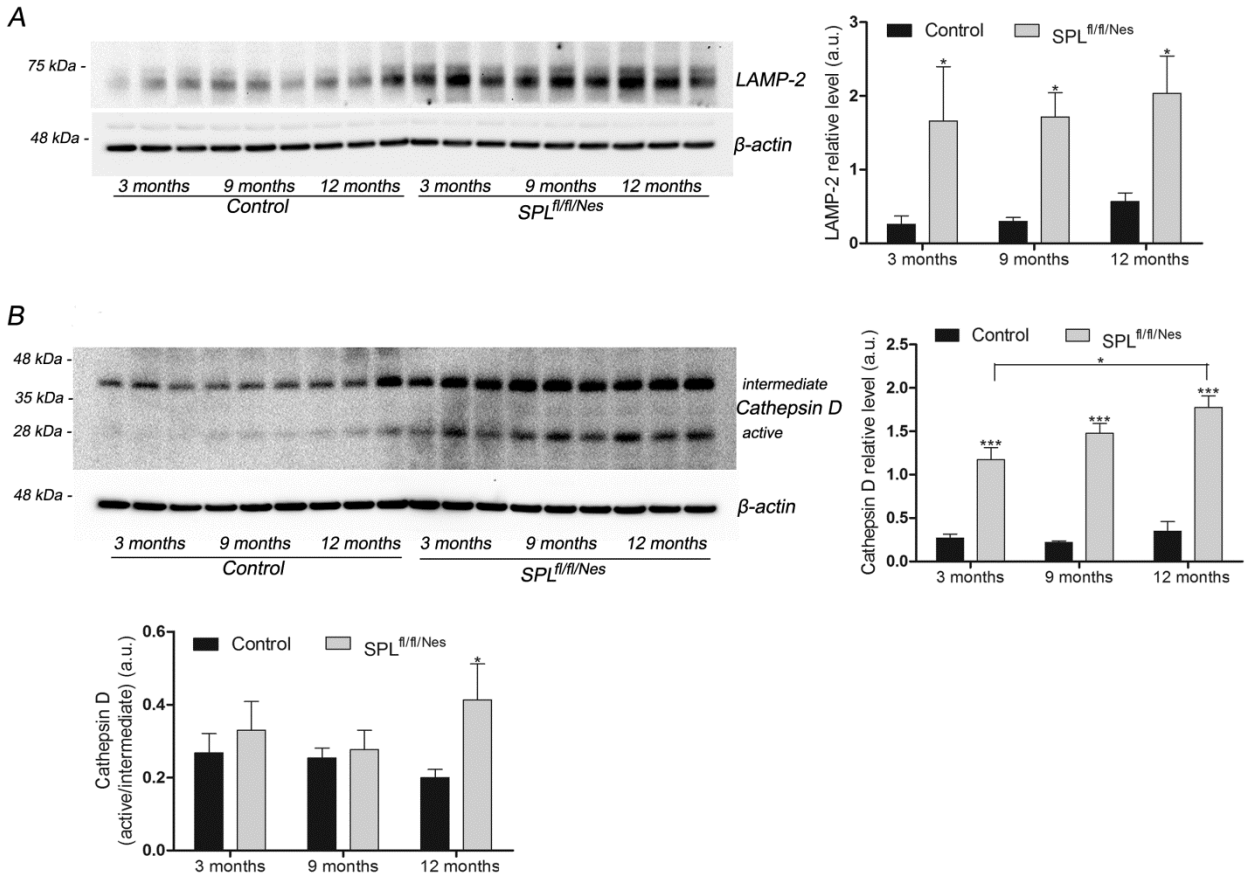

Figure 6. Up-regulation of lysosomal markers in SPL-deficient brains. Representative Western blot images and graphs showing mean ± SEM in brain extracts from control and $SPL^{fl/fl/Nes}$ mice for: **A**, LAMP-2 ($n \geq 3$; two-way ANOVA, $P_{3m} = 0.0197$, $P_{9m} = 0.013$, $P_{12m} = 0.0481$) and **B**, Cathepsin D (with indication of intermediate and active variants) ($n \geq 3$; two-way ANOVA, total Cathepsin D, $P_{time} = 0.0497$, $P_{genotype} < 0.0001$, and Cathepsin D active/intermediate, $P_{12m} = 0.0455$).

3.3.3 Autophagic flux is blocked at initial stages upon SPL deficiency

The biochemical analysis showing diminished LC3-II/LC3-I ratio but increased levels of Beclin-1 and p62 in SPL deficient mouse brains, together with reduced autophagolysosome-like but increased phagophore-like structures detected by electron microscopy (Fig. 4, 5), suggested a blockage in the autophagic flux at the initial stages. To gain further insight on autophagy flux we moved to the *in vitro* analysis in neuronal cultures from control and $SPL^{fl/fl/Nes}$ mice in which we expressed the EGFP-mRFP-LC3 construct. This tandem fluorescent-tagged autophagosomal marker in which LC3 was engineered with both red-fluorescent protein (mRFP) and green-fluorescent protein (EGFP) allows the labelling of autophagosomes in yellow (merged green

EGFP and red mRFP fluorescences), whereas autophagolysosomes appear red only as acidification after autophagosome–lysosome fusion quenches EGFP fluorescence (Kimura et al. 2007). Quantification of autophagolysosomes (red only structures) revealed a significant reduction in SPL-deficient neurons compared to controls (Fig. 7 A). We also employed a parallel approach in neurons in which SPL had been pharmacologically inhibited. THI was previosly known not to inhibit SPL *in vitro* either in cell-free or cell-based systems. A reason of this was that the *in vitro* experimental conditions were not suitable for the evaluation of SPL inhibition (Ohtoyo et al. 2015). A key factor might be the coenzyme pyridoxal 5'-phosphate (PLP), which is an active form of vitamin B6 that can be found in excess in culture media leading to the activation of SPL (Ohtoyo et al. 2015). Consistent with the observations made in the brains of $SPL^{fl/fl/Nes}$ mice, the treatment of 14 days *in vitro* hippocampal neurons from wild-type (wt) rats with the SPL inhibitor THI resulted in higher expression levels of the autophagy initiation protein Atg5-Atg12 and in diminished LC3-II/LC3-I ratio (Fig. 7 B). We next expressed the construct EGFP-mRFP-LC3 in wt cultured hippocampal neurons in which SPL was pharmacologically inhibited with THI and observed a significant reduction of autophagolysosomes in THI treated compared to non-treated cultured neurons (Fig. 7 C). These results are consistent with SPL inhibition blocking autophagic flux at early stages thus preventing the fusion of autophagosomes and lysosomes.

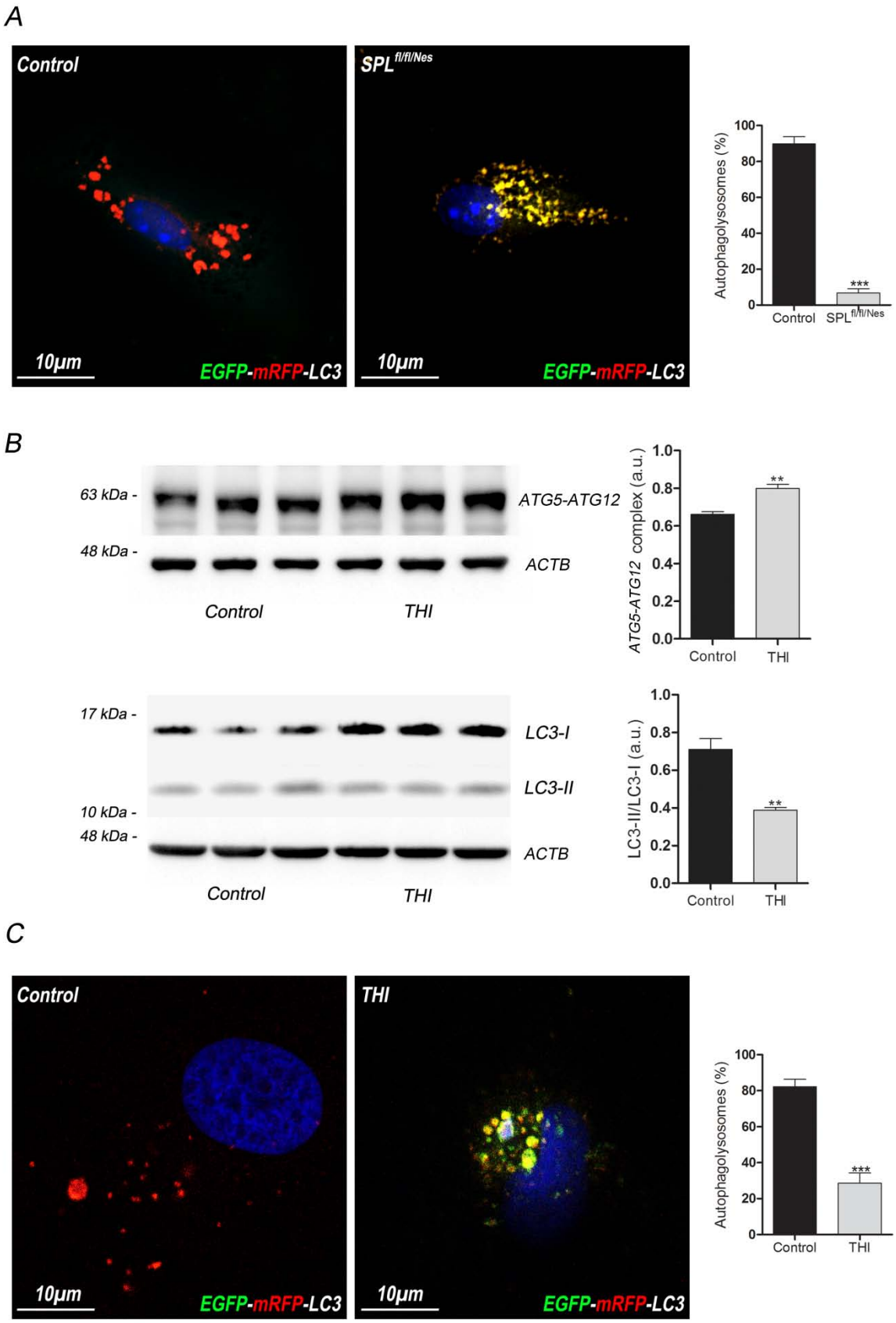
A
Control
SPL fl/fl/Nes
10μm
EGFP-mRFP-LC3
Autophagolysosomes (%)
100
80
60
40
20
0
***
Control
SPL fl/fl/Nes
B
63 kDa -
ATG5-ATG12
48 kDa -
ACTB
Control
THI
ATG5-ATG12 complex (a.u.)
1.0
0.8
0.6
0.4
0.2
0.0
**
17 kDa -
LC3-I
LC3-II
10 kDa -
48 kDa -
ACTB
LC3-II/LC3-I (a.u.)
C
Control
THI

Figure 7. Genetic and pharmacological inhibition of SPL impairs autophagy flux in cultured neurons. **A, C,** Images showing the fluorescence associated to mRFP-EGFP-LC3 construct expressed in cultured neurons from $SPL^{fl/fl/Nes}$ and control mice **(A)** (unpaired Student's *t* test, $P < 0.0001$) and in cultured hippocampal neurons from wt rats treated or not with THI **(C)** (unpaired Student's *t* test, $P < 0.0001$). DAPI staining indicates cell nuclei in blue. Graph shows mean ± SEM of the percentage of red structures corresponding to autophagolysosomes with respect to the total number of structures (red and yellow) per cell (n=20 cells in each of two different cultures) **B**, Representative Western blot images and graphs showing mean ± SEM in extracts from cultured hippocampal neurons from wt rats treated or not with THI for the ATG5-ATG12 complex (unpaired Student's *t* test, $P = 0.0067$) and for LC3 (unpaired Student's *t* test, $P = 0.0063$).

3.3.4 PE restores autophagic flux and control levels of p62, APP and α-synuclein in cultured neurons with pharmacological or genetic inhibition of SPL

We showed above that ablation of SPL decreases the levels of PE in the brain. Since PE is essential for the conversion of LC3-I into LC3-II, and thus for autophagosome formation, we checked whether this lipid was able to rescue autophagic flux in SPL-deficient neurons. As depicted in Figure 8 A addition of PE to cultured neurons derived from $SPL^{fl/fl/Nes}$ mice indeed restored the conversion of LC3-I into LC3-II and the amount of p62 to control levels. This was also the case in cultured neurons derived from wt rats treated with THI and PE (Fig. 8 B). In addition, PE supplementation reestablished the autophagy flux in EGFP-mRFP-LC3 expressing wt neurons in which SPL was pharmacologically inhibited by THI as evidenced by the enhanced number of red structures corresponding to autophagolysosomes (Fig. 8 C). Finally, PE addition prevented the accumulation of APP and of α-synuclein levels in cultured neurons from $SPL^{fl/fl/Nes}$ mice as determined by Western blot (Fig. 8 D).

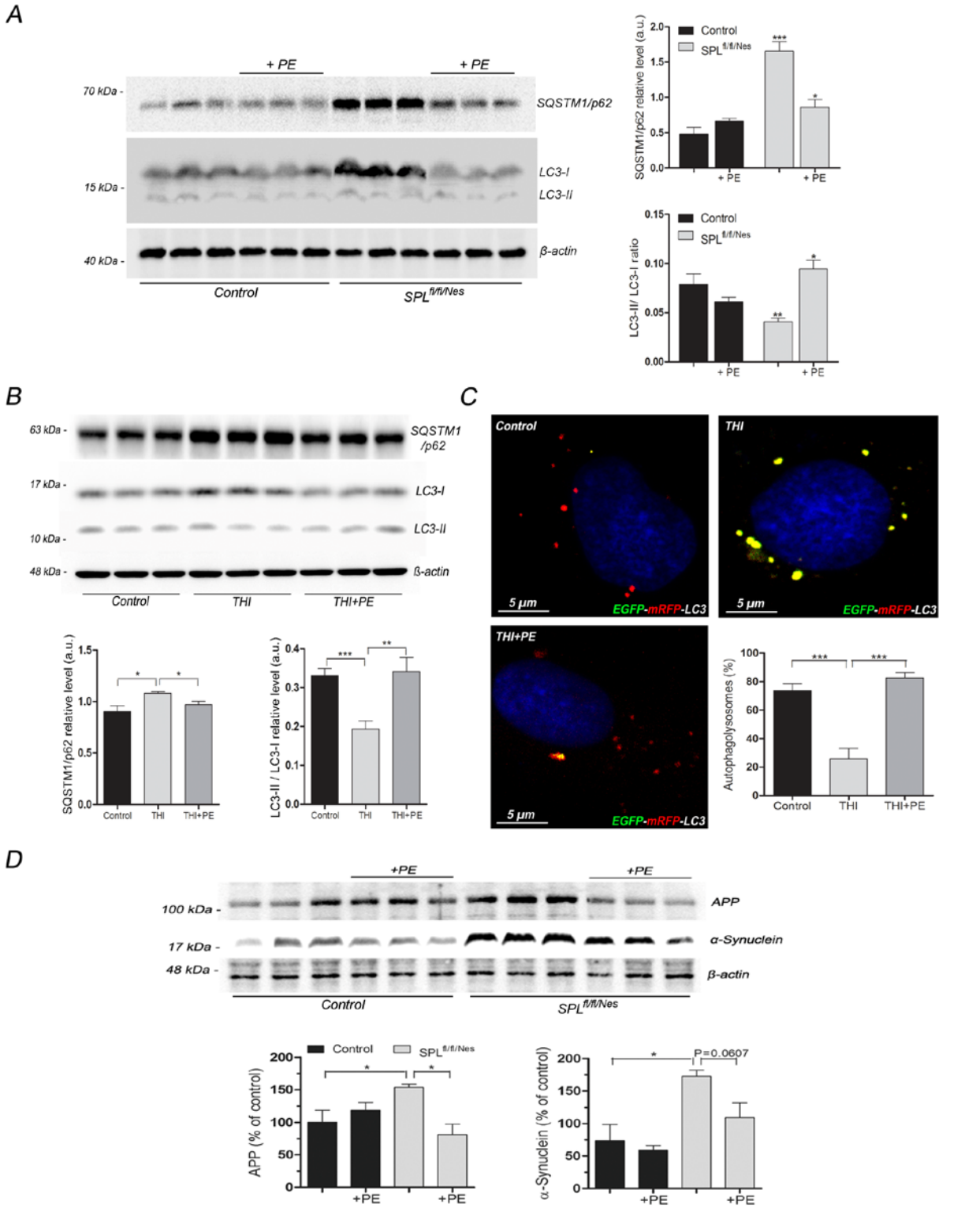

Figure 8. PE restores autophagic flux and prevents accumulation of APP and α-synuclein in SPL-deficient neurons. A, Representative Western blot images for LC3 and p62 and graphs showing mean ± SEM in extracts from cultured neurons treated or not with PE from: **A**, control and $SPL^{fl/fl/Nes}$ mice ($n \geq 3$;

two-way ANOVA, $P_{LC3,genotype} = 0.0072$, $P_{LC3,treatment} = 0.0293$, $P_{p62,genotype} = 0.0001$, $P_{p62,treatment} = 0.0158$); **B,** wt rats none treated (control), or treated with THI in the absence or presence of PE ($n \geq 3$; one-way ANOVA, $P_{LC3,THI} = 0.0005$, $P_{LC3,THI+PE} = 0.0056$, $P_{p62,THI} = 0.0112$, $P_{p62,THI+PE} = 0.0113$). **C**, Images showing the fluorescence associated to mRFP-EGFP-LC3 construct expressed in cultured neurons from wt rats none treated (control) or treated with THI in the absence or presence of PE. DAPI staining indicates cell nuclei in blue. Graph shows mean value ± SEM of the percentage of red structures corresponding to autophagolysosomes with respect to the total number of structures (red and yellow) per cell (n=20 cells in each of two different cultures) (one-way ANOVA, $P_{THI} < 0.0001$, $P_{THI+PE} < 0.0001$). **D,** Representative Western blot images for APP and α-synuclein and graphs showing means ± SEM values in extracts from cultured neurons from control and $SPL^{fl/fl/Nes}$ mice treated or not with PE ($n \geq 3$; one-way ANOVA, $P_{APP} = 0.0304$, $P_{syn} = 0.0204$).

3.3.4.1 PE restores control levels of p62 and LC3 in adult hippocampal slice cultures from $SPL^{fl/fl/Nes}$ mice

In vitro cell culture models are important in neuroscience research, but organotypic brain slices are found to be a potent model very close to the *in vivo* situation. Therefore, we prepared hippocampal slices and we incubated them with PE. The same results like in the neuronal cultures were obtained. PE could re-establish SQSTM1/p62 and LC3 to control levels in the $SPL^{fl/fl/Nes}$ slices (Fig. 9).

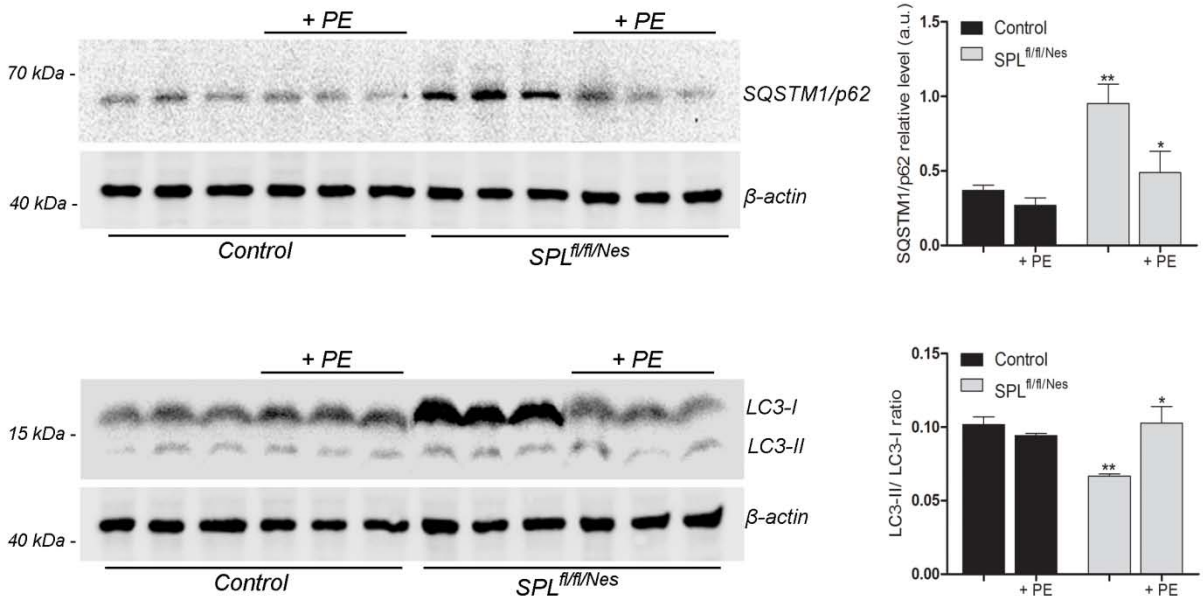

Figure 9. Ex vivo PE treatment of hippocampal slices re-establish autophagic markers in $SPL^{fl/fl/Nes}$ mice. Representative Western blot images for SQSTM1/p62 and LC3, and graphs showing mean ± SEM

in extracts from hippocampal slice cultures treated or not with PE from control and SPL$^{fl/fl/Nes}$ mice ($n \geq 3$; two-way ANOVA, $P_{p62,genotype} = 0.0041$, $P_{p62,treatment} = 0.0227$, $P_{LC3,genotype} = 0.0031$, $P_{LC3,treatment} = 0.0446$).

3.3.5 Impaired autophagy in SPL-deficient neurons is mTOR independent

Nutrient starvation induces autophagy in eukaryotic cells through inhibition of mTOR (mammalian target of rapamycin) protein kinase (Jung et al. 2010). Rapamycin binds to a domain separate from the catalytic site to block a subset of mTOR functions (Ballou et al. 2008). We observed that the treatment of Rapamycin has no effect on the neuronal cultures from SPL $^{fl/fl/Nes}$ mice, although in the neuronal cultures form control mice we could see an increase in autophagy illustrated by the increase in LC3 and decrease of SQSTM1/p62 levels (Fig. 10).

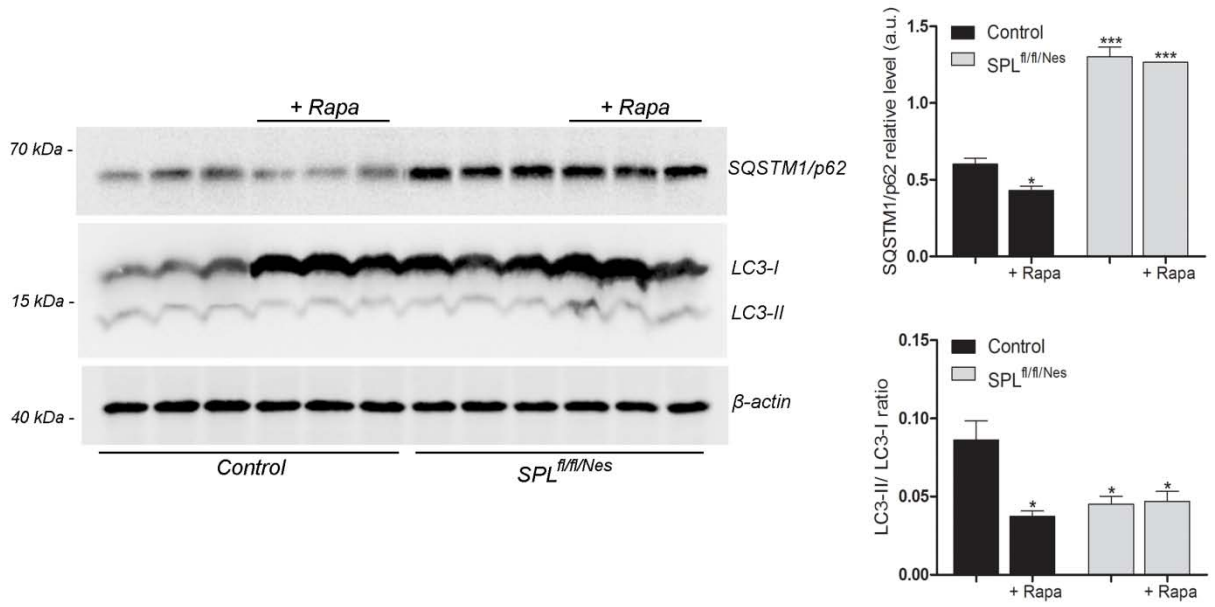

Figure 10. Rapamicyn stimulated autophagy could not save impaired autophagy in SPL$^{fl/fl/Nes}$ cultured neurons. Representative Western blot images for SQSTM1/p62 and LC3, and graphs showing mean ± SEM in extracts from neuronal cultures treated or not with 0.5 μM Rapamycin for 24h from control and SPL$^{fl/fl/Nes}$ mice ($n \geq 3$; two-way ANOVA, $P_{p62,genotype} < 0.0001$, $P_{p62,treatment} = 0.0174$, $P_{LC3,genotype} = 0.0105$, $P_{LC3,treatment} = 0.0151$).

3.4 Altered presynaptic morphology in hippocampal CA1 region of SPL$^{fl/fl/Nes}$ mice

Based on previous results on S1P neurotoxicity (Hagen et al. 2011), we tested whether brains of SPL$^{fl/fl/Nes}$ mice exhibit neuronal loss. In a first straight forward approach a neuron-specific nuclear protein (NeuN) immunohistochemical staining of coronal brain sections was performed. Although we did not observed massive neuronal loss (Fig. 11 A), closer quantitative examination of brain sections revealed a reduced thickness of the dentate gyrus in SPL$^{fl/fl/Nes}$ mice (Fig. 11 B). Neuropatholological processes are often accompanied by reactive gliosis or reactive astrogliosis, a term coined for the morphological and functional changes seen in astroglial cells/astrocytes (Pekny et al. 2014). We therefore performed immunohistochemical stainings using GFAP (glial fibrillary acidic protein) antibody and detected an age-dependent increase of reactive astrogliosis in the cortex of SPL$^{fl/fl/Nes}$ mice (Fig. 11 C). Western immunoblotting confirmed an age-dependent increase of GFAP, indicative for reactive astrogliosis in SPL-deficient brains (Fig. 11 C). These gross irregularities in the hippocampal region was further investigated by Dr. Oleg Shupliakov at the subcellular morphology of asymmetric (excitatory) synapses in the hippocampal CA1 region in SPL$^{fl/fl/Nes}$ mice (Mitroi et al. in press). Analysis of ultrathin sections revealed a significant decrease in number and density of synaptic vesicles in nerve terminals from SPL$^{fl/fl/Nes}$ mice compared to controls (Mitroi et al. in press).

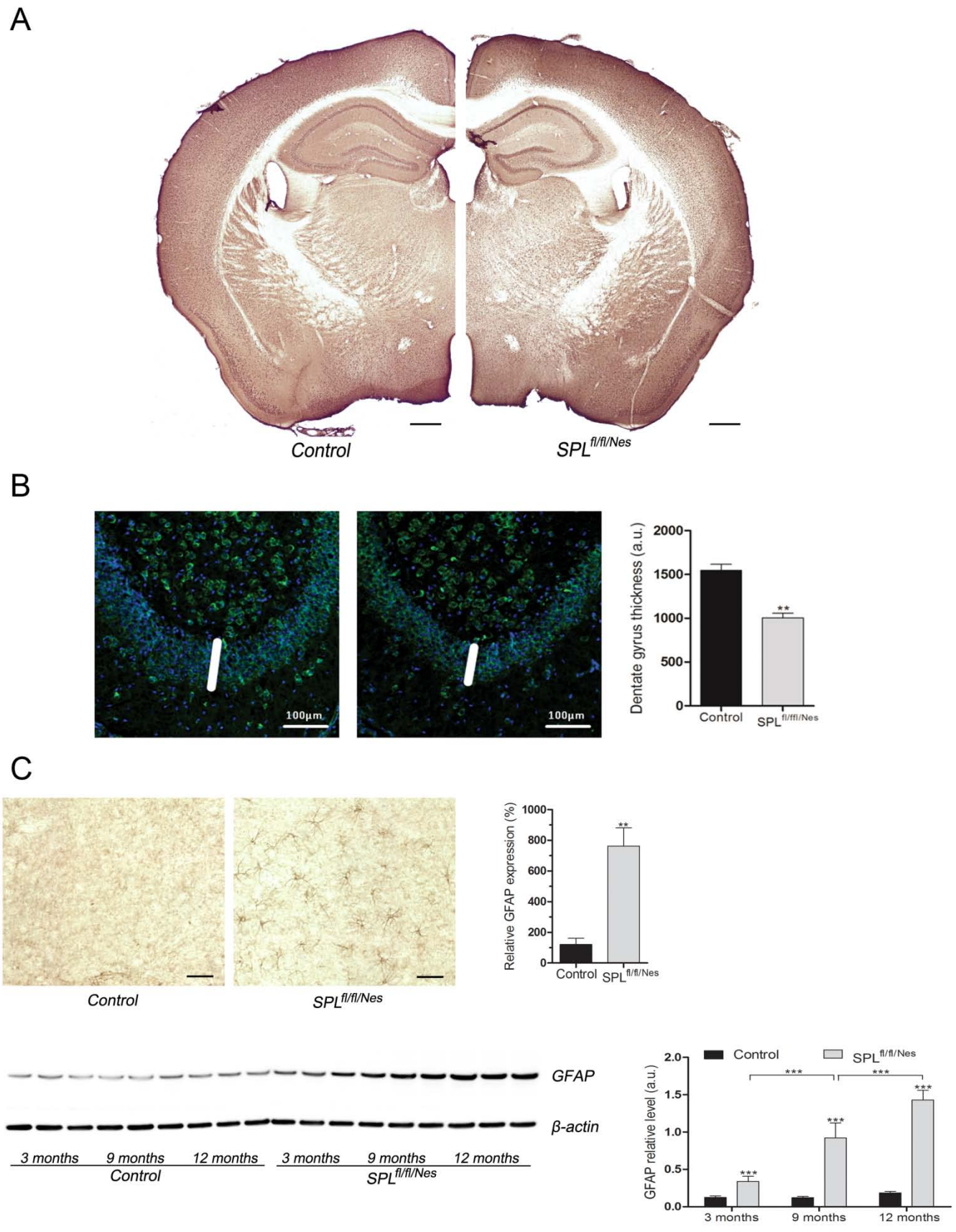
A
Control
SPL fl/fl/Nes
B
100µm
100µm
Dentate gyrus thickness (a.u.)
2000
1500
1000
500
0
**
Control
SPL fl/fl/Nes
C
Control
SPL fl/fl/Nes
Relative GFAP expression (%)
1000
800
600
400
200
0
**
Control
SPL fl/fl/Nes
GFAP
β-actin
3 months
9 months
12 months
3 months
9 months
12 months
Control
SPL fl/fl/Nes
GFAP relative level (a.u.)
2.0
1.5
1.0
0.5
0.0
Control
SPL fl/fl/Nes
***
***
***
***
***
3 months
9 months
12 months

Figure 11. T**he impact of SPL ablation on brain morphology**. **A**, Neuron-specific nuclear protein (NeuN) immunohistochemistry of coronal brain sections from 18-month-old control and $SPL^{fl/fl/Nes}$ mice (4 animals per group). Scale bar, 500 µm. **B**, Dentate gyrus from 6-month-old control and $SPL^{fl/fl/Nes}$ mice (3 animals per group) stained with DAPI (blue) and Nissl (green) (unpaired t test, P = 0.0014). **C,** Immunohistochemical staining of 18-month-old mice (unpaired t test, P = 0.0076) and western blot analysis of control and $SPL^{fl/fl/Nes}$ mice of the indicated age with anti-GFAP (glial fibrillary acidic protein) antibody reveals reactive astrogliosis in the cortex of $SPL^{fl/fl/Nes}$ mice (two-way ANOVA, $P_{genotype} < 0.0001$; $P_{time} = 0.0005$). Scale bar, 50 µm.

3.4.1 Altered expression of presynaptic proteins in $SPL^{fl/fl/Nes}$ mice

Next, we aimed to identify the molecular mechanism underlying the observed alterations in synaptic morphology in SPL-deficient mice. First we assessed whether the reduced number of synaptic vesicles or/and sphingosine which has been shown to facilitate SNARE complex assembly and to activate synaptic vesicle exocytosis (Darios et al. 2009) is also reflected in the expression of presynaptic proteins. We found that in hippocampi as well as in cultured cerebellar neurons of $SPL^{fl/fl/Nes}$ mice the expression of the presynaptic markers Bassoon and Synapsin-1 as well as the SNARE-proteins syntaxin and VAMP2 and the major synaptic vesicle protein synaptophysin was significantly decreased (Fig. 12 A-E). However, the expression of other presynaptic proteins including synaptotagmin, piccolo, SNAP25, MUNC18 and NCS1 was not affected (Fig. 13 A-E). The expression of the post-synaptic marker PSD-95 (Fig. 12 F) and other proteins including IDE (insulin degrading enzyme) (Fig. 13 F) and GAP-43 (Fig. 13 G) was not affected in $SPL^{fl/fl/Nes}$ mice. Similar results were obtained in cultured cerebellar neurons of $SPL^{fl/fl/Nes}$ mice (Fig. 12 G-H).

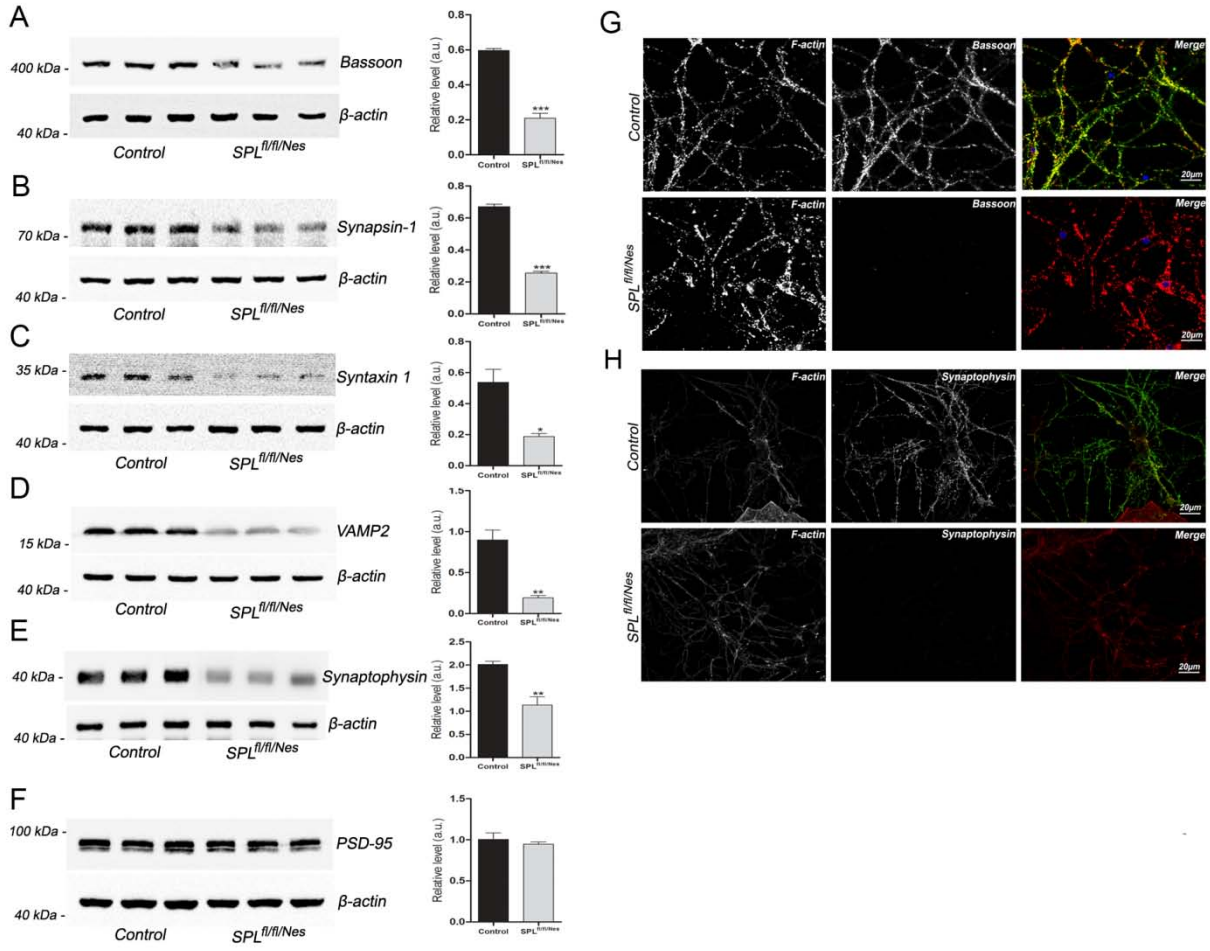

Figure 12. Expression of presynaptic proteins is reduced in SPL$^{fl/fl/Nes}$ mice. Protein amounts were assessed by (**A – F**) immunoblotting , (unpaired t test, $P_{Bassoon} = 0.0002$, $P_{Synapsin\text{-}1} < 0.0001$, $P_{syntaxin\ 1} = 0.0157$, $P_{VAMP2} = 0.0048$, $P_{Synaptophysin} = 0.0099$). Immunostaining of the presynaptic marker proteins (**H**) Bassoon and (**I**) synaptophysin in cerebellar granule cells after 2 weeks in culture. F-actin (red), bassoon and synaptophysin (green).

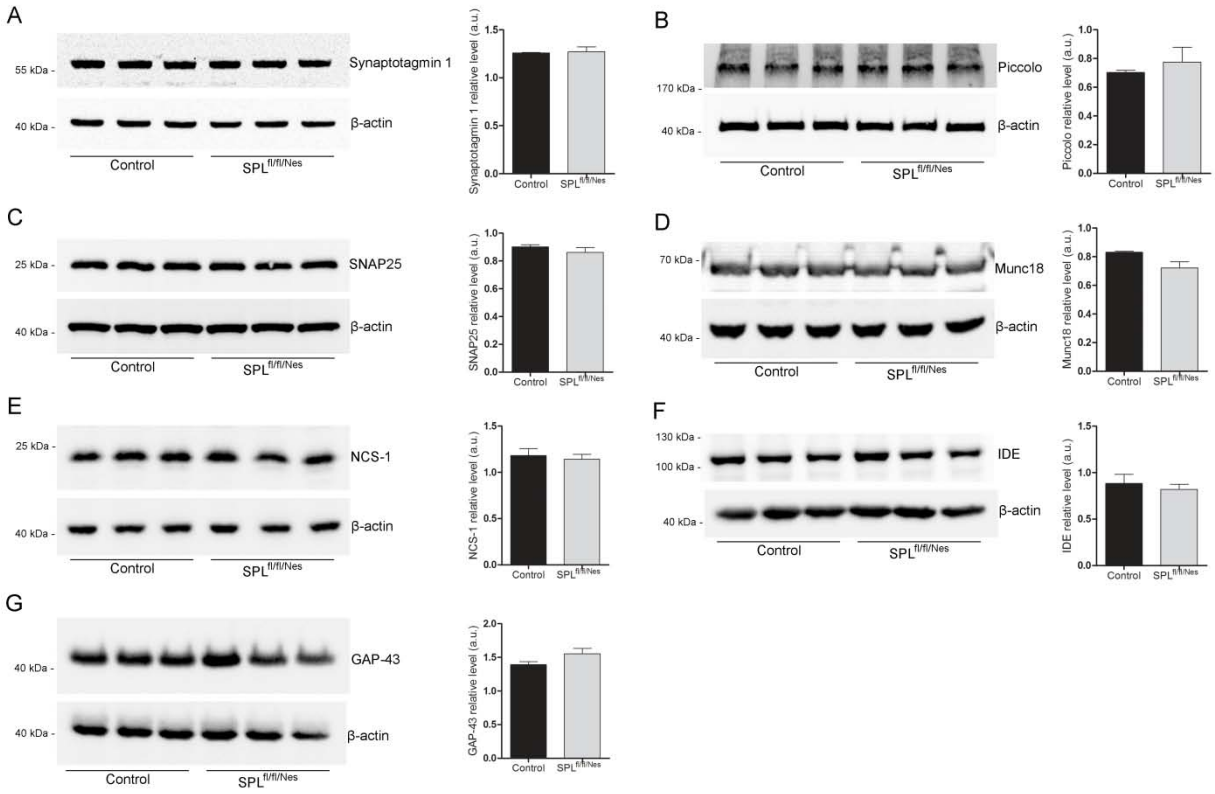

Figure 13. Proteins with unchanged expression in SPLfl/fl/Nes mice. (**A – G**) Protein amounts were assessed by immunoblotting.

3.4.1.1 Unaltered expression of mRNA of presynaptic proteins in SPL$^{fl/fl/Nes}$ mice

Since S1P was shown to modulate the activity of histone deacetylases (Hait et al. 2009), we checked whether the decreased expression of presynaptic proteins occurred at transcriptional level. Yet, no changes in transcript amounts were found in brains of SPL$^{fl/fl/Nes}$ mice (Fig. 14).

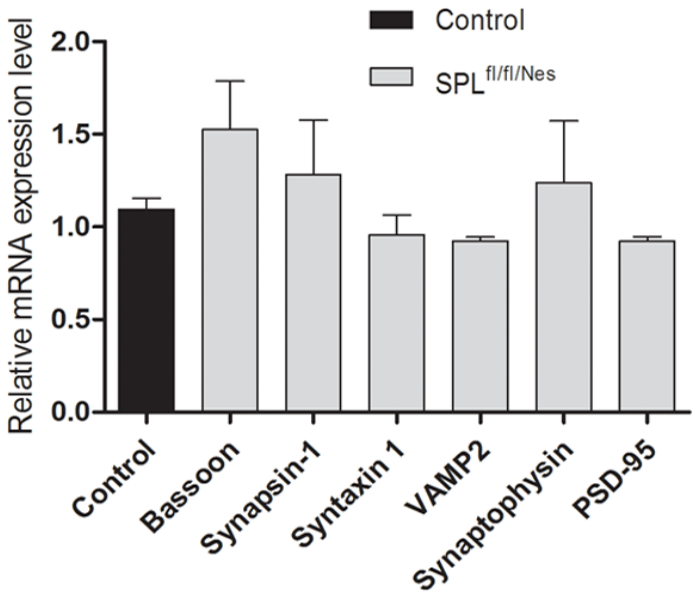

Figure 14. mRNA levels of presynaptic proteins in SPL$^{fl/fl/Nes}$ mice. Transcript amounts were determined by qRT-PCR in hippocampi of 6-month-old mice.

3.4.2 The ubiquitin-proteasomal system is up-regulated in SPL$^{fl/fl/Nes}$ mice

As many presynaptic proteins are known to be degraded by the UPS (Bingol et al. 2005, Hegde 2010), and there is a coordinated balance of protein ubiquitination, proteasomal activity and autophagy (Nedelsky et al. 2008, Korolchuk et al. 2010, Riley et al. 2010), we next assessed protein ubiquitination and proteasomal activity in SPL$^{fl/fl/Nes}$ brains. The amount of ubiquitinated proteins was indeed considerably elevated in brains of SPL$^{fl/fl/Nes}$ mice compared to the respective age matched controls (Fig. 15 A). Moreover, augmented protein ubiquitination was associated with increased proteasomal activity (Fig. 15 B). In addition, we found that presynaptic proteins with reduced expression were indeed included in the highly ubiquitinated protein fraction (Fig. 15 C).

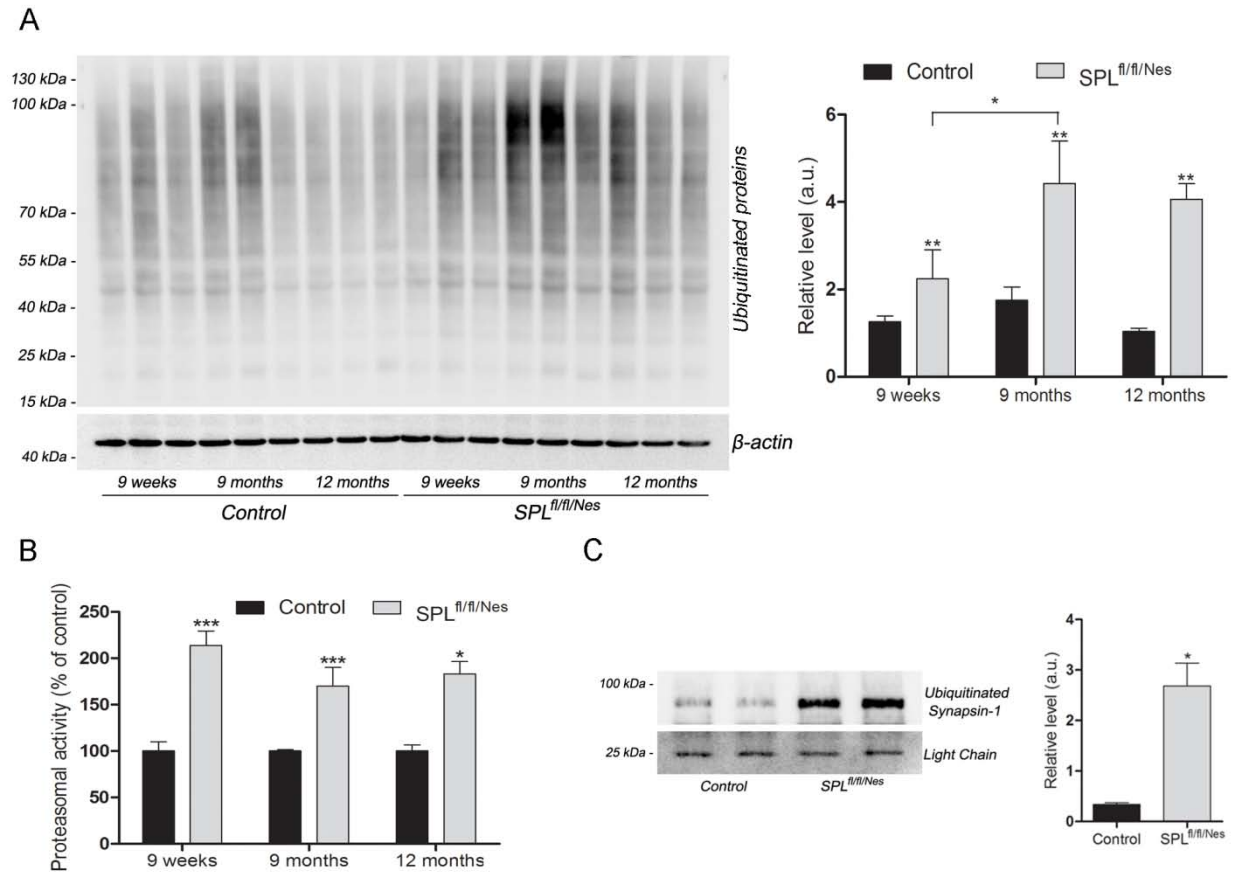

Figure 15. Ablation of SPL leads to an elevation of proteasome activity. Experiments were performed in brains of $SPL^{fl/fl/Nes}$ mice at the indicated ages. (**A**) Age-dependent increase of ubiquitinated proteins (two-way ANOVA, $P_{genotype} = 0.0058$, $P_{time} = 0.0284$). (**B**), increase of proteasomal activity (two-way ANOVA, $P_{genotype} = 0.0058$). (**C**) immunoprecipitation of ubiquitinated proteins followed by Western blotting of synapsin-1 (unpaired t test, $P_{Synapsin-1} = 0.0354$).

3.4.2.1 Decrease of deubiquitinating protein USP14 in $SPL^{fl/fl/Nes}$ mice

The proteasome-associated deubiquitinating enzyme USP14 on one hand is functionally coupled with proteasomal activity and on the other hand a critical regulator of synaptic plasticity (Kowalski et al. 2012). The loss of USP14 causes a large reduction in the number of synaptic vesicles and impairs paired pulse facilitation (PPF), indicating that UPS14 regulates presynaptic structure and function (Walters et al. 2014). We therefore studied the expression of USP14 at protein and mRNA level in $SPL^{fl/fl/Nes}$ mice. As depicted in Figure 16 A the expression of USP14 was considerably reduced in hippocampi of $SPL^{fl/fl/Nes}$ mice. However, there were no significant

differences in the amount of the respective transcripts (Fig. 16 B). On the other hand USP14 was included in the highly ubiquitinated protein fraction, suggesting that its decreased expression could be due to its degradation by the proteasome (Fig. 16 C).

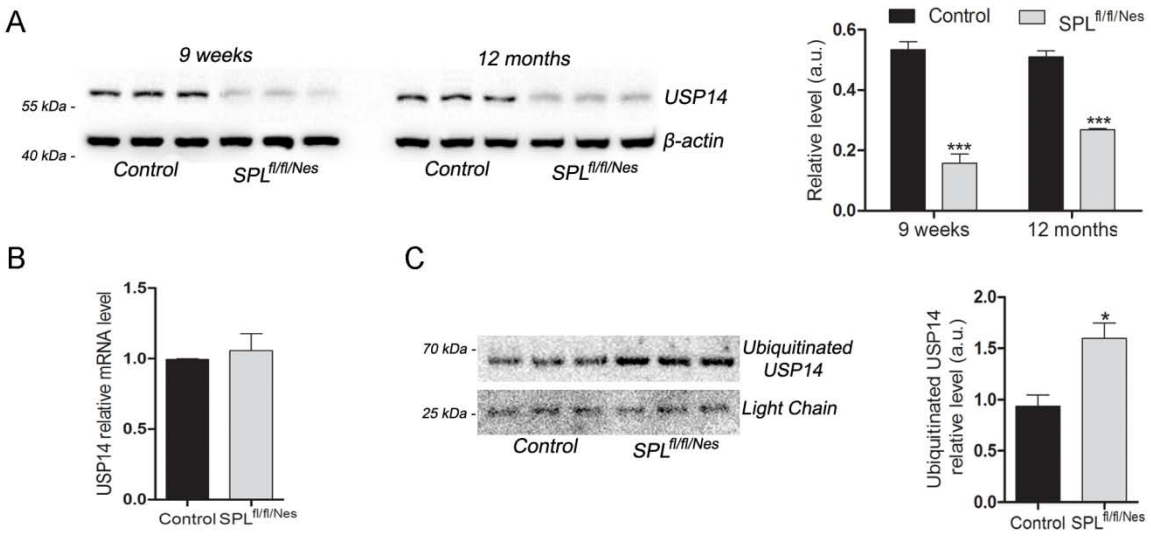

Figure 16. Ablation of SPL leads to a decreased expression of USP14. Experiments were performed in brains of $SPL^{fl/fl/Nes}$ mice at the indicated ages. (**A**) expression of USP14 (two-way ANOVA, $P_{genotype} < 0.0001$). (**B**) transcript levels of USP14. (**C**) immunoprecipitation of ubiquitinated proteins followed by Western blotting of USP14 (unpaired t test, $P_{USP14} = 0.0231$).

3.4.2.2 Proteasome inhibition restores expression of USP14 and of presynaptic proteins

To test whether slowing protein degradation would restore the changes in protein expression in the hippocampus of $SPL^{fl/fl/Nes}$ mice, hippocampal slices were treated with the proteasome-specific inhibitor epoxomicin for 5h, restoring the decreased expression of USP14 and the SNARE-proteins, syntaxin1 and VAMP2, in $SPL^{fl/fl/Nes}$ mice with no significant effect in controls (Fig. 17 A). Presynaptic proteins were also restored upon treatment with MG-132 for 24h in cultured cerebellar neurons from $SPL^{fl/fl/Nes}$ mice (Fig. 17 B, 18).

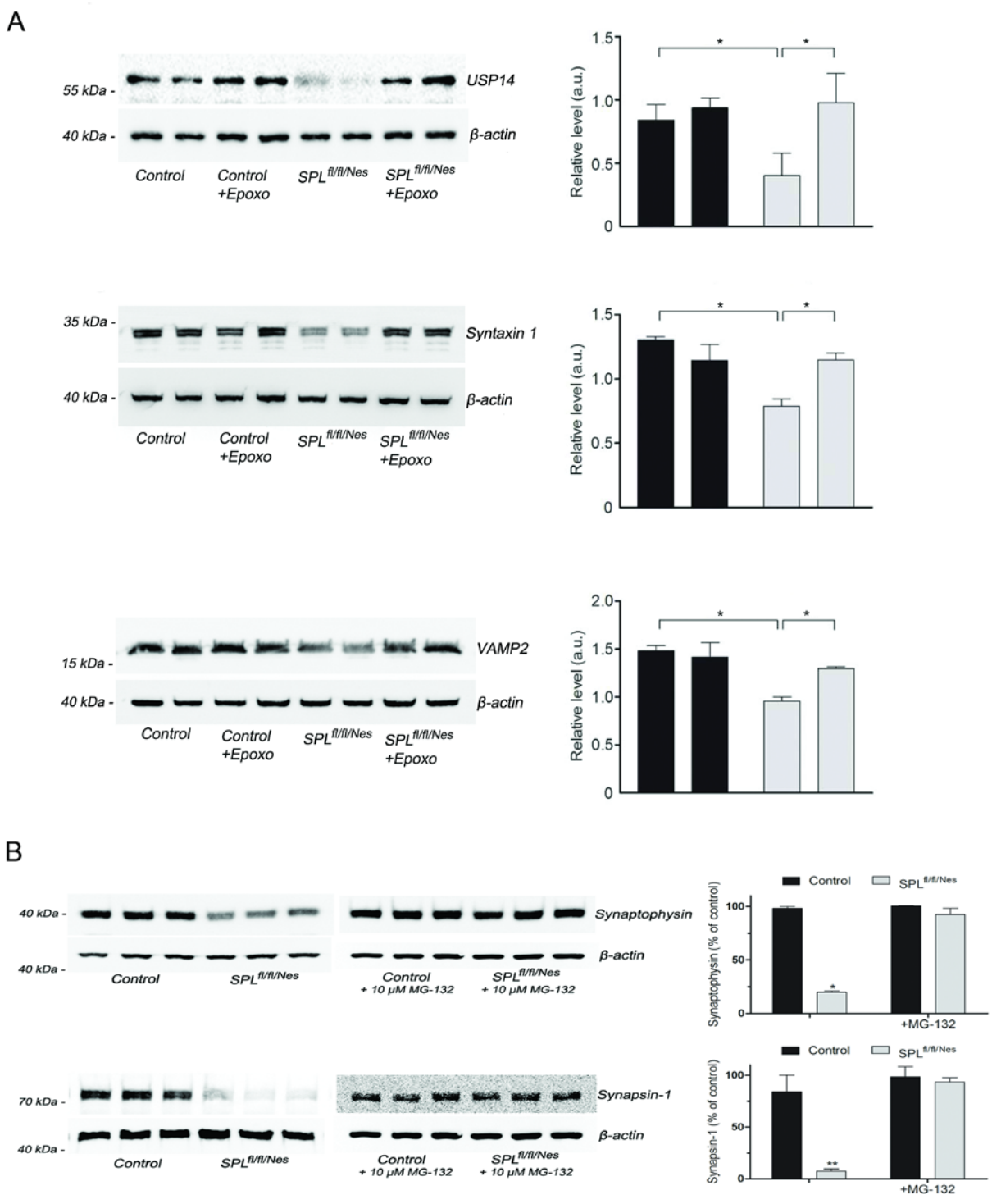

Figure 17. Proteasome inhibition restores expression of USP14 and of presynaptic proteins in SPL$^{fl/fl/Nes}$ mice. A, Hippocampal slices from control and SPL$^{fl/fl/Nes}$ mice were incubated in the absence or presence of 15 µM epoxomicin (Epoxo) for 5 h, immunoblotting of USP14 and SNARE-proteins (two-way ANOVA, $P_{USP14} = 0.0125$, $P_{Syntaxin\ 1} = 0.0315$, $P_{VAMP2} = 0.0390$). **B,** Neuronal cultures generated from

cerebella of mice with the indicated genotype were incubated at day 14 in culture with 10 µM proteasomal inhibitor MG-132 for 24 h, immunoblotting (two-way ANOVA, $P_{Synaptophysin} = 0.012$, $P_{Synapsin\text{-}1} = 0.0095$).

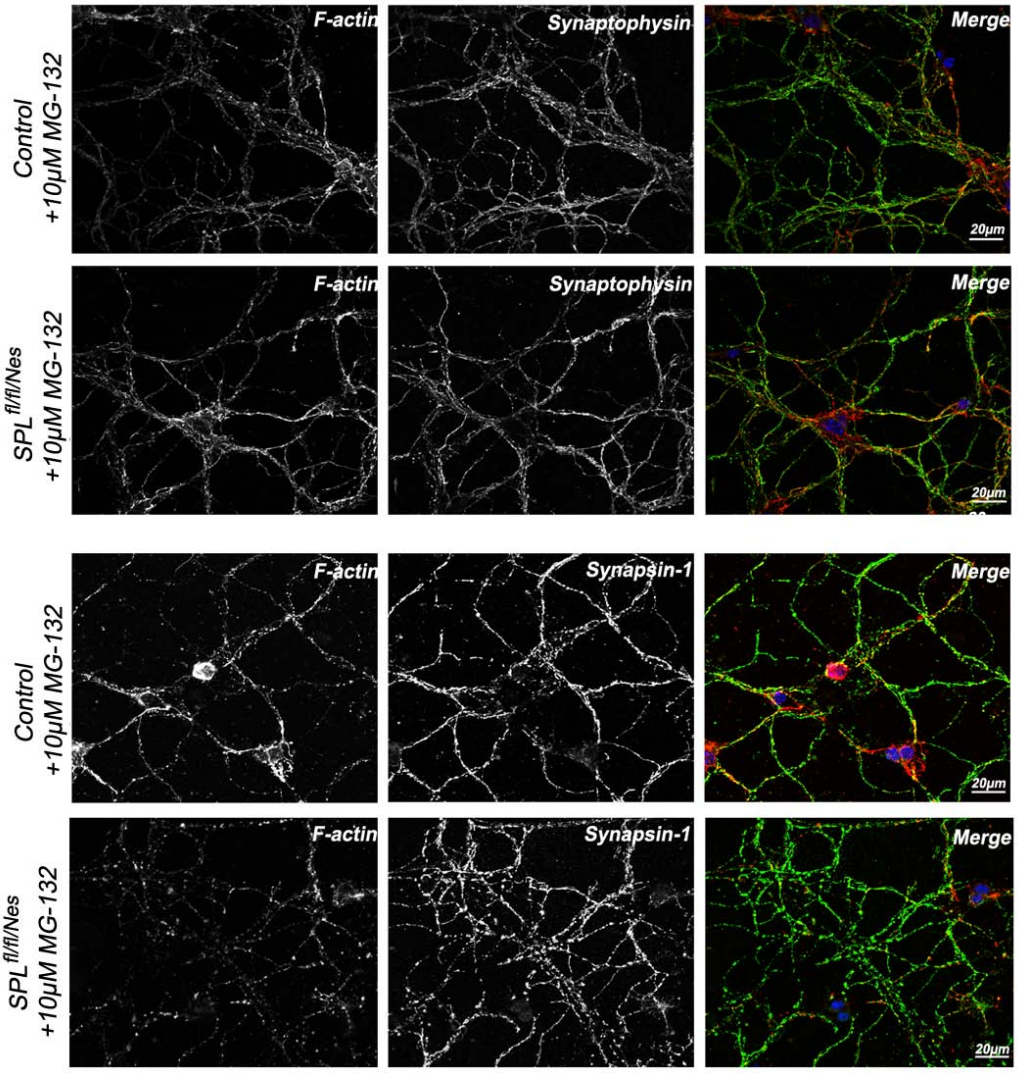

Figure 18. Proteasome inhibition restores expression of presynaptic proteins in SPL$^{fl/fl/Nes}$ mice. Immunostaining. F-actin (red), synaptophysin and synapsin-1 (green).

3.4.2.3 Proteasome activity is re-established by BAPTA-AM in SPL$^{fl/fl/Nes}$ mice

As calcium is a potential inducer of the UPS (Uvarov et al. 2008), and there is evidence that S1P accumulation induces calcium release from the ER (Hagen et al. 2011), the effect of calcium

chelation on UPS was assessed. Indeed addition of BAPTA-AM, a calcium chelator, completely re-established proteasomal activity in neurons derived from SPL$^{fl/fl/Nes}$ mice. (Fig. 19).

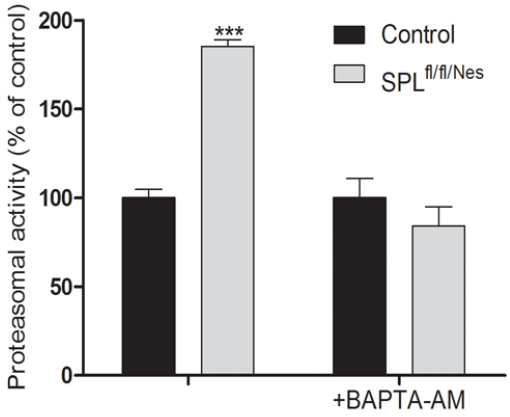

Figure 19. Proteasomal activity is normalized by calcium chelation in SPL$^{fl/fl/Nes}$ mice. Neuronal cultures were incubated in the presence of the calcium chelator BAPTA-AM (5 µM, 1 h) (two-way ANOVA, P = 0.0003).

3.5 SPL$^{fl/fl/Nes}$ mice exhibit deficits in spatial learning, memory and motor coordination

Based on all the changes regarding brain morphology, physiology and biochemistry described above we decided that it is very important to find out whether cognitive skills and motor coordination of SPL$^{fl/fl/Nes}$ mice are also affected. We started by analyzing in parallel exploratory activity in an open field of SPL$^{fl/fl/Nes}$ and control littermates. As illustrated in Figure 20 A no significant difference in the distance covered by control and SPL$^{fl/fl/Nes}$ mice could be detected. Next, we tested spatial learning and memory in an object-place-recognition task in the SPL$^{fl/fl/Nes}$ and control mice (Fig. 20 B, C). During training trials (3 x 6 min), mice were allowed to explore two identical objects situated in defined locations of arena. During the test, the position of one of the objects was shifted to a new location, while the other object remained in the known location. Total exploration times (new object + known object) did not differ during the test between experimental groups, indicating that the overall levels of exploratory activity were similar between SPL$^{fl/fl/Nes}$ mice and controls. There was, however, a difference in exploration patterns between genotypes: Controls spent significantly more time exploring the object in the novel location compared to the object in the known location, which is indicative of memory for the prior object locations during training. SPL$^{fl/fl/Nes}$ mice, in contrast, did not spend more time

exploring the objects in the familiar and novel locations and, hence, lacked evidence for proper object-place memory (Fig. 20 B, C). We also examined spatial learning and memory in a hidden version of the Morris water maze in $SPL^{fl/fl/Nes}$ and control mice. Shown are quadrant occupancy, target crossings and proximity in the probe trial at day 7 (Fig. 20 D-F). Note that escape latencies did not differ between the two groups (not shown). Moreover assessment of associative learning and memory in a contextual fear conditioning paradigm indicated reduced performance in $SPL^{fl/fl/Nes}$ mice as judged by higher activity suppression ratios compared to controls (Fig. 20 G). Finally, we examined motor coordination and balance with the accelerating rotarod, which revealed severe impairments in $SPL^{fl/fl/Nes}$ mice (Fig. 20 H). Altogether, these data demonstrate the presence of profound and complex neurological phenotypes in $SPL^{fl/fl/Nes}$ mice.

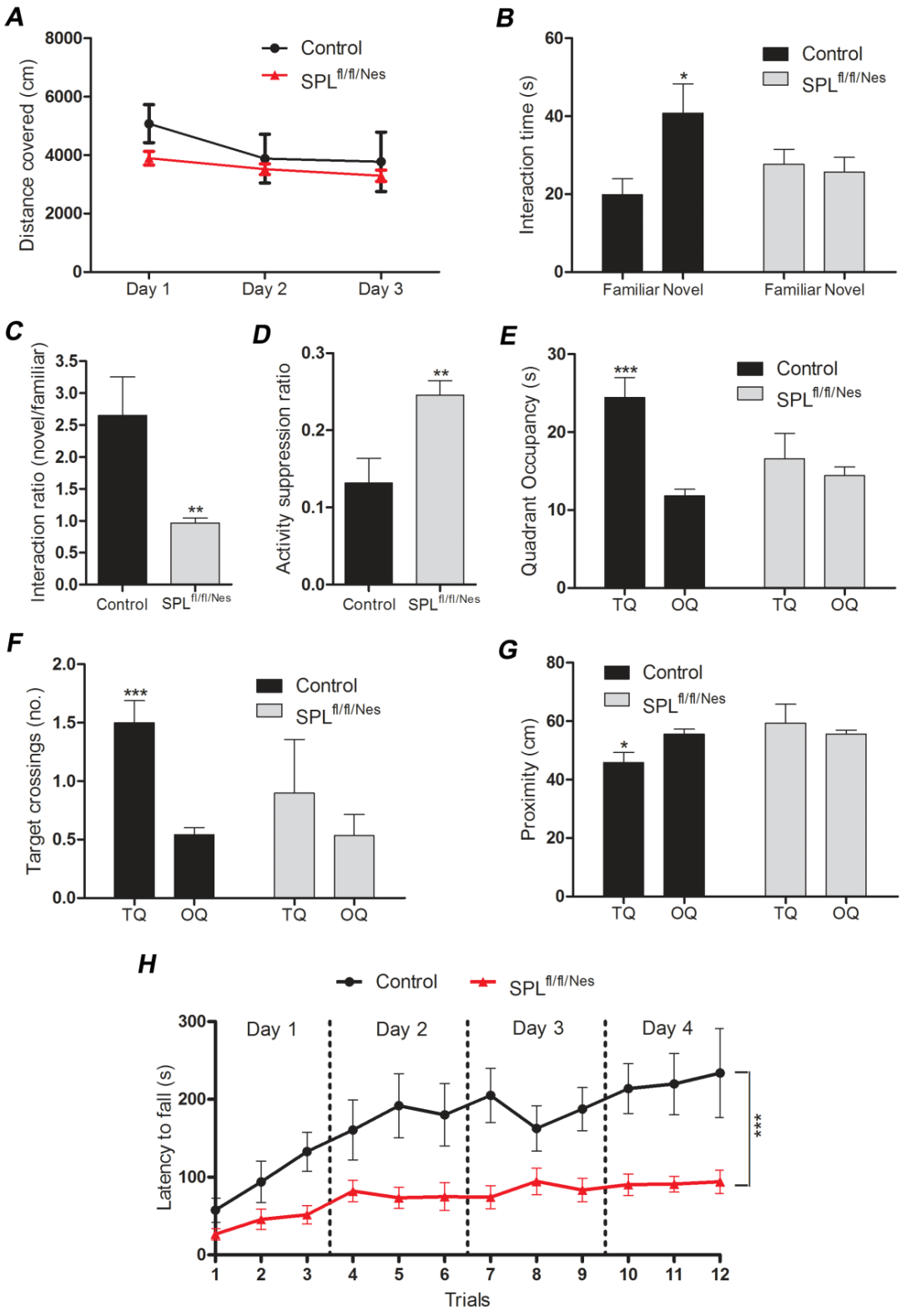

Figure 20. Profound deficits in spatial learning, memory and motor coordination in SPL$^{fl/fl/Nes}$ mice. **A**, Open field test: Exploratory activity is expressed as the distance covered during 20 min. **B**, Object placement recognition test; shown is the exploration time of the objects in the novel and familiar location,

respectively (two-way ANOVA, P = 0.0265). **C**, Novel object recognition ability; shown is the discrimination index, represented by the normalized ratio of time spent with the novel object and the familiar object (unpaired t test, P = 0.0097). **D**, Fear conditioning test. Shown is the relative time of activity expressed as the activity suppression ratio [(time of activity during test)/(time of activity during test + time of activity during baseline)]. Baseline activity was determined 2 min before aversive stimulus whereas time of activity was determined one day after associative training in a context fear conditioning paradigm (unpaired t test, P = 0.0053). **E-G**, Hidden version of the Morris water maze; TQ, target quadrant with hidden platform; OQ, other quadrants. **E**: Time of quadrant occupancy (two-way ANOVA, P = 0.001); **F**: Number of target crossings after completion of training (two-way ANOVA, P = 0.001). **G**: Time spent in the target area expressed as distance from the target (two-way ANOVA, P = 0.043) . **H**, Latency to fall in the context of a motor coordination test on the accelerating rotarod (two-way ANOVA, P < 0.0001) . All tests were assessed in mice at an age of 15-18-month with n=9 (control group), and n=10 ($SPL^{fl/fl/Nes}$ group).

4. DISCUSSION

The generation of a mouse model with neural specific ablation of SPL and the consequent accumulation of S1P and sphingosine leads to morphological, molecular, and behavioural abnormalities. Moreover, it has allowed us to identify a formerly overlooked direct role of SPL in neuronal autophagy.

On the one hand accumulation of S1P and sphingosine induced a calcium mediated elevation of the UPS and hence reduced expression of several presynaptic proteins. The inhibition of proteasomal activity restoring protein expression suggests the UPS as a possible link connecting sphingolipid metabolism and presynaptic pathology. On the other hand our results show that SPL deficiency blocks autophagy at its early stages because of reduced PE production.

4.1 The effects of SPL deficiency

Synaptic pathology has been acknowledged as a key early event in neurodegeneration, and presynaptic terminal changes during ageing and neurodegeneration have been reported (Wishart et al. 2006, Yasuda et al. 2013). However, the detailed mechanisms connecting sphingolipid metabolism to synaptic dysfunction remain poorly understood and the existing reports on the connection between S1P, sphingosine and synaptic function are rather contradictory (Kanno et al. 2010, Kanno et al. 2011, Chan et al. 2012, Chan et al. 2012, Kempf et al. 2014). Earlier reports argue for a positive role of S1P in synaptic transmission (Kanno et al. 2010, Kanno et al. 2011, Chan et al. 2012, Chan et al. 2012). In contrast, a recent report demonstrated a repressive effect of S1P signalling on synaptic plasticity (Kempf et al. 2014). Consistently, our results argue in favour of S1P and sphingosine accumulation leading to perturbations in synaptic morphology and function. Hence S1P can be viewed as a double edged sword wherein, despite its importance in normal cellular functions, both decrease and increase of the lipid beyond a threshold might be fatal for cellular functions. Reports regarding the function of enzymes involved in S1P metabolism are also controversial. There are two isoforms of sphingosine kinases (SK1 and SK2)

that generate S1P (Pitson 2011). Presynaptic SK1-derived S1P was reported to promote neurotransmitter release in hippocampal neurons (Kajimoto et al. 2007) and *C. elegans* (Chan et al. 2012), while studies in human and rodent brain suggest that SK2 is particularly important in neurons (Blondeau et al. 2007, Katsel et al. 2007). However, the major regulator of intracellular S1P levels is S1P-lyase (SPL). It catalyses the irreversible cleavage of S1P to hexadecenal and ethanolamine phosphate, the final step of sphingolipid catabolism (Serra et al. 2010).

We show that loss of SPL activity results in tissue-dependent accumulation of S1P and sphingosine. Similar results were also reported by others (Hagen et al. 2009, Bektas et al. 2010, Hagen-Euteneuer et al. 2012). Intriguingly, SPL-deficiency in neurons causes a predominant S1P accumulation and to a lesser degree, its metabolic precursor sphingosine with no significant alterations in ceramide, sphingomyelin and glycosphingolipids (Hagen-Euteneuer et al. 2012).

Neurodegenerative disorders are characterized by the loss of structure and function of specific neuronal circuitry in the brain. Behavioural science plays an important role when characterizing mouse models of human disorders. Therefore, standard test for assessing behavioural changes are used (Dumont 2011). The alterations in behaviour observed in the present study were accompanied by morphological and functional changes of hippocampal synapses (Mitroi et al. in press). Vesicle pools were largely reduced (60 %) and single vesicles were increased in diameter (Mitroi et al. in press). A major finding in the study by Walters et al. (Walters et al. 2014) was that the loss of presynaptic USP14 triggers a large reduction in the number of presynaptic vesicles including docked vesicles. Since the number of docked vesicles has been shown to correspond to the size of the readily releasable pool (Dobrunz et al. 1997, Schikorski et al. 2001), that is assumed to be reduced in stimulated synapses. Note that based on the known effects of increased calcium levels on endocytosis (Cousin et al. 2000, Wu et al. 2009) an increased recycling and delivery of vesicles to release sites may be expected. In agreement with this, no difference in the number of “docked” vesicles was detected in synapses at rest (Mitroi et al. in press). Moreover, an increased number of coated endocytic vesicles were observed in the $SPL^{fl/fl/Nes}$ mice (Mitroi et al. in press). Additional role of endocytosis and calcium on increased size of synaptic vesicles in hippocampi of $SPL^{fl/fl/Nes}$ mice remains unclear.

Astrocytes are ubiquitous glia and provide many supportive activities crucial for neuronal function in uninjured central nervous system (CNS) (Kimelberg et al. 2010), and most likely the

modeling and maintenance of synapses (Ullian et al. 2001). Astrocytes become “reactive” in response to all CNS insults. Evidence of neuroinflammatory processes has been found in several neurodegenerative diseases, like Alzheimer’s disease, Parkinson’s disease, Huntington’s disease and multiple sclerosis (Glass et al. 2010). Although substantial information regarding molecules that are able to induce reactive astrocytosis is available, the degree to which reactive astrocytes augment, maintain, or down-regulate the supportive activities when they become reactive is not known (Sofroniew 2005). Another function of astrocytes is the uptake of glutamate, which is the main route of glutamate removal, from glutamatergic synapses, conversion of glutamate to glutamine, and in the last step re-uptake of glutamine by presynaptic neurons to reconstitute neurotransmitter pools (Colangelo et al. 2014). Therefore, the upregulation of reactive astrocytes seen by an increased GFAP expression in the $SPL^{fl/fl/Nes}$ mouse brain may be due to the presynaptic changes, although there was still no significant neuronal death.

4.2 SPL involvement in autophagy

Studying the enzymes regulating S1P balance is a promising route to understand S1P regulated autophagic mechanisms (Lavieu et al. 2006, Lepine et al. 2011, Moruno Manchon et al. 2015). In neurons cytosolic SK1 responsible for S1P generation was shown to enhance flux through autophagy whereas S1P-degrading enzymes like SPPs or SPL decrease this flux (Moruno Manchon et al. 2015). In non-neuronal cells SK1 (S1P)-induced autophagy is nutrient sensitive and characterized by the inhibition of mammalian target of rapamycin (mTOR) (Lavieu et al. 2006). Alternatively, deletion of SPP1 has been shown to induce autophagy even in the presence of nutrients via an mTOR independent mechanism. Notably, several studies have described extrinsic S1P acting via its receptors as an inhibitor of autophagy through activation of the mTOR pathway (Maeurer et al. 2009, Taniguchi et al. 2012).

PE production from ethanolamine phosphate resulted from the breakdown of S1P could not constitute the major pathway for *de novo* synthesis, since there are other S1P-independent pathways for the synthesis of ethanolamine phosphate and/or PE (Rockenfeller et al. 2015). The precise control and regulation of sphingolipids is a complicated process and even slight changes in the concentration of these metabolites can inflict distinct and opposing effects on cellular

functions (Merrill 2002). The necessity for such an intricate regulation is also argued to be a reason behind why S1P degradation is not a predominant source of ethanolamine phosphate (Hannun et al. 2001). However, our findings concerning $SPL^{fl/fl/Nes}$ mice indeed point to an important role for PE generated from the S1P degradation products in autophagy and lysosomal function at least in neurons. Of note, an earlier study by Zhang et al. (Zhang et al. 2007) has shown evidence for a striking remodeling of the sphingolipid pathway for bulk production of ethanolamine in Leishmania (Zhang et al. 2007). On the other hand, a recent report by Rockenfeller et al. (Rockenfeller et al. 2015) has shown that the artificial increase of intracellular PE levels or overexpressing the PE-generating phosphatidylserine decarboxylase Psd, significantly increased autophagic flux which in turn extended the life span of yeast (Rockenfeller et al. 2015). Taken together, these findings establish on one hand the importance of PE in the autophagic pathway and on the other hand the significant contribution of S1P metabolism in regulating this pathway. Thus SPL apart from linking sphingolipid and glycerophospholipid metabolism (Kihara 2014) might also modulate autophagic flux via its reaction product ethanolamine phosphate in tissues which abundantly express sphingolipids as demonstrated here for neurons.

On a closer look, it is obvious that there are more layers of complexity to our results than they appear to be at the first glance. A bidirectional effect of SPL ablation leading to the reduction of its product ethanolamine phosphate and also the accumulation of its substrate S1P can be envisaged. S1P has its own specific routes through which it can influence autophagy. S1P treatment has been shown to counteract autophagy induction by amino acid starvation and this effect was mediated by the S1PR3 in an mTOR dependent manner (Taniguchi et al. 2012). It is to be noted that mTOR independent effects of S1P on autophagy have also been documented (Lepine et al. 2011) and these differences could be attributed to the extrinsic and intrinsic effects of S1P (Taniguchi et al. 2012). Our results show an mTOR independent effect as rapamycin treatment could not rescue the accumulation of p62 and the decreased conversion of LC3-I into LC3-II. Importantly, rapamycin increased LC3 levels and decreased p62 levels in control neurons. Nevertheless it was shown in earlier reports that accumulation of SK2-derived S1P induces ER stress (Hagen et al. 2011, Hagen-Euteneuer et al. 2012) known to up regulate cellular autophagy (Yang et al. 2010, Wang et al. 2016). At the same time accumulating S1P reduced neuronal *de novo* sphingolipid biosynthesis (Hagen-Euteneuer et al. 2012), which was reported to

be essential for induction of autophagy in non-neuronal cells (Sims et al. 2010). In line with this data, we detected both, an accumulation of p62, a generally accepted indicator of impaired autophagy (Rusten et al. 2010) as well as an elevated expression of beclin-1 and Atg5-Atg12 complex, which is rather indicative of increased autophagosome initiation (Yang et al. 2010). Moreover, pharmacological inhibition of SPL by 2-acetyl-4-(tetrahydroxybutyl)imidazole (THI) under conditions of vitamin B6 deficiency was able to produce the same phenotype of autophagy impairment. Accumulation of p62 was prevented by PE supply implying that an effect of S1P on autophagy in SPL-deficient neural tissue if present is rather secondary. Intriguingly, in Niemann-Pick disease type C1 caused by an impaired cholesterol trafficking and hence lysosomal storage of sphingolipids, autophagy was also found to be both induced and defective (Elrick et al. 2012, Ordonez et al. 2012).

Another possibility that cannot be fully excluded is the role of sphingosine in autophagy which is also accumulating to a certain extent in SPL-deficient neurons (Hagen-Euteneuer et al. 2012). Sphingosine has recently been demonstrated to trigger calcium release from acidic stores (Hoglinger et al. 2015) that in turn might activate autophagy. Intriguingly, our results regarding LAMP-2 and cathepsin D point to an increased lysosomal function. It could be assumed therefore that augmented lysosomal activity downstream of the autophagic block as well as enhanced number of phagophores upstream of this block might represent an attempt of SPL-deficient neurons to overcome impaired autophagy caused by reduced PE levels.

Defective autophagic flux and lysosomal activity are involved in the pathogenesis of neurodegenerative diseases (Nixon 2013, Menzies et al. 2015) by causing defective degradation of protein aggregates. Consistent with this hypothesis, we observed an accumulation of neurodegenerative biomarkers of Alzheimer’s disease and Parkinson’s disease in SPL-deficient mouse brains. A strong accumulation of APP and potentially amyloidogenic APP C-terminal fragments, as well as an increased generation of Aβ have been reported before in SPL-deficient mouse embryonic fibroblasts (Karaca et al. 2014).

4.3 Molecular mechanisms of neurodegeneration triggered by SPL ablation

Deletion studies have helped to identify presynaptic proteins which are essential for synaptic function and integrity. Removal of such key proteins often leads to impaired neurotransmitter release, changes of the vesicle pools or cytomatrix at the active zone. However, in some cases the loss of function can be compensated by other presynaptic proteins (Gundelfinger et al. 2012, Sudhof 2012, Sudhof 2013). On analyzing the levels of selected key proteins involved in different stages of the vesicle cycle, we found that several of these proteins were reduced in $SPL^{fl/fl/Nes}$ mice. Since we did not observed morphological changes in the active zone we conclude that the observed reductions in key proteins do not underlie or at least are not sufficient (Arancillo et al. 2013) to cause the observed changes in synaptic transmission in $SPL^{fl/fl/Nes}$ mice (Mitroi et al. in press). At the structural level a reduction in number of synaptic vesicles in the pool has been reported in synapsin I and synapsin triple-knockout mice (Li et al. 1995, Siksou et al. 2007). Accordingly, a profound reduction in number of vesicles has been reported also in a study of Mitroi et al. (Mitroi et al. in press). A redistribution of synapsin has been recently reported following application of S1P in nanomolar concentration to synapses (Riganti et al. 2016) thus supporting that this protein is the target of S1P action.

Speese et al. (Speese et al. 2003) have shown that parts of the ubiquitin proteasome system (UPS) are present in the presynaptic terminal and that UPS acutely regulates presynaptic protein turnover modulating synaptic efficiency and neurotransmission strength. Moreover, acute pharmacological inhibition of the proteasome causes a rapid strengthening of neurotransmission by 50 % because of increased presynaptic efficacy (Speese et al. 2003). According to a previous study of Speese et al. (Speese et al. 2003) in the $SPL^{fl/fl/Nes}$ mice there is an increase in proteasomal activity and a decrease of several presynaptic proteins. Pharmacological inhibition of proteasomal activity rescued presynaptic proteins and USP14 expression in $SPL^{fl/fl/Nes}$ mice. We therefore propose the degradation of USP14 by UPS could be the underlying molecular mechanism responsible for the morphological and behaviour impairments observed. Localized in the 19S regulatory subunit of the proteasome, USP14 has been proposed as a negative modulator of proteasome-mediated degradation (Lee et al. 2010).

Certain studies suggest a compensatory mechanism between UPS and autophagy allowing cells to reduce the accumulation of UPS substrates. This observation is referring to an increased

function of autophagy due to the impairment of the UPS (Iwata et al. 2005, Ding et al. 2007, Pandey et al. 2007). However the reverse mechanism is not available since a deficiency in autophagy leads to accumulation of polyubiquitinated proteins with no alteration in proteasome function (Hara et al. 2006, Komatsu et al. 2006). Hence, we cannot exclude that the increase of ubiquitinated proteins observed in the brains of $SPL^{fl/fl/Nes}$ mice could be a result of autophagy alteration. Notably, p62, an autophagic marker, is increased in the brains of $SPL^{fl/fl/Nes}$ mice. p62 competes with other ubiquitin-binding proteins for binding to ubiquitylated proteins (Korolchuk et al. 2009). When is accumulating, p62 oligomerizes, preventing the delivery of the p62-bound ubiquitylated proteins to the proteasome for degradation (Korolchuk et al. 2010). This might be a good explanation for the accumulation of ubiquityled proteins in spite of the fact that the proteasomal function is activated in $SPL^{fl/fl/Nes}$ mice. The enhancement of proteasomal activity might be a consequence of increased cytosolic Ca2+ (Uvarov et al. 2008) due to the ER-stress caused by high levels of S1P and sphingosine (Hagen et al. 2011, Hagen-Euteneuer et al. 2012).

Our results indicate an important role of proteasomal activity and hence deregulated protein degradation at the presynapse induced by SPL deficiency. Although, we cannot conclusively pinpoint the exact underlying molecular mechanism, our results, which are in line with recent findings of Jarome et al. (Jarome et al. 2014), suggest that the decrease of USP14 by the elevated UPS activity might be the central switch that propagates the observed long-term memory impairment for the fear conditioning task in $SPL^{fl/fl/Nes}$ mice, making USP14 an important regulator of long-term memory formation. Since presynaptic dysfunction might be an early pathogenic event in neurodegeneration (Zhang et al. 2009), our findings could have important implications for diseases where S1P analogues are used as disease modifying therapies.

In addition to earlier data providing a calpain mediated link that connects S1P and neurodegeneration (Hagen et al. 2011) the present study provides an additional route that connects SPL deficiency and neurodegeneration via a PE-mediated defective autophagy mechanism.

CONCLUSIONS

Our results demonstrate an involvement of sphingolipid metabolism in maintaining presynaptic nerve terminal architecture leading to cognitive deficits. We are the first to observe that S1P accumulation is essential for the assessed elevation of ubiquitin-proteasomal system (UPS) which is responsible for the decrease of several presynaptic proteins and the deubiquitinating protease USP14. The latter was shown to play a critical role in synaptic plasticity and its loss is associated with several physiological impairments in the central nervous system (Kowalski et al. 2012). The inhibition of proteasomal activity restoring protein expression suggests the UPS as a possible link connecting sphingolipid metabolism and presynaptic pathology. Since presynaptic dysfunction might be an early pathogenic event in neurodegeneration (Zhang et al. 2009), our findings could have important implications for diseases where S1P analogues are used as disease modifying therapies.

Our study brings further insights for another important aspect of S1P mediated autophagy regulation, which has not been investigated so far; the role of the SPL degradation product ethanolamine phosphate. The latter is easily incorporated into PE, which is important for autophagosome initiation and elongation. We were able to see a decrease in PE, followed by an impaired autophagy and a consequent accumulation of neurodegenerative biomarkers in the mice with neural specific ablation of SPL. Our results show that PE paucity is leading to the blockage of autophagic flux at the early stages of autophagosome formation. These findings identify a formerly overlooked direct role of SPL in neuronal autophagy that could be of great interest in a better understanding of neurodegenerative diseases in which autophagy is dysfunctional. However, the detailed mechanism involved in the regulation of autophagy by PE linked via SPL to S1P metabolism is yet to be explored.

References

Arancillo, M., S. W. Min, S. Gerber, A. Munster-Wandowski, Y. J. Wu, M. Herman, T. Trimbuch, J. C. Rah, G. Ahnert-Hilger, D. Riedel, T. C. Sudhof and C. Rosenmund (2013). "Titration of Syntaxin1 in mammalian synapses reveals multiple roles in vesicle docking, priming, and release probability." J Neurosci **33**(42): 16698-16714.

Ballou, L. M. and R. Z. Lin (2008). "Rapamycin and mTOR kinase inhibitors." J Chem Biol **1**(1-4): 27-36.

Bandhuvula, P. and J. D. Saba (2007). "Sphingosine-1-phosphate lyase in immunity and cancer: silencing the siren." Trends Mol Med **13**(5): 210-217.

Bankowska, A., M. Gacko, E. Chyczewska and A. Worowska (1997). "Biological and diagnostic role of cathepsin D." Rocz Akad Med Bialymst **42 Suppl 1**: 79-85.

Bedia, C., T. Levade and P. Codogno (2011). "Regulation of autophagy by sphingolipids." Anticancer Agents Med Chem **11**(9): 844-853.

Bektas, M., M. L. Allende, B. G. Lee, W. Chen, M. J. Amar, A. T. Remaley, J. D. Saba and R. L. Proia (2010). "S1P lyase deficiency disrupts lipid homeostasis in liver." J Biol Chem **285**: 10880-10889.

Beljanski, V., C. Knaak and C. D. Smith (2010). "A novel sphingosine kinase inhibitor induces autophagy in tumor cells." J Pharmacol Exp Ther **333**(2): 454-464.

Beljanski, V., C. Knaak, Y. Zhuang and C. D. Smith (2011). "Combined anticancer effects of sphingosine kinase inhibitors and sorafenib." Invest New Drugs **29**(6): 1132-1142.

Bhattacharyya, B. J., S. M. Wilson, H. Jung and R. J. Miller (2012). "Altered neurotransmitter release machinery in mice deficient for the deubiquitinating enzyme Usp14." Am J Physiol Cell Physiol **302**(4): C698-708.

Bingol, B. and E. M. Schuman (2005). "Synaptic protein degradation by the ubiquitin proteasome system." Curr Opin Neurobiol **15**(5): 536-541.

Bjorkoy, G., T. Lamark, A. Brech, H. Outzen, M. Perander, A. Overvatn, H. Stenmark and T. Johansen (2005). "p62/SQSTM1 forms protein aggregates degraded by autophagy and has a protective effect on huntingtin-induced cell death." J Cell Biol **171**(4): 603-614.

Blondeau, N., Y. Lai, S. Tyndall, M. Popolo, K. Topalkara, J. K. Pru, L. Zhang, H. Kim, J. K. Liao, K. Ding and C. Waeber (2007). "Distribution of sphingosine kinase activity and mRNA in rodent brain." J Neurochem **103**(2): 509-517.

Bode, C. and M. H. Graler (2012). "Quantification of sphingosine-1-phosphate and related sphingolipids by liquid chromatography coupled to tandem mass spectrometry." Methods Mol Biol **874**: 33-44.

Boya, P., R. A. Gonzalez-Polo, N. Casares, J. L. Perfettini, P. Dessen, N. Larochette, D. Metivier, D. Meley, S. Souquere, T. Yoshimori, G. Pierron, P. Codogno and G. Kroemer (2005). "Inhibition of macroautophagy triggers apoptosis." Mol Cell Biol **25**(3): 1025-1040.

Brindley, D. N. (2004). "Lipid phosphate phosphatases and related proteins: signaling functions in development, cell division, and cancer." J Cell Biochem **92**(5): 900-912.

Brinkmann, V., A. Billich, T. Baumruker, P. Heining, R. Schmouder, G. Francis, S. Aradhye and P. Burtin (2010). "Fingolimod (FTY720): discovery and development of an oral drug to treat multiple sclerosis." Nat Rev Drug Discov **9**(11): 883-897.

Brooks, S. P. and S. B. Dunnett (2009). "Tests to assess motor phenotype in mice: a user's guide." Nat Rev Neurosci **10**(7): 519-529.

Carter, R. J., L. A. Lione, T. Humby, L. Mangiarini, A. Mahal, G. P. Bates, S. B. Dunnett and A. J. Morton (1999). "Characterization of progressive motor deficits in mice transgenic for the human Huntington's disease mutation." J Neurosci **19**(8): 3248-3257.

Causeret, C., L. Geeraert, G. Van der Hoeven, G. P. Mannaerts and P. P. Van Veldhoven (2000). "Further characterization of rat dihydroceramide desaturase: tissue distribution, subcellular localization, and substrate specificity." Lipids **35**(10): 1117-1125.

Chan, J. P., Z. Hu and D. Sieburth (2012). "Recruitment of sphingosine kinase to presynaptic terminals by a conserved muscarinic signaling pathway promotes neurotransmitter release." Genes Dev **26**(10): 1070-1085.

Chan, J. P. and D. Sieburth (2012). "Localized sphingolipid signaling at presynaptic terminals is regulated by calcium influx and promotes recruitment of priming factors." J Neurosci **32**(49): 17909-17920.

Chang, C. L., M. C. Ho, P. H. Lee, C. Y. Hsu, W. P. Huang and H. Lee (2009). "S1P(5) is required for sphingosine 1-phosphate-induced autophagy in human prostate cancer PC-3 cells." Am J Physiol Cell Physiol **297**(2): C451-458.

Chen, H., S. Polo, P. P. Di Fiore and P. V. De Camilli (2003). "Rapid Ca2+-dependent decrease of protein ubiquitination at synapses." Proc Natl Acad Sci U S A **100**(25): 14908-14913.

Chen, Y. and D. J. Klionsky (2011). "The regulation of autophagy - unanswered questions." J Cell Sci **124**(Pt 2): 161-170.

Chen, Y., Y. Liu, M. C. Sullards and A. H. Merrill, Jr. (2010). "An introduction to sphingolipid metabolism and analysis by new technologies." Neuromolecular Med **12**(4): 306-319.

Chin, L. S., J. P. Vavalle and L. Li (2002). "Staring, a novel E3 ubiquitin-protein ligase that targets syntaxin 1 for degradation." J Biol Chem **277**(38): 35071-35079.

Ciechanover, A. (2005). "Intracellular protein degradation: from a vague idea thru the lysosome and the ubiquitin-proteasome system and onto human diseases and drug targeting." Cell Death Differ **12**(9): 1178-1190.

Ciechanover, A. (2005). "Proteolysis: from the lysosome to ubiquitin and the proteasome." Nat Rev Mol Cell Biol **6**(1): 79-87.

Ciechanover, A., H. Heller, S. Elias, A. L. Haas and A. Hershko (1980). "ATP-dependent conjugation of reticulocyte proteins with the polypeptide required for protein degradation." Proc Natl Acad Sci U S A **77**(3): 1365-1368.

Colangelo, A. M., L. Alberghina and M. Papa (2014). "Astrogliosis as a therapeutic target for neurodegenerative diseases." Neurosci Lett **565**: 59-64.

Cousin, M. A. and P. J. Robinson (2000). "Ca(2+) influx inhibits dynamin and arrests synaptic vesicle endocytosis at the active zone." J Neurosci **20**(3): 949-957.

Couttas, T. A., N. Kain, B. Daniels, X. Y. Lim, C. Shepherd, J. Kril, R. Pickford, H. Li, B. Garner and A. S. Don (2014). "Loss of the neuroprotective factor Sphingosine 1-phosphate early in Alzheimer's disease pathogenesis." Acta Neuropathol Commun **2**(1): 9.

Curzon, P., N. R. Rustay and K. E. Browman (2009). Cued and Contextual Fear Conditioning for Rodents. Methods of Behavior Analysis in Neuroscience. J. J. Buccafusco. Boca Raton (FL).

Cutler, R. G., W. A. Pedersen, S. Camandola, J. D. Rothstein and M. P. Mattson (2002). "Evidence that accumulation of ceramides and cholesterol esters mediates oxidative stress-induced death of motor neurons in amyotrophic lateral sclerosis." Ann Neurol **52**(4): 448-457.

D'Amato, C. J. and S. P. Hicks (1965). "Neuropathologic alterations in the ataxia (paralytic) mouse." Arch Pathol **80**(6): 604-612.

D.R. Herr, H. F., V. Phan, K. Heinecke, R. Georges, G.L. Harris, J.D. Saba (2003). " Sply regulation of sphingolipid signaling molecules is essential for Drosophila

development." Development **130**: 2443–2453.

Darios, F., C. Wasser, A. Shakirzyanova, A. Giniatullin, K. Goodman, J. L. Munoz-Bravo, J. Raingo, J. Jorgacevski, M. Kreft, R. Zorec, J. M. Rosa, L. Gandia, L. M. Gutierrez, T. Binz, R. Giniatullin, E. T. Kavalali and B. Davletov (2009). "Sphingosine facilitates SNARE complex assembly and activates synaptic vesicle exocytosis." Neuron **62**(5): 683-694.

Degagne, E., A. Pandurangan, P. Bandhuvula, A. Kumar, A. Eltanawy, M. Zhang, Y. Yoshinaga, M. Nefedov, P. J. de Jong, L. G. Fong, S. G. Young, R. Bittman, Y. Ahmedi and J. D. Saba (2014). "Sphingosine-1-phosphate lyase downregulation promotes colon carcinogenesis through STAT3-activated microRNAs." J Clin Invest **124**(12): 5368-5384.

Ding, W. X., H. M. Ni, W. Gao, T. Yoshimori, D. B. Stolz, D. Ron and X. M. Yin (2007). "Linking of autophagy to ubiquitin-proteasome system is important for the regulation of endoplasmic reticulum stress and cell viability." Am J Pathol **171**(2): 513-524.

Dobrunz, L. E. and C. F. Stevens (1997). "Heterogeneity of release probability, facilitation, and depletion at central synapses." Neuron **18**(6): 995-1008.

Du, Y., D. Yang, L. Li, G. Luo, T. Li, X. Fan, Q. Wang, X. Zhang, Y. Wang and W. Le (2009). "An insight into the mechanistic role of p53-mediated autophagy induction in response to proteasomal inhibition-induced neurotoxicity." Autophagy **5**(5): 663-675.

Dubois, N. C., D. Hofmann, K. Kaloulis, J. M. Bishop and A. Trumpp (2006). "Nestin-Cre transgenic mouse line Nes-Cre1 mediates highly efficient Cre/loxP mediated recombination in the nervous system, kidney, and somite-derived tissues." Genesis **44**(8): 355-360.

Dumont, M. (2011). "Behavioral phenotyping of mouse models of neurodegeneration." Methods Mol Biol **793**: 229-237.

Dunham, N. W. and T. S. Miya (1957). "A note on a simple apparatus for detecting neurological deficit in rats and mice." J Am Pharm Assoc Am Pharm Assoc **46**(3): 208-209.

Elrick, M. J., T. Yu, C. Chung and A. P. Lieberman (2012). "Impaired proteolysis underlies autophagic dysfunction in Niemann-Pick type C disease." Hum Mol Genet **21**(22): 4876-4887.

France-Lanord, V., B. Brugg, P. P. Michel, Y. Agid and M. Ruberg (1997). "Mitochondrial free radical signal in ceramide-dependent apoptosis: a putative mechanism for neuronal death in Parkinson's disease." J Neurochem **69**(4): 1612-1621.

Fuertes, G., J. J. Martin De Llano, A. Villarroya, A. J. Rivett and E. Knecht (2003). "Changes in the proteolytic activities of proteasomes and lysosomes in human fibroblasts produced by serum withdrawal, amino-acid deprivation and confluent conditions." Biochem J **375**(Pt 1): 75-86.

Fuertes, G., A. Villarroya and E. Knecht (2003). "Role of proteasomes in the degradation of short-lived proteins in human fibroblasts under various growth conditions." Int J Biochem Cell Biol **35**(5): 651-664.

Fushman, D. and O. Walker (2010). "Exploring the linkage dependence of polyubiquitin conformations using molecular modeling." J Mol Biol **395**(4): 803-814.

Futerman, A. H. (2006). "Intracellular trafficking of sphingolipids: relationship to biosynthesis." Biochim Biophys Acta **1758**(12): 1885-1892.

Futerman, A. H. and H. Riezman (2005). "The ins and outs of sphingolipid synthesis." Trends Cell Biol **15**(6): 312-318.

Fyrst, H. and J. D. Saba (2008). "Sphingosine-1-phosphate lyase in development and disease: sphingolipid metabolism takes flight." Biochim Biophys Acta **1781**(9): 448-458.

G. Li, C. F., S. Alexander, H. Alexander (2001). "Sphingosine-1-phosphate lyase has a central role in the development of Dictyostelium discoideum." Development **128**: 3473–3483.

Galadari, S., B. X. Wu, C. Mao, P. Roddy, S. El Bawab and Y. A. Hannun (2006). "Identification of a novel amidase motif in neutral ceramidase." Biochem J **393**(Pt 3): 687-695.

Gault, C. R., L. M. Obeid and Y. A. Hannun (2010). "An overview of sphingolipid metabolism: from synthesis to breakdown." Adv Exp Med Biol **688**: 1-23.

Geetha, T., M. L. Seibenhener, L. Chen, K. Madura and M. W. Wooten (2008). "p62 serves as a shuttling factor for TrkA interaction with the proteasome." Biochem Biophys Res Commun **374**(1): 33-37.

Glass, C. K., K. Saijo, B. Winner, M. C. Marchetto and F. H. Gage (2010). "Mechanisms underlying inflammation in neurodegeneration." Cell **140**(6): 918-934.

Gotz, J. and L. M. Ittner (2008). "Animal models of Alzheimer's disease and frontotemporal dementia." Nat Rev Neurosci **9**(7): 532-544.

Gundelfinger, E. D. and A. Fejtova (2012). "Molecular organization and plasticity of the cytomatrix at the active zone." Curr Opin Neurobiol **22**(3): 423-430.

Hagen-Euteneuer, N., D. Luetjohann, H. Park, A. H. Merrill, Jr. and G. van Echten-Deckert (2012). "S1P-lyase-deficiency increases sphingolipid formation via recycling at the expense of de novo biosynthesis in neurons." J Biol Chem.

Hagen-Euteneuer, N., D. Lutjohann, H. Park, A. H. Merrill, Jr. and G. van Echten-Deckert (2012). "Sphingosine 1-phosphate (S1P) lyase deficiency increases sphingolipid formation via recycling at the expense of de novo biosynthesis in neurons." J Biol Chem **287**(12): 9128-9136.

Hagen-Euteneuer, N., D. Lutjohann, H. Park, A. H. Merrill and G. van Echten-Deckert (2012). "Sphingosine 1-Phosphate (S1P) Lyase Deficiency Increases Sphingolipid Formation via Recycling at the Expense of de Novo Biosynthesis in Neurons." Journal of Biological Chemistry **287**(12): 9128-9136.

Hagen, N., M. Hans, D. Hartmann, D. Swandulla and G. van Echten-Deckert (2011). "Sphingosine-1-phosphate links glycosphingolipid metabolism to neurodegeneration via a calpain-mediated mechanism." Cell Death Differ **18**(8): 1356-1365.

Hagen, N., M. Hans, D. Hartmann, D. Swandulla and G. van Echten-Deckert (2011). "Sphingosine-1-phosphate links glycosphingolipid metabolism to neurodegeneration via a calpain-mediated mechanism." Cell Death and Differentiation **18**(8): 1356-1365.

Hagen, N., P. P. Van Veldhoven, R. L. Proia, H. Park, A. H. Merrill, Jr. and G. van Echten-Deckert (2009). "Subcellular Origin of Sphingosine 1-Phosphate Is Essential for Its Toxic Effect in Lyase-deficient Neurons." J Biol Chem **284**(17): 11346-11353.

Hagen, N., P. P. Van Veldhoven, R. L. Proia, H. Park, A. H. Merrill and G. van Echten-Deckert (2009). "Subcellular Origin of Sphingosine 1-Phosphate Is Essential for Its Toxic Effect in Lyase-deficient Neurons." Journal of Biological Chemistry **284**(17): 11346-11353.

Hait, N. C., J. Allegood, M. Maceyka, G. M. Strub, K. B. Harikumar, S. K. Singh, C. Luo, R. Marmorstein, T. Kordula, S. Milstien and S. Spiegel (2009). "Regulation of histone acetylation in the nucleus by sphingosine-1-phosphate." Science **325**(5945): 1254-1257.

Hait, N. C., C. A. Oskeritzian, S. W. Paugh, S. Milstien and S. Spiegel (2006). "Sphingosine kinases, sphingosine 1-phosphate, apoptosis and diseases." Biochim Biophys Acta **1758**(12): 2016-2026.

Hanada, K. (2003). "Serine palmitoyltransferase, a key enzyme of sphingolipid metabolism." Biochim Biophys Acta **1632**(1-3): 16-30.

Hanada, K., K. Kumagai, S. Yasuda, Y. Miura, M. Kawano, M. Fukasawa and M. Nishijima (2003). "Molecular machinery for non-vesicular trafficking of ceramide." Nature **426**(6968): 803-809.

Hannun, Y. A., C. Luberto and K. M. Argraves (2001). "Enzymes of sphingolipid metabolism: from modular to integrative signaling." Biochemistry **40**(16): 4893-4903.

Hannun, Y. A. and L. M. Obeid (2008). "Principles of bioactive lipid signalling: lessons from sphingolipids." Nat Rev Mol Cell Biol **9**(2): 139-150.

Hara, T., K. Nakamura, M. Matsui, A. Yamamoto, Y. Nakahara, R. Suzuki-Migishima, M. Yokoyama, K. Mishima, I. Saito, H. Okano and N. Mizushima (2006). "Suppression of basal autophagy in neural cells causes neurodegenerative disease in mice." Nature **441**(7095): 885-889.

Harvald, E. B., A. S. Olsen and N. J. Faergeman (2015). "Autophagy in the light of sphingolipid metabolism." Apoptosis **20**(5): 658-670.

Haughey, N. J., R. G. Cutler, A. Tamara, J. C. McArthur, D. L. Vargas, C. A. Pardo, J. Turchan, A. Nath and M. P. Mattson (2004). "Perturbation of sphingolipid metabolism and ceramide production in HIV-dementia." Ann Neurol **55**(2): 257-267.

Hegde, A. N. (2010). "The ubiquitin-proteasome pathway and synaptic plasticity." Learn Mem **17**(7): 314-327.

Heinemeyer, W., M. Fischer, T. Krimmer, U. Stachon and D. H. Wolf (1997). "The active sites of the eukaryotic 20 S proteasome and their involvement in subunit precursor processing." J Biol Chem **272**(40): 25200-25209.

Heinen M1, H. M., Ryan DP, Schnell S, Paesler K, Ehninger D. (2012). "Adult-onset fluoxetine treatment does not improve behavioral impairments and may have adverse effects on the Ts65Dn mouse model of Down syndrome." Neural Plast.

Hershko, A., A. Ciechanover, H. Heller, A. L. Haas and I. A. Rose (1980). "Proposed role of ATP in protein breakdown: conjugation of protein with multiple chains of the polypeptide of ATP-dependent proteolysis." Proc Natl Acad Sci U S A **77**(4): 1783-1786.

Hershko, A., H. Heller, S. Elias and A. Ciechanover (1983). "Components of ubiquitin-protein ligase system. Resolution, affinity purification, and role in protein breakdown." J Biol Chem **258**(13): 8206-8214.

Hoglinger, D., P. Haberkant, A. Aguilera-Romero, H. Riezman, F. D. Porter, F. M. Platt, A. Galione and C. Schultz (2015). "Intracellular sphingosine releases calcium from lysosomes." Elife **4**.

Hoyer-Hansen, M. and M. Jaattela (2007). "Connecting endoplasmic reticulum stress to autophagy by unfolded protein response and calcium." Cell Death Differ **14**(9): 1576-1582.

Huwiler, A., T. Kolter, J. Pfeilschifter and K. Sandhoff (2000). "Physiology and pathophysiology of sphingolipid metabolism and signaling." Biochim Biophys Acta **1485**(2-3): 63-99.

Iwata, A., B. E. Riley, J. A. Johnston and R. R. Kopito (2005). "HDAC6 and microtubules are required for autophagic degradation of aggregated huntingtin." J Biol Chem **280**(48): 40282-40292.

J. Mendel, K. H., H. Fyrst, J.D. Saba (2003). "Sphingosine phosphate lyase expression is essential for normal development in Caenorhabditis elegans." J. Biol. Chem. **278**: 22341–22349.

J. Zhou, J. S. (1998). "Identification of the first mammalian sphingosine phosphate lyase gene and its functional expression in yeast." Biochem. Biophys. Res. Commun. **242**: 502–507.

J.D. Saba, F. N., A. Bielawska, S. Garrett, Y.A. Hannun (1997). "The BST1 gene of

Saccharomyces cerevisiae is the sphingosine-1-phosphate lyase." J. Biol. Chem. **272**: 26087–26090.

Jarome, T. J., J. L. Kwapis, J. J. Hallengren, S. M. Wilson and F. J. Helmstetter (2014). "The ubiquitin-specific protease 14 (USP14) is a critical regulator of long-term memory formation." Learn Mem **21**(1): 9-13.

Jin, L. W., F. S. Shie, I. Maezawa, I. Vincent and T. Bird (2004). "Intracellular accumulation of amyloidogenic fragments of amyloid-beta precursor protein in neurons with Niemann-Pick type C defects is associated with endosomal abnormalities." Am J Pathol **164**(3): 975-985.

Johnson, K. R., K. Y. Johnson, K. P. Becker, J. Bielawski, C. Mao and L. M. Obeid (2003). "Role of human sphingosine-1-phosphate phosphatase 1 in the regulation of intra- and extracellular sphingosine-1-phosphate levels and cell viability." J Biol Chem **278**(36): 34541-34547.

Jones, B. J. and D. J. Roberts (1968). "A rotarod suitable for quantitative measurements of motor incoordination in naive mice." Naunyn Schmiedebergs Arch Exp Pathol Pharmakol **259**(2): 211.

Jung, C. H., S. H. Ro, J. Cao, N. M. Otto and D. H. Kim (2010). "mTOR regulation of autophagy." FEBS Lett **584**(7): 1287-1295.

K. Zhang, J. P., F. Hsu, J. Turk, P. Bandhuvula, J. Saba, S. Beverley (2007). "Redirection of sphingolipid metabolism towards de novo synthesis of ethanolamine in

Leishmania." EMBO J **26**.

Kaech, S. and G. Banker (2006). "Culturing hippocampal neurons." Nat Protoc **1**(5): 2406-2415.

Kajimoto, T., T. Okada, H. Yu, S. K. Goparaju, S. Jahangeer and S. Nakamura (2007). "Involvement of sphingosine-1-phosphate in glutamate secretion in hippocampal neurons." Mol Cell Biol **27**(9): 3429-3440.

Kanno, T. and T. Nishizaki (2011). "Endogenous sphingosine 1-phosphate regulates spontaneous glutamate release from mossy fiber terminals via S1P(3) receptors." Life Sci **89**(3-4): 137-140.

Kanno, T., T. Nishizaki, R. L. Proia, T. Kajimoto, S. Jahangeer, T. Okada and S. Nakamura (2010). "Regulation of synaptic strength by sphingosine 1-phosphate in the hippocampus." Neuroscience **171**(4): 973-980.

Karaca, I., I. Y. Tamboli, K. Glebov, J. Richter, L. H. Fell, M. O. Grimm, V. J. Haupenthal, T. Hartmann, M. H. Graler, G. van Echten-Deckert and J. Walter (2014). "Deficiency of sphingosine-1-phosphate lyase impairs lysosomal metabolism of the amyloid precursor protein." J Biol Chem **289**(24): 16761-16772.

Karaca, I., I. Y. Tamboli, K. Glebov, J. Richter, L. H. Fell, M. O. Grimm, V. J. Haupenthal, T. Hartmann, M. H. Graler, G. van Echten-Deckert and J. Walter (2014). "Deficiency of sphingosine-1-phosphate lyase impairs lysosomal metabolism of the amyloid precursor protein." J Biol Chem.

Katsel, P., C. Li and V. Haroutunian (2007). "Gene expression alterations in the sphingolipid metabolism pathways during progression of dementia and Alzheimer's disease: a shift toward ceramide accumulation at the earliest recognizable stages of Alzheimer's disease?" Neurochem Res **32**(4-5): 845-856.

Kempf, A., B. Tews, M. E. Arzt, O. Weinmann, F. J. Obermair, V. Pernet, M. Zagrebelsky, A. Delekate, C. Iobbi, A. Zemmar, Z. Ristic, M. Gullo, P. Spies, D. Dodd, D. Gygax, M. Korte and M. E. Schwab (2014). "The sphingolipid receptor S1PR2 is a receptor for Nogo-a repressing synaptic plasticity." PLoS Biol **12**(1): e1001763.

Kihara, A. (2014). "Sphingosine 1-phosphate is a key metabolite linking sphingolipids to glycerophospholipids." Biochim Biophys Acta **1841**(5): 766-772.

Kim, I. and J. J. Lemasters (2011). "Mitophagy selectively degrades individual damaged mitochondria after photoirradiation." Antioxid Redox Signal **14**(10): 1919-1928.

Kimelberg, H. K. and M. Nedergaard (2010). "Functions of astrocytes and their potential as therapeutic targets." Neurotherapeutics **7**(4): 338-353.

Kimura, S., T. Noda and T. Yoshimori (2007). "Dissection of the autophagosome maturation process by a novel reporter protein, tandem fluorescent-tagged LC3." Autophagy **3**(5): 452-460.

Kirkin, V., T. Lamark, T. Johansen and I. Dikic (2009). "NBR1 cooperates with p62 in selective autophagy of ubiquitinated targets." Autophagy **5**(5): 732-733.

Kirkin, V., D. G. McEwan, I. Novak and I. Dikic (2009). "A role for ubiquitin in selective autophagy." Mol Cell **34**(3): 259-269.

Klionsky, D. J. (2005). "The molecular machinery of autophagy: unanswered questions." J Cell Sci **118**(Pt 1): 7-18.

Klionsky, D. J. (2007). "Autophagy: from phenomenology to molecular understanding in less than a decade." Nat Rev Mol Cell Biol **8**(11): 931-937.

Klionsky, D. J., H. Abeliovich, P. Agostinis, D. K. Agrawal, G. Aliev, D. S. Askew, M. Baba, E. H. Baehrecke, B. A. Bahr, A. Ballabio, B. A. Bamber, D. C. Bassham, E. Bergamini, X. Bi, M. Biard-Piechaczyk, J. S. Blum, D. E. Bredesen, J. L. Brodsky, J. H. Brumell, U. T. Brunk, W. Bursch, N. Camougrand, E. Cebollero, F. Cecconi, Y. Chen, L. S. Chin, A. Choi, C. T. Chu, J. Chung, P. G. Clarke, R. S. Clark, S. G. Clarke, C. Clave, J. L. Cleveland, P. Codogno, M. I. Colombo, A. Coto-Montes, J. M. Cregg, A. M. Cuervo, J. Debnath, F. Demarchi, P. B. Dennis, P. A. Dennis, V. Deretic, R. J. Devenish, F. Di Sano, J. F. Dice, M. Difiglia, S. Dinesh-Kumar, C. W. Distelhorst, M. Djavaheri-Mergny, F. C. Dorsey, W. Droge, M. Dron, W. A. Dunn, Jr., M. Duszenko, N. T. Eissa, Z. Elazar, A. Esclatine, E. L. Eskelinen, L. Fesus, K. D. Finley, J. M. Fuentes, J. Fueyo, K. Fujisaki, B. Galliot, F. B. Gao, D. A. Gewirtz, S. B. Gibson, A. Gohla, A. L. Goldberg, R. Gonzalez, C. Gonzalez-Estevez, S. Gorski, R. A. Gottlieb, D. Haussinger, Y. W. He, K. Heidenreich, J. A. Hill, M. Hoyer-Hansen, X. Hu, W. P. Huang, A. Iwasaki, M. Jaattela, W. T. Jackson, X. Jiang, S. Jin, T. Johansen, J. U. Jung, M. Kadowaki, C. Kang, A. Kelekar, D. H. Kessel, J. A. Kiel, H. P. Kim, A. Kimchi, T. J. Kinsella, K. Kiselyov, K. Kitamoto, E. Knecht, M. Komatsu, E. Kominami, S. Kondo, A. L. Kovacs, G. Kroemer, C. Y. Kuan, R. Kumar, M. Kundu, J. Landry, M. Laporte, W. Le, H. Y. Lei, M. J. Lenardo, B. Levine, A. Lieberman, K. L. Lim, F. C. Lin, W. Liou, L. F. Liu, G. Lopez-Berestein, C. Lopez-Otin, B. Lu, K. F. Macleod, W. Malorni, W. Martinet, K. Matsuoka, J. Mautner, A. J. Meijer, A. Melendez, P. Michels, G. Miotto, W. P. Mistiaen, N. Mizushima, B. Mograbi, I. Monastyrska, M. N. Moore, P. I. Moreira, Y. Moriyasu, T. Motyl, C. Munz, L. O. Murphy, N. I. Naqvi, T. P. Neufeld, I. Nishino, R. A. Nixon, T. Noda, B. Nurnberg, M. Ogawa, N. L. Oleinick, L. J. Olsen, B. Ozpolat, S. Paglin, G. E. Palmer, I. Papassideri, M. Parkes, D. H. Perlmutter, G. Perry, M. Piacentini, R. Pinkas-Kramarski, M. Prescott, T. Proikas-Cezanne, N. Raben, A. Rami, F. Reggiori, B. Rohrer, D. C. Rubinsztein, K. M. Ryan, J. Sadoshima, H. Sakagami, Y. Sakai, M. Sandri, C. Sasakawa, M. Sass, C. Schneider, P. O. Seglen, O. Seleverstov, J. Settleman, J. J. Shacka, I. M. Shapiro, A. Sibirny, E. C. Silva-Zacarin, H. U. Simon, C. Simone, A. Simonsen, M. A. Smith, K. Spanel-Borowski, V. Srinivas, M. Steeves, H. Stenmark, P. E. Stromhaug, C. S. Subauste, S. Sugimoto, D. Sulzer, T. Suzuki, M. S. Swanson, I. Tabas, F. Takeshita, N. J. Talbot, Z. Talloczy, K. Tanaka, I. Tanida, G. S. Taylor, J. P. Taylor, A. Terman, G. Tettamanti, C. B. Thompson, M. Thumm, A. M. Tolkovsky, S. A. Tooze, R. Truant, L. V. Tumanovska, Y. Uchiyama, T. Ueno, N. L. Uzcategui, I. van der Klei, E. C. Vaquero, T. Vellai, M. W. Vogel, H. G. Wang, P. Webster, J. W. Wiley, Z. Xi, G. Xiao, J. Yahalom, J. M. Yang, G. Yap, X. M. Yin, T. Yoshimori, L. Yu, Z. Yue, M. Yuzaki, O.

Zabirnyk, X. Zheng, X. Zhu and R. L. Deter (2008). "Guidelines for the use and interpretation of assays for monitoring autophagy in higher eukaryotes." Autophagy **4**(2): 151-175.

Klionsky, D. J., J. M. Cregg, W. A. Dunn, Jr., S. D. Emr, Y. Sakai, I. V. Sandoval, A. Sibirny, S. Subramani, M. Thumm, M. Veenhuis and Y. Ohsumi (2003). "A unified nomenclature for yeast autophagy-related genes." Dev Cell **5**(4): 539-545.

Koike, M., H. Nakanishi, P. Saftig, J. Ezaki, K. Isahara, Y. Ohsawa, W. Schulz-Schaeffer, T. Watanabe, S. Waguri, S. Kametaka, M. Shibata, K. Yamamoto, E. Kominami, C. Peters, K. von Figura and Y. Uchiyama (2000). "Cathepsin D deficiency induces lysosomal storage with ceroid lipofuscin in mouse CNS neurons." J Neurosci **20**(18): 6898-6906.

Koike, M., M. Shibata, S. Waguri, K. Yoshimura, I. Tanida, E. Kominami, T. Gotow, C. Peters, K. von Figura, N. Mizushima, P. Saftig and Y. Uchiyama (2005). "Participation of autophagy in storage of lysosomes in neurons from mouse models of neuronal ceroid-lipofuscinoses (Batten disease)." Am J Pathol **167**(6): 1713-1728.

Komatsu, M., S. Waguri, T. Chiba, S. Murata, J. Iwata, I. Tanida, T. Ueno, M. Koike, Y. Uchiyama, E. Kominami and K. Tanaka (2006). "Loss of autophagy in the central nervous system causes neurodegeneration in mice." Nature **441**(7095): 880-884.

Komatsu, M., S. Waguri, M. Koike, Y. S. Sou, T. Ueno, T. Hara, N. Mizushima, J. Iwata, J. Ezaki, S. Murata, J. Hamazaki, Y. Nishito, S. Iemura, T. Natsume, T. Yanagawa, J. Uwayama, E. Warabi, H. Yoshida, T. Ishii, A. Kobayashi, M. Yamamoto, Z. Yue, Y. Uchiyama, E. Kominami and K. Tanaka (2007). "Homeostatic levels of p62 control cytoplasmic inclusion body formation in autophagy-deficient mice." Cell **131**(6): 1149-1163.

Kopp, F., R. Steiner, B. Dahlmann, L. Kuehn and H. Reinauer (1986). "Size and shape of the multicatalytic proteinase from rat skeletal muscle." Biochim Biophys Acta **872**(3): 253-260.

Korolchuk, V. I., A. Mansilla, F. M. Menzies and D. C. Rubinsztein (2009). "Autophagy inhibition compromises degradation of ubiquitin-proteasome pathway substrates." Mol Cell **33**(4): 517-527.

Korolchuk, V. I., F. M. Menzies and D. C. Rubinsztein (2009). "A novel link between autophagy and the ubiquitin-proteasome system." Autophagy **5**(6): 862-863.

Korolchuk, V. I., F. M. Menzies and D. C. Rubinsztein (2010). "Mechanisms of cross-talk between the ubiquitin-proteasome and autophagy-lysosome systems." FEBS Lett **584**(7): 1393-1398.

Kowalski, J. R. and P. Juo (2012). "The Role of Deubiquitinating Enzymes in Synaptic Function and Nervous System Diseases." Neural Plasticity.

Kroemer, G., G. Marino and B. Levine (2010). "Autophagy and the integrated stress response." Mol Cell **40**(2): 280-293.

Lane, R. M. and M. R. Farlow (2005). "Lipid homeostasis and apolipoprotein E in the development and progression of Alzheimer's disease." J Lipid Res **46**(5): 949-968.

Lavieu, G., F. Scarlatti, G. Sala, S. Carpentier, T. Levade, R. Ghidoni, J. Botti and P. Codogno (2006). "Regulation of autophagy by sphingosine kinase 1 and its role in cell survival during nutrient starvation." J Biol Chem **281**(13): 8518-8527.

Le Stunff, H., I. Galve-Roperh, C. Peterson, S. Milstien and S. Spiegel (2002). "Sphingosine-1-phosphate phosphohydrolase in regulation of sphingolipid metabolism and apoptosis." J Cell Biol **158**(6): 1039-1049.

Ledesma, M. D., A. Prinetti, S. Sonnino and E. H. Schuchman (2011). "Brain pathology in Niemann Pick disease type A: insights from the acid sphingomyelinase knockout mice." J Neurochem **116**(5): 779-788.

Lee, B. H., M. J. Lee, S. Park, D. C. Oh, S. Elsasser, P. C. Chen, C. Gartner, N. Dimova, J. Hanna, S. P. Gygi, S. M. Wilson, R. W. King and D. Finley (2010). "Enhancement of proteasome activity by a small-molecule inhibitor of USP14." Nature **467**(7312): 179-184.

Lepine, S., J. C. Allegood, M. Park, P. Dent, S. Milstien and S. Spiegel (2011). "Sphingosine-1-phosphate phosphohydrolase-1 regulates ER stress-induced autophagy." Cell Death Differ **18**(2): 350-361.

Li, L., L. S. Chin, O. Shupliakov, L. Brodin, T. S. Sihra, O. Hvalby, V. Jensen, D. Zheng, J. O. McNamara, P. Greengard and et al. (1995). "Impairment of synaptic vesicle clustering and of synaptic transmission, and increased seizure propensity, in synapsin I-deficient mice." Proc Natl Acad Sci U S A **92**(20): 9235-9239.

Long, J., T. R. Gallagher, J. R. Cavey, P. W. Sheppard, S. H. Ralston, R. Layfield and M. S. Searle (2008). "Ubiquitin recognition by the ubiquitin-associated domain of p62 involves a novel conformational switch." J Biol Chem **283**(9): 5427-5440.

Lowe, J., D. Stock, B. Jap, P. Zwickl, W. Baumeister and R. Huber (1995). "Crystal structure of the 20S proteasome from the archaeon T. acidophilum at 3.4 A resolution." Science **268**(5210): 533-539.

M. Ikeda, A. K., Y. Igarashi (2004). "Sphingosine-1-phosphate lyase SPL is an endoplasmic reticulum-resident, integral membrane protein with the pyridoxal 5'-phosphate binding domain exposed to the cytosol." Biochem. Biophys. Res. Commun. **325**: 338–343.

Maeurer, C., S. Holland, S. Pierre, W. Potstada and K. Scholich (2009). "Sphingosine-1-phosphate induced mTOR-activation is mediated by the E3-ubiquitin ligase PAM." Cell Signal **21**(2): 293-300.

Massey, A. C., C. Zhang and A. M. Cuervo (2006). "Chaperone-mediated autophagy in aging and disease." Curr Top Dev Biol **73**: 205-235.

Mencarelli, C., M. Losen, C. Hammels, J. De Vry, M. K. Hesselink, H. W. Steinbusch, M. H. De Baets and P. Martinez-Martinez (2010). "The ceramide transporter and the Goodpasture antigen binding protein: one protein--one function?" J Neurochem **113**(6): 1369-1386.

Menzies, F. M., A. Fleming and D. C. Rubinsztein (2015). "Compromised autophagy and neurodegenerative diseases." Nat Rev Neurosci **16**(6): 345-357.

Merrill, A. H., Jr. (2002). "De novo sphingolipid biosynthesis: a necessary, but dangerous, pathway." J Biol Chem **277**(29): 25843-25846.

Merrill, A. H., Jr., M. D. Wang, M. Park and M. C. Sullards (2007). "(Glyco)sphingolipidology: an amazing challenge and opportunity for systems biology." Trends Biochem Sci **32**(10): 457-468.

Mielke, M. M. and C. G. Lyketsos (2010). "Alterations of the sphingolipid pathway in Alzheimer's disease: new biomarkers and treatment targets?" Neuromolecular Med **12**(4): 331-340.

Milani, M., T. Rzymski, H. R. Mellor, L. Pike, A. Bottini, D. Generali and A. L. Harris (2009). "The role of ATF4 stabilization and autophagy in resistance of breast cancer cells treated with Bortezomib." Cancer Res **69**(10): 4415-4423.

Mitroi D.N., André Deutschmann, Maren Raucamp, Indulekha Karunakaran, Konstantine Glebov, Michael Hans, Jochen Walter, Julie Saba, Markus Gräler, Dan Ehninger, Elena Sopova, Oleg Shupliakov, Dieter Swandulla, Gerhild van Echten-Deckert: Sphingosine 1-phosphate lyase ablation disrupts presynaptic architecture and function via an ubiquitin- proteasome mediated mechanism, Scientific Reports, in press

Mizugishi, K., T. Yamashita, A. Olivera, G. F. Miller, S. Spiegel and R. L. Proia (2005). "Essential role for sphingosine kinases in neural and vascular development." Mol Cell Biol **25**(24): 11113-11121.

Mizushima, N. (2005). "The pleiotropic role of autophagy: from protein metabolism to bactericide." Cell Death Differ **12 Suppl 2**: 1535-1541.

Monville, C., E. M. Torres and S. B. Dunnett (2006). "Comparison of incremental and accelerating protocols of the rotarod test for the assessment of motor deficits in the 6-OHDA model." J Neurosci Methods **158**(2): 219-223.

Moruno Manchon, J. F., N. E. Uzor, Y. Dabaghian, E. E. Furr-Stimming, S. Finkbeiner and A. S. Tsvetkov (2015). "Cytoplasmic sphingosine-1-phosphate pathway modulates neuronal autophagy." Sci Rep **5**: 15213.

Nag, D. K. and D. Finley (2012). "A small-molecule inhibitor of deubiquitinating enzyme USP14 inhibits Dengue virus replication." Virus Res **165**(1): 103-106.

Nandi, D., P. Tahiliani, A. Kumar and D. Chandu (2006). "The ubiquitin-proteasome system." J Biosci **31**(1): 137-155.

Nedelsky, N. B., P. K. Todd and J. P. Taylor (2008). "Autophagy and the ubiquitin-proteasome system: collaborators in neuroprotection." Biochim Biophys Acta **1782**(12): 691-699.

Nixon, R. A. (2013). "The role of autophagy in neurodegenerative disease." Nat Med **19**(8): 983-997.

Ogretmen, B. and Y. A. Hannun (2004). "Biologically active sphingolipids in cancer pathogenesis and treatment." Nat Rev Cancer **4**(8): 604-616.

Ohtoyo, M., M. Tamura, N. Machinaga, F. Muro and R. Hashimoto (2015). "Sphingosine 1-phosphate lyase inhibition by 2-acetyl-4-(tetrahydroxybutyl)imidazole (THI) under conditions of vitamin B6 deficiency." Mol Cell Biochem **400**(1-2): 125-133.

Ordonez, M. P., E. A. Roberts, C. U. Kidwell, S. H. Yuan, W. C. Plaisted and L. S. Goldstein (2012). "Disruption and therapeutic rescue of autophagy in a human neuronal model of Niemann Pick type C1." Hum Mol Genet **21**(12): 2651-2662.

P.P. Van Veldhoven, S. G., G.P. Mannaerts, J.R. Vermeesch, V. Brys (2000). "Human sphingosine-1-phosphate lyase: cDNA cloning, functional expression studies and mapping to chromosome 10q22." Biochimica et Biophysica Acta **1487**: 128–134.

Pan, T., S. Kondo, W. Zhu, W. Xie, J. Jankovic and W. Le (2008). "Neuroprotection of rapamycin in lactacystin-induced neurodegeneration via autophagy enhancement." Neurobiol Dis **32**(1): 16-25.

Pandey, U. B., Z. Nie, Y. Batlevi, B. A. McCray, G. P. Ritson, N. B. Nedelsky, S. L. Schwartz, N. A. DiProspero, M. A. Knight, O. Schuldiner, R. Padmanabhan, M. Hild, D. L. Berry, D. Garza, C. C. Hubbert, T. P. Yao, E. H. Baehrecke and J. P. Taylor (2007). "HDAC6 rescues neurodegeneration and provides an essential link between autophagy and the UPS." Nature **447**(7146): 859-863.

Pankiv, S., T. H. Clausen, T. Lamark, A. Brech, J. A. Bruun, H. Outzen, A. Overvatn, G. Bjorkoy and T. Johansen (2007). "p62/SQSTM1 binds directly to Atg8/LC3 to facilitate degradation of ubiquitinated protein aggregates by autophagy." J Biol Chem **282**(33): 24131-24145.

Pekny, M. and M. Pekna (2014). "Astrocyte reactivity and reactive astrogliosis: costs and benefits." Physiol Rev **94**(4): 1077-1098.

Pelletier, D. and D. A. Hafler (2012). "Fingolimod for multiple sclerosis." N Engl J Med **366**(4): 339-347.

Pewzner-Jung, Y., S. Ben-Dor and A. H. Futerman (2006). "When do Lasses (longevity assurance genes) become CerS (ceramide synthases)?: Insights into the regulation of ceramide synthesis." J Biol Chem **281**(35): 25001-25005.

Pickart, C. M. and M. J. Eddins (2004). "Ubiquitin: structures, functions, mechanisms." Biochim Biophys Acta **1695**(1-3): 55-72.

Pitson, S. M. (2011). "Regulation of sphingosine kinase and sphingolipid signaling." Trends Biochem Sci **36**(2): 97-107.

Prasad, M. R., M. A. Lovell, M. Yatin, H. Dhillon and W. R. Markesbery (1998). "Regional membrane phospholipid alterations in Alzheimer's disease." Neurochem Res **23**(1): 81-88.

Qiao, L. and J. Zhang (2009). "Inhibition of lysosomal functions reduces proteasomal activity." Neurosci Lett **456**(1): 15-19.

Randow, F. and P. J. Lehner (2009). "Viral avoidance and exploitation of the ubiquitin system." Nat Cell Biol **11**(5): 527-534.

Rao, R. P. and J. K. Acharya (2008). "Sphingolipids and membrane biology as determined from genetic models." Prostaglandins Other Lipid Mediat **85**(1-2): 1-16.

Ravikumar, B., A. Acevedo-Arozena, S. Imarisio, Z. Berger, C. Vacher, C. J. O'Kane, S. D. Brown and D. C. Rubinsztein (2005). "Dynein mutations impair autophagic clearance of aggregate-prone proteins." Nat Genet **37**(7): 771-776.

Ravikumar, B., Z. Berger, C. Vacher, C. J. O'Kane and D. C. Rubinsztein (2006). "Rapamycin pre-treatment protects against apoptosis." Hum Mol Genet **15**(7): 1209-1216.

Ravikumar, B., S. Sarkar, J. E. Davies, M. Futter, M. Garcia-Arencibia, Z. W. Green-Thompson, M. Jimenez-Sanchez, V. I. Korolchuk, M. Lichtenberg, S. Luo, D. C. Massey, F. M. Menzies, K. Moreau, U. Narayanan, M. Renna, F. H. Siddiqi, B. R. Underwood, A. R. Winslow and D. C. Rubinsztein (2010). "Regulation of mammalian autophagy in physiology and pathophysiology." Physiol Rev **90**(4): 1383-1435.

Recchia, A., P. Debetto, A. Negro, D. Guidolin, S. D. Skaper and P. Giusti (2004). "Alpha-synuclein and Parkinson's disease." FASEB J **18**(6): 617-626.

Riganti, L., F. Antonucci, M. Gabrielli, I. Prada, P. Giussani, P. Viani, F. Valtorta, E. Menna, M. Matteoli and C. Verderio (2016). "Sphingosine-1-Phosphate (S1P) Impacts Presynaptic Functions by Regulating Synapsin I Localization in the Presynaptic Compartment." J Neurosci **36**(16): 4624-4634.

Riley, B. E., S. E. Kaiser, T. A. Shaler, A. C. Ng, T. Hara, M. S. Hipp, K. Lage, R. J. Xavier, K. Y. Ryu, K. Taguchi, M. Yamamoto, K. Tanaka, N. Mizushima, M. Komatsu and R. R. Kopito (2010). "Ubiquitin accumulation in autophagy-deficient mice is dependent on the Nrf2-mediated stress response pathway: a potential role for protein aggregation in autophagic substrate selection." J Cell Biol **191**(3): 537-552.

Rockenfeller, P., M. Koska, F. Pietrocola, N. Minois, O. Knittelfelder, V. Sica, J. Franz, D. Carmona-Gutierrez, G. Kroemer and F. Madeo (2015). "Phosphatidylethanolamine positively regulates autophagy and longevity." Cell Death Differ **22**(3): 499-508.

Rubinsztein, D. C. (2006). "The roles of intracellular protein-degradation pathways in neurodegeneration." Nature **443**(7113): 780-786.

Rusten, T. E. and H. Stenmark (2010). "p62, an autophagy hero or culprit?" Nat Cell Biol **12**(3): 207-209.

Scarlatti, F., C. Bauvy, A. Ventruti, G. Sala, F. Cluzeaud, A. Vandewalle, R. Ghidoni and P. Codogno (2004). "Ceramide-mediated macroautophagy involves inhibition of protein kinase B and up-regulation of beclin 1." J Biol Chem **279**(18): 18384-18391.

Schikorski, T. and C. F. Stevens (2001). "Morphological correlates of functionally defined synaptic vesicle populations." Nat Neurosci **4**(4): 391-395.

Schmahl, J., C. S. Raymond and P. Soriano (2007). "PDGF signaling specificity is mediated through multiple immediate early genes." Nat Genet **39**(1): 52-60.

Schmahl J, R. C., Soriano P. (2007). "PDGF signaling specificity is mediated through multiple immediate early genes." Nat Genet **39**: 52-60.

Serra, M. and J. D. Saba (2010). "Sphingosine 1-phosphate lyase, a key regulator of sphingosine 1-phosphate signaling and function." Adv Enzyme Regul **50**(1): 349-362.

Shacka, J. J., B. J. Klocke, C. Young, M. Shibata, J. W. Olney, Y. Uchiyama, P. Saftig and K. A. Roth (2007). "Cathepsin D deficiency induces persistent neurodegeneration in the absence of Bax-dependent apoptosis." J Neurosci **27**(8): 2081-2090.

Sigal, Y. J., M. I. McDermott and A. J. Morris (2005). "Integral membrane lipid phosphatases/phosphotransferases: common structure and diverse functions." Biochem J **387**(Pt 2): 281-293.

Siksou, L., P. Rostaing, J. P. Lechaire, T. Boudier, T. Ohtsuka, A. Fejtova, H. T. Kao, P. Greengard, E. D. Gundelfinger, A. Triller and S. Marty (2007). "Three-dimensional architecture of presynaptic terminal cytomatrix." J Neurosci **27**(26): 6868-6877.

Sims, K., C. A. Haynes, S. Kelly, J. C. Allegood, E. Wang, A. Momin, M. Leipelt, D. Reichart, C. K. Glass, M. C. Sullards and A. H. Merrill, Jr. (2010). "Kdo2-lipid A, a TLR4-specific agonist, induces de novo sphingolipid biosynthesis in RAW264.7 macrophages, which is essential for induction of autophagy." J Biol Chem **285**(49): 38568-38579.

Sofroniew, M. V. (2005). "Reactive astrocytes in neural repair and protection." Neuroscientist **11**(5): 400-407.

Sowa, M. E., E. J. Bennett, S. P. Gygi and J. W. Harper (2009). "Defining the human deubiquitinating enzyme interaction landscape." Cell **138**(2): 389-403.

Speese, S. D., N. Trotta, C. K. Rodesch, B. Aravamudan and K. Broadie (2003). "The ubiquitin proteasome system acutely regulates presynaptic protein turnover and synaptic efficacy." Current Biology **13**(11): 899-910.

Spiegel, S. and S. Milstien (2003). "Sphingosine-1-phosphate: an enigmatic signalling lipid." Nat Rev Mol Cell Biol **4**(5): 397-407.

Sudhof, T. C. (2012). "The presynaptic active zone." Neuron **75**(1): 11-25.

Sudhof, T. C. (2013). "Neurotransmitter release: the last millisecond in the life of a synaptic vesicle." Neuron **80**(3): 675-690.

Suzuki, K. and Y. Ohsumi (2007). "Molecular machinery of autophagosome formation in yeast, Saccharomyces cerevisiae." FEBS Lett **581**(11): 2156-2161.

Takasugi, N., T. Sasaki, K. Suzuki, S. Osawa, H. Isshiki, Y. Hori, N. Shimada, T. Higo, S. Yokoshima, T. Fukuyama, V. M. Lee, J. Q. Trojanowski, T. Tomita and T. Iwatsubo (2011). "BACE1 activity is modulated by cell-associated sphingosine-1-phosphate." J Neurosci **31**(18): 6850-6857.

Taniguchi, M., K. Kitatani, T. Kondo, M. Hashimoto-Nishimura, S. Asano, A. Hayashi, S. Mitsutake, Y. Igarashi, H. Umehara, H. Takeya, J. Kigawa and T. Okazaki (2012). "Regulation of autophagy and its associated cell death by "sphingolipid rheostat": reciprocal role of ceramide and sphingosine 1-phosphate in the mammalian target of rapamycin pathway." J Biol Chem **287**(47): 39898-39910.

Thrower, J. S., L. Hoffman, M. Rechsteiner and C. M. Pickart (2000). "Recognition of the polyubiquitin proteolytic signal." EMBO J **19**(1): 94-102.

Tian, Z., P. D'Arcy, X. Wang, A. Ray, Y. T. Tai, Y. Hu, R. D. Carrasco, P. Richardson, S. Linder, D. Chauhan and K. C. Anderson (2014). "A novel small molecule inhibitor of deubiquitylating enzyme USP14 and UCHL5 induces apoptosis in multiple myeloma and overcomes bortezomib resistance." Blood **123**(5): 706-716.

Tuscher, J. J., A. M. Fortress, J. Kim and K. M. Frick (2015). "Regulation of object recognition and object placement by ovarian sex steroid hormones." Behav Brain Res **285**: 140-157.

U. Reiss, B. O., J. Zhou, V. Gupta, P. Sooriyakumaran, S. Kelly, E. Wang, A.H. Merrill Jr., J.D. Saba (2004). " Sphingosine-phosphate lyase enhances stress-induced ceramide generation and apoptosis." J. Biol. Chem. **279**: 1281–1290.

Ullian, E. M., S. K. Sapperstein, K. S. Christopherson and B. A. Barres (2001). "Control of synapse number by glia." Science **291**(5504): 657-661.

Ullrich, C., N. Daschil and C. Humpel (2011). "Organotypic vibrosections: novel whole sagittal brain cultures." J Neurosci Methods **201**(1): 131-141.

Uvarov, A. V. and N. Mesaeli (2008). "Enhanced ubiquitin-proteasome activity in calreticulin deficient cells: a compensatory mechanism for cell survival." Biochim Biophys Acta **1783**(6): 1237-1247.

van Echten-Deckert, G., N. Hagen-Euteneuer, I. Karaca and J. Walter (2014). "Sphingosine-1-phosphate: boon and bane for the brain." Cell Physiol Biochem **34**(1): 148-157.

van Echten-Deckert, G. and J. Walter (2012). "Sphingolipids: Critical players in Alzheimer's disease." Prog Lipid Res **51**(4): 378-393.

van Echten-Deckert, G., A. Zschoche, T. Bar, R. R. Schmidt, A. Raths, T. Heinemann and K. Sandhoff (1997). "cis-4-Methylsphingosine decreases sphingolipid biosynthesis by specifically interfering with serine palmitoyltransferase activity in primary cultured neurons." J Biol Chem **272**(25): 15825-15833.

Walter, J. and G. van Echten-Deckert (2013). "Cross-talk of membrane lipids and Alzheimer-related proteins." Mol Neurodegener **8**: 34-45.

Walters, B. J., J. J. Hallengren, C. S. Theile, H. L. Ploegh, S. M. Wilson and L. E. Dobrunz (2014). "A catalytic independent function of the deubiquitinating enzyme USP14 regulates hippocampal synaptic short-term plasticity and vesicle number." J Physiol **592**(Pt 4): 571-586.

Wang, H., R. Q. Sun, D. Camera, X. Y. Zeng, E. Jo, S. M. Chan, T. P. Herbert, J. C. Molero and J. M. Ye (2016). "Endoplasmic reticulum stress up-regulates Nedd4-2 to induce autophagy." FASEB J **30**(7): 2549-2556.

Wei, Y., S. Pattingre, S. Sinha, M. Bassik and B. Levine (2008). "JNK1-mediated phosphorylation of Bcl-2 regulates starvation-induced autophagy." Mol Cell **30**(6): 678-688.

Welchman, R. L., C. Gordon and R. J. Mayer (2005). "Ubiquitin and ubiquitin-like proteins as multifunctional signals." Nat Rev Mol Cell Biol **6**(8): 599-609.

Wheeler, T. C., L. S. Chin, Y. Li, F. L. Roudabush and L. Li (2002). "Regulation of synaptophysin degradation by mammalian homologues of seven in absentia." J Biol Chem **277**(12): 10273-10282.

Wilson-Zbinden, C., A. X. dos Santos, I. Stoffel-Studer, A. van der Vaart, K. Hofmann, F. Reggiori, H. Riezman, C. Kraft and M. Peter (2015). "Autophagy competes for a common phosphatidylethanolamine pool with major cellular PE-consuming pathways in Saccharomyces cerevisiae." Genetics **199**(2): 475-485.

Wilson, S. M., B. Bhattacharyya, R. A. Rachel, V. Coppola, L. Tessarollo, D. B. Householder, C. F. Fletcher, R. J. Miller, N. G. Copeland and N. A. Jenkins (2002). "Synaptic defects in ataxia mice result from a mutation in Usp14, encoding a ubiquitin-specific protease." Nat Genet **32**(3): 420-425.

Wishart, T. M., S. H. Parson and T. H. Gillingwater (2006). "Synaptic vulnerability in neurodegenerative disease." J Neuropathol Exp Neurol **65**(8): 733-739.

Wooten, M. W., T. Geetha, J. R. Babu, M. L. Seibenhener, J. Peng, N. Cox, M. T. Diaz-Meco and J. Moscat (2008). "Essential role of sequestosome 1/p62 in regulating accumulation of Lys63-ubiquitinated proteins." J Biol Chem **283**(11): 6783-6789.

Wu, X. S., B. D. McNeil, J. Xu, J. Fan, L. Xue, E. Melicoff, R. Adachi, L. Bai and L. G. Wu (2009). "Ca(2+) and calmodulin initiate all forms of endocytosis during depolarization at a nerve terminal." Nat Neurosci **12**(8): 1003-1010.

Xu, R., J. Jin, W. Hu, W. Sun, J. Bielawski, Z. Szulc, T. Taha, L. M. Obeid and C. Mao (2006). "Golgi alkaline ceramidase regulates cell proliferation and survival by controlling levels of sphingosine and S1P." FASEB J **20**(11): 1813-1825.

Y. Liu, R. W., T. Yamashita, Y. Mi, C.X. Deng, J.P. Hobson, H.M. Rosenfeldt, V.E. and S. S. C. Nava, M.J. Lee, C.H. Liu, T. Hla, S. Spiegel, R.L. Proia (2000). "Edg-1, the G proteincoupled receptor for sphingosine-1-phosphate, is essential for vascular maturation." J. Clin. Invest. **106**: 951–961.

Yang, Z. and D. J. Klionsky (2010). "Mammalian autophagy: core molecular machinery and signaling regulation." Curr Opin Cell Biol **22**(2): 124-131.

Yasuda, T., Y. Nakata, C. J. Choong and H. Mochizuki (2013). "Neurodegenerative changes initiated by presynaptic dysfunction." Transl Neurodegener **2**(1): 16.

Zhang, C., B. Wu, V. Beglopoulos, M. Wines-Samuelson, D. Zhang, I. Dragatsis, T. C. Sudhof and J. Shen (2009). "Presenilins are essential for regulating neurotransmitter release." Nature **460**(7255): 632-636.

Zhang, K., J. M. Pompey, F. F. Hsu, P. Key, P. Bandhuvula, J. D. Saba, J. Turk and S. M. Beverley (2007). "Redirection of sphingolipid metabolism toward de novo synthesis of ethanolamine in Leishmania." EMBO J **26**(4): 1094-1104.

Zhao, J., J. J. Brault, A. Schild, P. Cao, M. Sandri, S. Schiaffino, S. H. Lecker and A. L. Goldberg (2007). "FoxO3 coordinately activates protein degradation by the autophagic/lysosomal and proteasomal pathways in atrophying muscle cells." Cell Metab **6**(6): 472-483.

Zhu, K., K. Dunner, Jr. and D. J. McConkey (2010). "Proteasome inhibitors activate autophagy as a cytoprotective response in human prostate cancer cells." Oncogene **29**(3): 451-462.

ACKNOWLEDGEMENTS

I would like to express my deepest gratitude to PD Dr. Gerhild van Echen-Deckert for providing me the opportunity to work in her group. I am thankful for her ideas and guidance that helped me all these years. I am also grateful for her support in exchanging my ideas with other scientists at local, national or international meetings. She was also the initiator of the collaborations that helped me building up the thesis.

I would like to thank Prof. Dr. Walter Witke who kindly agreed to participate as the second referee for the thesis dissertation.

I am also grateful to Prof. Dr. Jörg Höhfeld and Prof. Dr. Dirk Menche for agreeing to participate as referee for my thesis.

I very much appreciate the support received through the collaborative work undertaken with Dr. Maria Dolores Ledesma at the Centre of Molecular Biology “Severo Ochoa” while I was an ERASMUS+ exchange student at the Autonomous University of Madrid.

I would like to thank to Dr. Dan Ehninger from German Center for Neurodegenerative Diseases for his supervision and help in doing the behavioural tests of the mice.

I gratefully acknowledge the funding received from the German Academic Exchange Service (DAAD).

I would like to thank all current and former members of the Life and Medical Sciences and to Bonn International Graduate School of Neuroscience (BIGS) for creating an inspiring scientific environment.

Finally, I wish to thank my family for their support and encouragement throughout my studies.

Publications

Daniel N Mitroi, Indulekha Karunakaran, Markus Gräler, Julie Saba, María Dolores Ledesma, Gerhild van Echten-Deckert: Sphingosine 1-phosphate-lyase modulates neuronal autophagy via phosphatidylethanolamine production, Autophagy, **accepted, in press**

Mitroi DN, Deutschmann AU, Raucamp M, Karunakaran I, Glebov K, Hans M, Walter J, Saba J, Gräler M, Ehninger D, Sopova E, Shupliakov O, Swandulla D, van Echten-Deckert G, Sphingosine 1-phosphate lyase ablation disrupts presynaptic architecture and function via an ubiquitin- proteasome mediated mechanism, Sci Rep. 2016 Nov 24;6:37064. doi: 10.1038/srep37064. PMID:27883090

Odent Grigorescu G, Preda MB, Radu E, Rosca AM, Tutuianu R, **Mitroi DN**, Simionescu M, Burlacu A: Combinatorial approach for improving the outcome of angiogenic therapy in ischemic tissues, Biomaterials, 2015 Aug; 60:72-81, Epub 2015 May 15.